TRAKYA UNIVERSITY
JOURNAL OF NATURAL SCIENCES

20 Volume 1 Number April 2019

TRAKYA UNIVERSITY JOURNAL OF NATURAL SCIENCES

TUJNS

Trakya Univ J Nat Sci
ISSN 2147-0294
e-ISSN 2528-9691

Trakya University
Journal of Natural Sciences

Volume: 20 **Number: 1** **April** **2019**

Trakya Univ J Nat Sci

http://dergipark.gov.tr/trkjnat
e-mail: tujns@trakya.edu.tr

ISSN 2147-0294
e-ISSN 2528-9691

ISSN 2147-0294
e-ISSN 2528-9691

Trakya University Journal of Natural Sciences
http://dergipark.gov.tr/trkjnat
Volume 20, Number 1, April 2019

Correspondence Address
Trakya Üniversitesi Fen Bilimleri Enstitüsü Binası, Balkan Yerleşkesi – 22030 Edirne / TÜRKİYE
e-mail: tujns@trakya.edu.tr
Tel: +90 284 2358230
Fax: +90 284 2358237

This Journal is a peer reviewed journal and is indexed by CAB Abstract, CiteFactor, DOAJ (Directory of Open Access Journal), DRJI (Directory of Research Journal Indexing), ESCI (Emerging Sources Citation Index), Google Scholar, ResearchBib, Science Library Index, SIS (Scientific Indexing Services), TUBITAK-ULAKBIM Life Sciences Database (Turkish Journal Index) and Zoological Record.

Publisher
Trakya Üniversitesi Matbaa Tesisleri / Trakya University Publishing Centre

TRAKYA UNIVERSITY JOURNAL OF NATURAL SCIENCES

Volume 20 **Number 1** **April** **2019**

REVIEWER LIST

ISSN 2147-0294
e-ISSN 2528-9691

Trakya University Journal of Natural Sciences
http://dergipark.gov.tr/trkjnat
Volume 20, Number 1, April 2019

CONTENTS

Research Article

http://dergipark.gov.tr/trkjnat
Trakya University Journal of Natural Sciences, 20(1): 1-8, 2019
ISSN 2147-0294, e-ISSN 2528-9691
DOI: 10.23902/trkjnat.435384

Research Article

FITNESS AND PATHOGENICITY OF OUTBREAK CAUSING *Salmonella* UPON SHORT-TERM EXPOSURE TO GROUNDWATER WITH RESIDUAL ANTIBIOTICS

Berat Zeki HAZNEDAROĞLU

Institute of Environmental Sciences, Boğaziçi University, Hisar Campus, 34342 Bebek, İstanbul, TURKEY
ORCID ID: orcid.org/0000-0002-0081-8801, e-mail: berat.haznedaroglu@boun.edu.tr

Cite this article as:

Haznedaroğlu B.Z. 2019. Fitness and Pathogenicity of Outbreak Causing *Salmonella* Upon Short-Term Exposure to Groundwater with Residual Antibiotics. *Trakya Univ J Nat Sci*, 20(1): 1-8, DOI: 10.23902/trkjnat.435384

Received: 21 June 2018, Accepted: 18 November 2018, Online First: 23 December 2018, Published: 15 April 2019

Abstract: The changes in survival and pathogenicity of three *Salmonella enterica* subsp. *enterica* serotypes upon short term exposure to groundwater with residual antibiotics have been studied in relationship to overall microbial fitness. A wild type flagellated *Salmonella enterica* ser. Typhimurium outbreak strain, a mutant *Salmonella enterica* ser. Typhimurium strain, and a wild type avian disease-causing *Salmonella enterica* ser. Pullorum strain were exposed to a range of ionic strength (3-30 mM) groundwater with residual antibiotics for 6-24 hours. Exposed organisms' pathogenicity was tested in vitro exposure to a human epithelial cell line (HEp2). Resistance profiles against 10 common antibiotics were also tested and compared to unexposed controls. Results show minor antibiotic resistance changes for *S. enterica* ser. Typhimurium strains in response to some antibiotic classes mediated with active efflux pumps. This trend was not observed for *S. enterica* ser. Pullorum, suggesting that resistance found in groundwater exposed organisms might be strain-dependent. In vitro epithelial cell invasion assays showed bacterial invasion of HEp2 cells initially decreases with time and increases after 24 hours. It is concluded that *S. enterica* serotypes reaching groundwater environments in the presence of residual antibiotics may exhibit increased levels of pathogenicity, strain-dependent resistance to antibiotics, and sustained levels of viability.

Key words: *Salmonella*, antibiotic resistance, invasion, groundwater, pathogenicity.

Özet: Bu çalışmada kalıntı miktarda antibiyotik içeren yeraltı sularına kısa süreli maruz bırakılan üç *Salmonella enterica* subsp. *enterica* serotipinin hastalık yapıcı özelliklerindeki değişiklikler ve hayatta kalabilme seviyeleri genel mikrobiyel fitnes çerçevesinde incelenmiştir. Serotipler gerçek bir salgından izole edilen kamçılı doğal fenotip *Salmonella enterica* ser. Typhimurium, kamçısı fonksiyonel olmayan bir başka *Salmonella enterica* ser. Typhimurium suşu ve kuş türlerinde salgına yol açan doğal fenotip *Salmonella enterica* ser. Pullorum'dan oluşup, iyon şiddeti değişken (3-30 mM) ve kalıntı miktarda antibiyotik içeren yeraltı suyuna 6-24 saat sürecince maruz bırakılmıştır. Serotiplerin hastalık yapıcı özellikleri in vitro koşullarda HEp2 türü insan epitel hücre kültürleri kullanılarak ölçülmüştür. Antibiyotik direnç seviyeleri ise yaygın kullanılan 10 antibitiyotiğe karşı disk difüzyon testi yardımıyla belirlenmiştir. Deneyler sonucunda *S. enterica* ser. Typhimurium suşlarında antibiyotik direnç seviyelerinde az miktarda artış gözlenirken *S. enterica* ser. Pullorum suşunda değişiklik gözlenmemiştir. In vitro deneylerde ise suşların HEp2 hücrelerini enfekte etmeleri zamanla önce azalmış, 24 saatlik dilim sonunda ise artmıştır. Sonuç olarak, kalıtsal antibiyotik içeren yeraltı sularına temas eden *S. enterica* serotiplerinin hastalık yapıcı karakterlerinin arttığı, antibiyotik direnç seviyelerinin suşa bağlı olarak değişkenlik gösterirken hayatta kalma oranlarının yüksek olduğu gözlenmiştir.

Introduction

Salmonella is a robust zoonotic pathogen threatening both human and animal health significantly. Non-typhoidal *Salmonella* infections are increasing worldwide with at least nine to ten incidents reported each year since 2009 only in the U.S. (Vugia *et al.* 2004). A recent major outbreak caused by *S. enterica* ser. Typhimurium has affected 714 individuals in 46 states (CDC 2009). One of the reservoirs for pathogenic bacteria including *Salmonella* following excretion from infected individuals is groundwater environments (Schmoll *et al.* 2006). Pathogens released from various point and non-point sources of human and/or animal waste will likely reach groundwater and create health related issues in individuals who are directly or indirectly exposed to the groundwater (Crane & Moore 1984). Considering the facts that antibiotics are frequently detected in various groundwater systems (Barber *et al.* 2009, Barnes *et al.* 2008, Vulliet & Cren-Olivé 2011) and 26% of the total freshwater demand is supplied through groundwater (Hutson 2004), it is essential to understand the effects of groundwater environments with residual antibiotics on the fitness of waterborne pathogens as it pertains to several physiological

characteristics such as pathogenicity, survivability and gained or lost resistance to certain antibiotics.

Another unknown issue with the ion-rich nature of groundwater systems is how bacterial efflux pumps are affected with respect to antimicrobial resistance, especially against aminoglyglycosides (Bradford 2008), tetracyclines (Chopra & Roberts 2001) and quinolones (Poole 2000). It has been previously documented that working mechanisms of these bacterial efflux pumps are directly and/or indirectly linked to the ionic components in the external environment. For example, the insertion of aminoglycosides into bacterial LPS (Bradford 2008) follows a proton gradient (energy) dependent transport across the cytoplasmic membrane. Additionally, a tetracycline efflux pump system is induced under the presence of Mg^{2+} in the external environment (Roberts 1996, Orth *et al.* 2000), which results in the excretion of the antibiotic in an energy-dependent manner with proton exchange for a tetracycline-cation complex (Yamaguchi *et al.* 1993). The majority of efflux pumps work in this manner, *i.e.*, compound-ion antiporter, and are reviewed in detail elsewhere (Kumar & Schweizer 2005). Similarly, efflux pump systems in *Salmonella* also assist the bacteria in resistance to antibiotics such as ciprofloxacin (Giraud *et al.* 2000), β-lactams (Nikaido *et al.* 1998), as well as creating simultaneous resistance to multiple drugs (Abouzeed *et al.* 2008, Piddock *et al.* 2000, Quinn 2006). Resistance to β-lactams in *Salmonella* is mediated by the AcrAB efflux system and AcrB is also required for virulence of *S. enterica* ser. Typhimurium (Lacroix 1996), suggesting that drug transporters may contribute not only to antibiotic resistance but also to virulence (Kunihiko Nishino 2006). Despite these findings, comprehensive studies on changes of antibiotic resistance in waterborne *Salmonella* spp. exposed to groundwater with residual antibiotics have not been performed so far.

This study aims to investigate whether the fitness of *Salmonella* is affected when exposed to ion-rich groundwater conditions with residual antibiotics in the external environment. The fitness was evaluated with respect to decreased antibiotic resistance, viability and pathogenicity against human cell lines. For these purposes, an outbreak-causing wild type *S. enterica* ser. Typhimurium, a non-motile mutant phenotype of *S. enterica* ser. Typhimurium and *S. enterica* ser. Pullorum, an important avian outbreak-causing strain, were selected as model organisms. These particular strains were chosen due to their different genotypic and phenotypic variation and their low-level susceptibility to the tested antibiotics as control groups to monitor any suspected changes in their profiles.

Materials and Methods

Bacterial strain selection and preparation

All *Salmonella* strains used in the study were obtained from the Salmonella Genetic Stock Centre (SGSC) of University of Calgary, Alberta, Canada. *S. enterica* ser. Typhimurium strain ST5383 is a wild type strain and was originally isolated from an outbreak infecting more than 1700 people (Bezanson *et al.* 1985). The strain designated as SGSC1512 is a non-motile mutant of *S. enterica* ser. Typhimurium TM2 (Yamaguchi *et al.* 1986). The non-motile, non-flagellated avian pathogenic *S. pullorum* wild type strain SA1685 (CDC number 2863-65) was originally isolated from an infected turkey.

S. enterica serotypes used during the course of the study was pre-cultured in Luria-Bertani (LB) broth (Fisher Scientific, Fair Lawn, NJ) at 37°C overnight, and shaken continuously at 120 rpm. Overnight grown cultures were inoculated into fresh LB broth in 1:100 dilutions and harvested at the mid-exponential phase determined by the growth curve analysis for each bacterium. A refrigerated bench-top centrifuge (5804R; Eppendorf, Hamburg, Germany) equipped with a fixed angle rotor (F-34-6-38; Eppendorf) was used to pellet the cells with an applied 3,700×*g* force for 15 min at 4°C. Growth medium was decanted and the pellet was resuspended in 10 mM potassium chloride (KCl) solution. The process was repeated twice in order to ensure complete removal of the growth medium. Electrolyte solutions used in cell preparation and other experiments were prepared with de-ionized water (DIW) (Millipore, Billerica, MA) and reagent-grade KCl (Fisher Scientific). The concentration of the cell stock solution was determined by using a cell counting hemocytometer (Bürker-Turk, Germany) under a light microscope (Fisher Scientific).

Groundwater exposure conditions

Bacteria cultured and harvested as described above were exposed to groundwater (GW) for 6, 12, 18 and 24 hours. GW was prepared with a slight modification of a previously used procedure (Bolster *et al.* 1999) by dissolving $CaCl_2.2H_2O$ (36 mg), $CaSO_4.2H_2O$ (25 mg), KNO_3 (20 mg), $NaHCO_3$ (36 mg), $Ca(NO_3)_2.4H_2O$ (35 mg) and $MgSO_4.7H_2O$ (60 mg) in 1 L of sterile deionized water (DIW) and the ionic strength (IS) of GW were adjusted to 3.33 mM (original recipe), 10 mM and 30 mM accordingly. For the test group, 1 μg/L of each the following antibiotics were added to GW: amoxicillin (MP Biomedicals), tetracycline (EMD Chemicals, Darmstadt, Germany), ampicillin (EMD Chemicals), chloramphenicol (EMD Chemicals), kanamycin (EMD Chemicals), gentamicin (MP Biomedicals), streptomycin (MP Biomedicals), sulfamethoxazole (MP Biomedicals), and penicillin (Fisher Scientific). The pH of GW was kept constant at 7.0±0.2. Bacteria suspensions of 10^8 cells per mL were exposed to the aforementioned GW conditions in 100 mL tissue culture flasks with 0.2 μm vented caps (Corning) wrapped in aluminum foil, placed on orbital shakers, and mildly shaken (70 rpm) for the tested time period. Bacterial isolates exposed to GW without the residual antibiotics were referred as the control group.

Cell viability analysis

At the end of exposure to GW, viability of both the control and the test groups was determined by using the Live/Dead BacLight® kit (L-7012; Molecular Probes,

Eugene, OR) according to the manufacturer's directions. Direct counting of the stained live and dead cells was done using an inverted microscope (IX70; Olympus, Japan) operated under red/green fluorescence filter set (Chroma Technology Corp., Brattleboro, VT).

Antibiotic susceptibility analysis

Antibiotic susceptibility tests were employed to assay any change in susceptibility of *Salmonella* isolates against 10 different antimicrobial chemicals commonly used by the U.S. National Antimicrobial Resistance Monitoring System (NARMS). Tests were performed in compliance with the Clinical Laboratory Standards (CLSI), formerly National Committee for Clinical Laboratory Standards (NCCLS), (CLSI 2003) for the following antimicrobial agents (numbers in parentheses denote the amount of antimicrobial chemical impregnated in 6 mm disks): amikacin (30 µg), amoxicillin-clavulanic acid (30 µg) cefoxitin (30 µg), ceftriaxone (30 µg), cephalothin (30 µg), chloramphenicol (30 µg), ciprofloxacin (5 µg), nalidixic acid (30 µg), tetracycline (30 µg) and trimethoprim-sulfamethoxazole (25 µg).

Epithelial cell culture and invasion assays

The human epithelial cell line HEp-2 was obtained from American Type Culture Collection (ATCC) (CCL-23; ATCC, Manassas, VA) and was grown in Eagle's Minimum Essential Medium (EMEM) (ATCC) supplemented with 10% fetal bovine serum (ATCC) and 1% penicillin-streptomycin (Sigma-Aldrich, St. Louis, MO). Epithelial cells were incubated at 37˚C under 5% CO_2.

Invasion of *Salmonella* into epithelial cells was quantified with slight modifications of the protocols described in Burnham *et al.* (2007). Briefly, a monolayer of HEp-2 cells was grown until confluence in 24-well plates (Corning, Corning, NY). *Salmonella,* at a concentration of 10^5 cells per mL, was inoculated into cell-culture plates and incubated for 2 hours at 37˚C to allow internalization. Following the incubation, each well of the plates was washed three times with phosphate buffered saline (PBS) to remove unbound bacteria. Bacteria that were bound to epithelial cells but had not been internalized were killed by applying fresh growth medium containing 5 µg penicillin per mL and 100 µg gentamicin per mL, and incubated for 2 hours at 37˚C. Following the incubation, cells were washed with PBS, treated with trypsin-EDTA complex (ATCC), and lysed with 0.1 % Triton-X100 (Fisher Scientific). The lysates were spread onto LB agar plates and incubated for 18 hours at 37˚C. The number of colony forming units (CFUs) was counted to quantify the number of *Salmonella* that had successfully invaded the monolayer of the epithelial cells.

Statistical analysis of data

Changes in the diameters of antibiotic inhibition zones (for determining antibiotic susceptibility profiles), viability, and the number of CFUs of *Salmonella* infecting HEp2 cells were statistically compared using the unpaired Student's t-test using Minitab® Version 14 (State College, PA). Differences between the control and the test groups were considered to be significant at 95% confidence interval ($P < 0.05$).

Light microscopy imaging of epithelial cells

Representative images of both uninfected and *Salmonella*-invaded HEp2 cells were obtained by using a light microscope (Micromaster, Fisher Scientific) (Fig. 1). The Giemsa stain (Fisher Scientific) which differentially stains human and bacterial cells in purple and pink, respectively was used. Chambered cover glass slides (Nunc Lab-Tek, Fisher Scientific) were used to grow HEp2 cells until desired confluence and infected with *Salmonella* as described above. After the chambered cover glasses were manually removed, the slides were placed in Giemsa stain (2.5%) for 45-60 minutes. Slides were rinsed by dipping in a buffer solution [0.59% (w/v) Na_2HPO_4, 0.36% (w/v) $NaH_2PO_4H_2O$] three-four times and left to air dry. Stained slides were observed under light microscope and their images were taken at 400× magnification.

Results

Antibiotic susceptibility analysis

The control group of the non-motile mutant SGSC1512 was susceptible to all antibiotics except cephalothin and nalidixic acid, where intermediate level resistance was observed (Table 1). SGSC1512 exposed to GW for 6, 12, 18 and 24 hours did not change in resistance to antibiotics except for cephalothin to which the isolates became susceptible after exposure periods of 12, 18, and 24 hours at all IS (with the exception of 30 mM IS exposure at 12 hours). For 6 hours of exposure, SGSC1512 showed decreased susceptibility to cephalothin only at 3.33 mM IS, whereas at 10 and 30 mM IS the isolates remained with intermediate resistance (Table 1).

The control group of the wild type *S. enterica* ser. Typhimurium strain ST5383 showed full susceptibility to all antibiotics except amoxicillin-clavulanic acid and nalidixic acid, for which only intermediate resistance was observed (Table 2). Interestingly, exposure to GW increased the resistance of ST5383 against nalidixic acid for all conditions except for 12 hours at 30 mM IS. ST5383's intermediate resistance to amoxicillin-clavulanic acid decreased to the susceptible level when it was exposed to GW for 24 hours at all IS and after 18 hours at 10 mM IS (Table 2).

The control group of the wild type and non-motile *S. enterica* ser. Pullorum strain SA1685 was susceptible to all tested antibiotics. This strain did not show any changes in its antibiotic resistance profile and remained susceptible to all antibiotics tested for all experimental conditions as shown in Table 3.

Table 1. Antibiotic susceptibility profile of SGSC1512 exposed to different IS (in mM) GW with residual antibiotics for four different time periods. The letters denote the degree of resistance as S; Susceptible, I; Intermediate Susceptible and R; Resistant.

Antibiotic[a]	Control	6 Hours			12 Hours			18 Hours			24 Hours		
		3.33 mM	10 mM	30 mM	3.33 mM	10 mM	30 mM	3.33 mM	10 mM	30 mM	3.33 mM	10 mM	30 mM
AMK30[b]	S	S	S	S	S	S	S	S	S	S	S	S	S
AMC30	S	S	S	S	S	S	S	S	S	S	S	S	S
FOX30	S	S	S	S	S	S	S	S	S	S	S	S	S
CRO30	S	S	S	S	S	S	S	S	S	S	S	S	S
KF30	I	S	I	I	S	S	I	S	S	S	S	S	S
C30	S	S	S	S	S	S	S	S	S	S	S	S	S
CIP5	S	S	S	S	S	S	S	S	S	S	S	S	S
NA30	I	I	I	I	I	I	I	I	I	I	I	I	I
TE30	S	S	S	S	S	S	S	S	S	S	S	S	S
SXT25	S	S	S	S	S	S	S	S	S	S	S	S	S

[a]Antibiotic abbreviations are as follows: Amikacin: (AMK); Amoxicillin-clavulanic acid: (AMC); Cefoxitin: (FOX); Ceftriaxone: (CRO); Cephalothin: KF 30; Chloramphenicol: (C); Ciprofloxacin: (CIP); Nalidixic acid: (NA); Tetracycline: (TE); Trimethoprim-sulfamethoxazole: (SXT).
[b]Numbers denote the concentration (in µg) of the given antibiotic impregnated on 6mm disks.

Table 2. Antibiotic susceptibility profile of ST5383 exposed to different IS (in mM) groundwater (GW) with residual antibiotics compared for four different time periods. The letters denote the degree of resistance as S; Susceptible, I; Intermediate Susceptible and R; Resistant.

Antibiotic[a]	Control	6 Hours			12 Hours			18 Hours			24 Hours		
		3.33 mM	10 mM	30 mM	3.33 mM	10 mM	30 mM	3.33 mM	10 mM	30 mM	3.33 mM	10 mM	30 mM
AMK30[b]	S	S	S	S	S	S	S	S	S	S	S	S	S
AMC30	I	I	I	I	I	I	I	I	S	I	S	S	S
FOX30	S	S	S	S	S	S	S	S	S	S	S	S	S
CRO30	S	S	S	S	S	S	S	S	S	S	S	S	S
KF30	I	I	I	I	I	I	I	I	I	I	I	I	I
C30	S	S	S	S	S	S	S	S	S	S	S	S	S
CIP5	S	S	S	S	S	S	S	S	S	S	S	S	S
NA30	S	I	I	I	I	I	S	I	I	I	I	I	I
TE30	S	S	S	S	S	S	S	S	S	S	S	S	S
SXT25	S	S	S	S	S	S	S	S	S	S	S	S	S

[a]Antibiotic abbreviations are as follows: Amikacin: (AMK); Amoxicillin-clavulanic acid: (AMC); Cefoxitin: (FOX); Ceftriaxone: (CRO); Cephalothin: KF 30; Chloramphenicol: (C); Ciprofloxacin: (CIP); Nalidixic acid: (NA); Tetracycline: (TE); Trimethoprim-sulfamethoxazole: (SXT).
[b]Numbers denote the concentration (in µg) of the given antibiotic impregnated on 6 mm disks.

Table 3. Antibiotic susceptibility profile of SA1685 exposed to different IS (in mM) groundwater (GW) with residual antibiotics compared for four different time periods. The letters denote the degree of resistance as S; Susceptible, I; Intermediate Susceptible and R; Resistant

Antibiotic[a]	Control	6 Hours			12 Hours			18 Hours			24 Hours		
		3.33 mM	10 mM	30 mM	3.33 mM	10 mM	30 mM	3.33 mM	10 mM	30 mM	3.33 mM	10 mM	30 mM
AMK30[b]	S	S	S	S	S	S	S	S	S	S	S	S	S
AMC30	S	S	S	S	S	S	S	S	S	S	S	S	S
FOX30	S	S	S	S	S	S	S	S	S	S	S	S	S
CRO30	S	S	S	S	S	S	S	S	S	S	S	S	S
KF30	S	S	S	S	S	S	S	S	S	S	S	S	S
C30	S	S	S	S	S	S	S	S	S	S	S	S	S
CIP5	S	S	S	S	S	S	S	S	S	S	S	S	S
NA30	S	S	S	S	S	S	S	S	S	S	S	S	S
TE30	S	S	S	S	S	S	S	S	S	S	S	S	S
SXT25	S	S	S	S	S	S	S	S	S	S	S	S	S

[a]Antibiotic abbreviations are as follows: Amikacin: (AMK); Amoxicillin-clavulanic acid: (AMC); Cefoxitin: (FOX); Ceftriaxone: (CRO); Cephalothin: KF 30; Chloramphenicol: (C); Ciprofloxacin: (CIP); Nalidixic acid: (NA); Tetracycline: (TE); Trimethoprim-sulfamethoxazole: (SXT).
[b]Numbers denote the concentration (in µg) of the given antibiotic impregnated on 6 mm disks.

Epithelial cell invasion assay

The number of CFUs for control groups invading HEp2 cells ranged approximately from 300 to 420 (Fig. 1). After exposure to GW for 6 and 12 hours at all IS tested, the number of all *Salmonella* strains invading the epithelial cells lines decreased significantly. The same trend was also observed after 18 hours of exposure to GW for all strains except ST5383 at 10 mM and 33 mM and SGSC1512 at 30 mM IS. Longer exposure periods (i.e. 24 hours) to GW was associated with an increase in the number of bacteria invading the HEp2 cells at all IS, with the exception of 3.33 mM for SGSC1512 and ST5383. The invasiveness of SA1685 exposed to all IS for 24 hours increased significantly compared to the control group (Fig. 1).

Representative images of SGSC1512 strain invading HEp2 cells are presented in Fig. 2.

Viability of Salmonella under stress

The percentages of viable cells of both the control and test groups of all *Salmonella* isolates exposed to 3.33, 10, and 30 mM GW with residual antibiotics for 6, 12, 18, and 24 hours were given in Fig. 3. As can be seen in Fig. 3, viability values of the control groups were determined to be over 90%. Throughout the spectrum of exposure conditions, residual antibiotics did not cause major viability loss; the lowest viability values observed were approximately 85%, 83% and 86% for SGSC1512, ST5383 and SA1685, respectively.

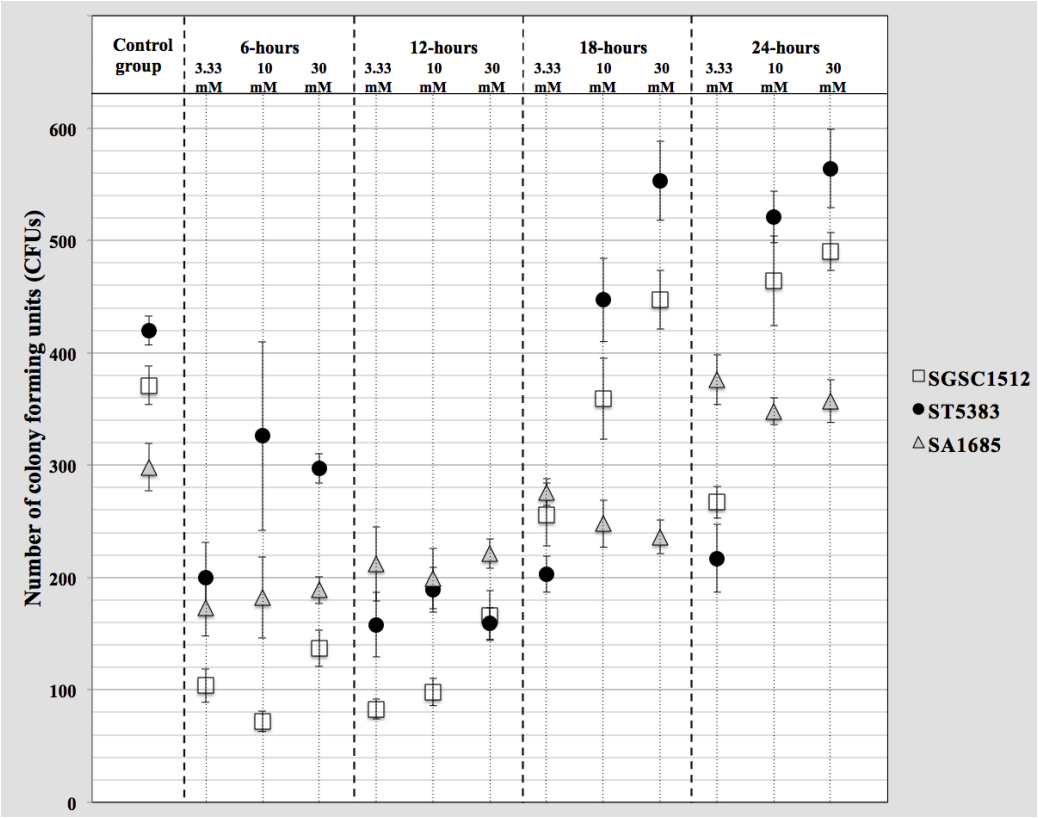

Fig. 1. Changes in the number of *Salmonella* CFUs infecting HEp2 cells upon exposure to GW with residual antibiotics at different IS (in mM) for four different time periods. Data represent average values of three biological replicates and the error bars reflect standard deviations.

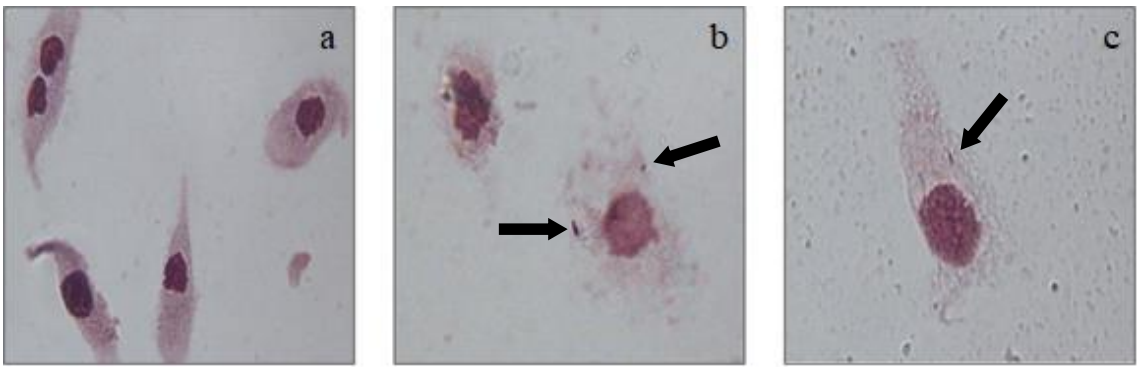

Fig. 2. Representative light microscopy (400×) images of (a) uninfected HEp2 cells and (b,c) HEp2 cells (pointed with the black arrows) infected with SGSC1512.

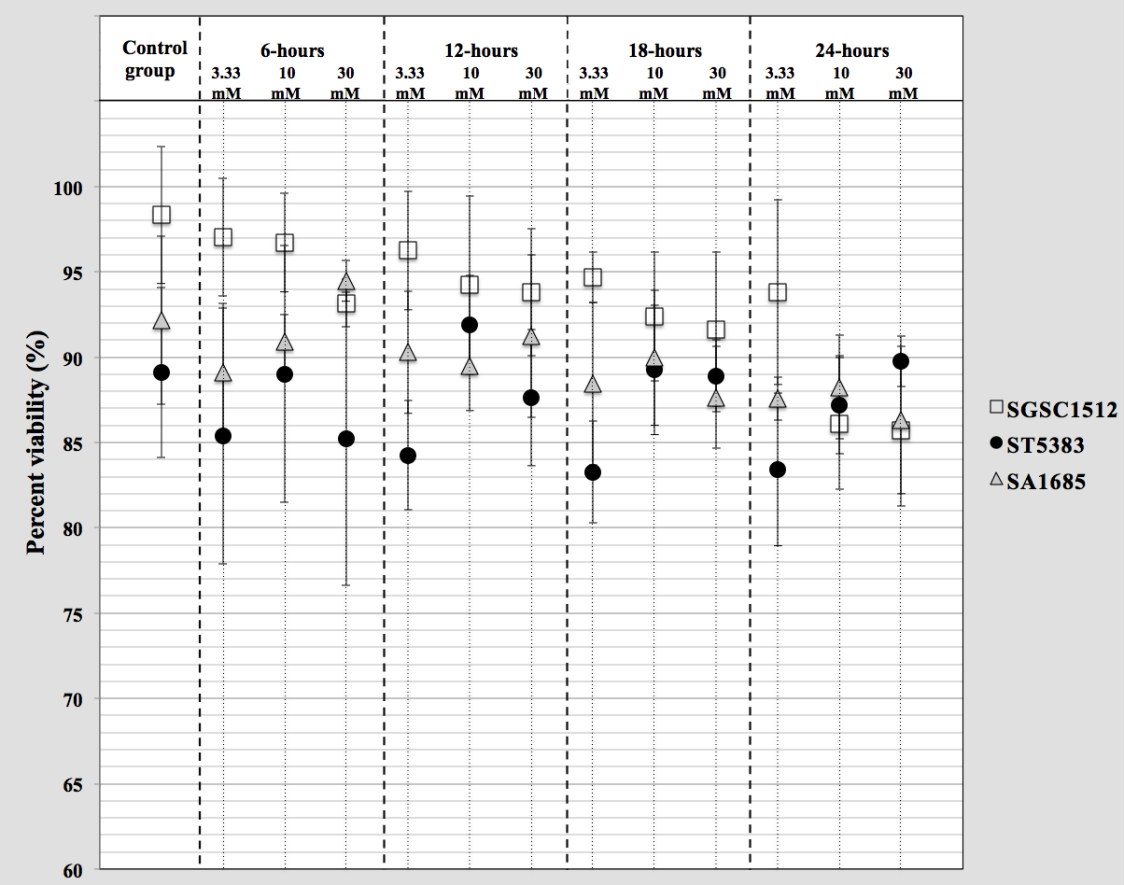

Fig. 3. Changes in the percent viability of *Salmonella* isolates upon exposure to GW with residual antibiotics at different IS (in mM) for four different time periods. Data represent average values of three biological replicates and the error bars reflect standard deviations.

Discussion

In this study, the changes in pathogenicity and viability of outbreak causing *S. enterica* serotypes exposed to groundwater with residual antibiotics were investigated to determine whether this groundwater matrix might impose fitness changes in terms of pathogenicity (invasiveness to target cell lines) and survivability. In addition, different IS conditions were tested to see if any correlation would exist between bacterial efflux pumps (as antibiotic resistance mechanisms) and the external GW environment with varying IS. The results showed increased virulence to be more evident at longer durations (i.e. 24 hours), sustained viability, and strain-dependent decreased antibiotic resistance among *S. enterica* serotypes upon exposure to GW with residual antibiotics. However, no conclusive evidence has been found to link the contribution of efflux pumps to antibiotic resistance of the bacteria under varying IS.

The first organism tested was *S. enterica* ser. Typhimurium strain SGSC1512 with dysfunctional flagella making it a non-motile strain. During exposure to GW, SGSC1512's resistance to cephalothin decreased from an intermediate resistance to a susceptible level for the exposure period of 12 hours and further (with the exception of 30 mM IS exposure at 12 hours). Although cephalothin is a member of the β-lactam class antibiotics, the same trend was not observed for the other β-lactam antibiotics. The influence of efflux pumps (that are likely to be impacted with varying IS of the external environment) on resistance to β-lactams class antibiotics was previously documented in the literature (Lacroix, 1996; Nikaido et al., 1998) but the results of the present study did not confirm this influence. Both the control and the test groups of SGSC1512 showed intermediate levels of susceptibility when tested against nalidixic acid. Nalidixic acid is a quinolone class antibiotic which is normally pumped out of the Gram-negative bacteria cytoplasm via their active efflux pumps. This is in agreement with previous studies showing the effects of efflux pumps mediating reduced quinolone susceptibility in *Salmonella* (Cebrián *et al.* 2005, Chu *et al.* 2005) However, we did not observe an increased resistance in the case of ciprofloxacin, another quinolone antibiotic, most probably due to the slightly different physical and chemical structures of the two drugs, with possible variations in the influx and efflux trends.

The second organism tested was a wild type, outbreak-causing *S. enterica* ser. Typhimurium strain (ST5383). Exposure to GW resulted in increased resistance of the control group from susceptible level to an intermediate resistance for all tested conditions, which was apparent by the statistically significant increased zone diameters at 3.33 mM for 12 hours and at 10 mM for 18 hours against

nalidixic acid. As in the case of resistance profile of SGSC1512, no change was observed against the other quinolone ciprofloxacin for the tested conditions. At longer exposure conditions (i.e. 24 hours for all IS) the intermediate level of resistance of the control group of ST5383 against amoxicillin-clavulanic acid decreased to susceptible levels. The same decrease was also observed at 10 mM GW after 18 hours of exposure. As mentioned earlier, *S. enterica* serotypes shows resistance to β-lactams by the AcrAB efflux system. However, there was no change in the resistance profiles of ST5383 against cefoxitin, ceftriaxone, and cephalothin, all in β-lactam group. This suggest that there is either no direct correlation between the efflux pumps assisting the ST5383 strain to sustain resistance against amoxicillin-clavulanic acid or the fitness of the strain was weakened following the 24 hours GW exposure. Another possibility is the secretion and release of β-lactamases by pathogenic bacteria is a more direct way of mediating the β-lactams. Long-term GW exposure might have negatively impacted the synthesis of β-lactamase in ST5383, which is observed as increased susceptibility.

The last organism tested was *S. enterica* ser. Pullorum strain SA1685, a non-flagellated serovar responsible for avian diseases in the poultry industry. The control group of SA1685 was observed to be susceptible to all antibiotics tested. The exposure of this strain to GW did not cause a change in the antibiotic resistance profile. Since SA1685 is a genotypically and phenotypically different serotype than SGSC1512 and ST5383, this trend might be due to the morphological features and overall fitness of the bacterium and its response to GW stress conditions.

Epithelial cell invasion assay results showed that exposure to GW for 6 and 12 hours resulted in decreased invasiveness of *S. enterica* serotypes into HEp2 cell lines for all tested IS conditions (Fig. 1). In addition, the number of SA1685 that can invade epithelial cells also decreased at all IS for 18 hours of exposure. The number of bacteria that can invade HEp2 cells decreased for 3.33 mM and 10 mM GW, and 3.33 mM for 18 hours of exposure in the cases of SGSC1512 and ST5383, respectively. However, at 24 hours of exposure to GW, increased number of ST5383 and SGSC1512 that can invade the epithelial cells were observed at 10 and 30 mM IS. In the case of SA1685, the number of invading CFU increased for all tested IS for 24 hours of exposure. The decreases in the number of invading bacteria observed up to 18 hours of exposure might be related to the decreased fitness induced by the residual antibiotics in the GW. After 24 hours of exposure, the bacteria might have metabolically become accustomed to the GW matrix, which in return increased the number of invading bacteria. Another possibility is that prolonged exposure to GW with divalent cations such as Ca^{2+} in this case may have contributed to the increased number of CFUs infecting HEp2 cells, which is in parallel to previous studies that showed increased invasion of human cell lines with increased Ca^{2+} concentrations (Niesel & Peterson 1987, Peterson 1988).

In conclusion, although the occurrence of residual antibiotics in groundwater systems is common, there is very limited knowledge on the effects of these antibiotics on the fitness levels of pathogenic bacteria with respect to their pathogenicity and survivability. In this initial study, outbreak-causing *S. enterica* serotypes with different morphologies were exposed to groundwater conditions with residual antibiotics to test for any changes in invasiveness against human cell lines. Their viabilities were also monitored. In addition, as an ion-rich environment, groundwater may affect the active efflux pumps of bacteria, which in turn change their resistance profiles against certain antibiotic classes. The results showed that relatively short-term exposure to residual antibiotics at μg per liter levels will not decrease viabilities, but may still induce increased invasiveness of *S. enterica* serotypes into human epithelial cell lines, which was more evident at 24 hours of exposure in the present conditions. Although there was no clear evidence to link the efflux pump mediated antibiotic resistance to different concentrations of ions tested in this study, subtle changes in resistance profiles were observed in certain quinolone and β-lactam class antibiotics. Further analyses might elaborate these findings to investigate the fate of *S. enterica* serotypes in groundwater settings.

References

1. Abouzeed, Y.M., Baucheron, S. & Cloeckaert, A. 2008. Ramr mutations involved in efflux-mediated multidrug resistance in *Salmonella enterica* serovar *Typhimurium. Antimicrobial Agents and Chemotherapy*, 52 (7): 2428-2434.
2. Barber, L.B., Keefe, S.H., LeBlanc, D.R., Bradley, P.M., Chapelle, F.H., Meyer, M.T., Loftin, K.A., Kolpin, D.W. & Rubio, F. 2009. Fate of sulfamethoxazole, 4-nonylphenol, and 17β-estradiol in groundwater contaminated by wastewater treatment plant effluent. *Environmental Science & Technology*, 43 (13): 4843-4850.
3. Barnes, K.K., Kolpin, D.W., Furlong, E.T., Zaugg, S.D., Meyer, M.T. & Barber, L.B. 2008. A national reconnaissance of pharmaceuticals and other organic wastewater contaminants in the United States - i) groundwater. *Science of The Total Environment*, 402 (2-3): 192-200.
4. Bezanson, G.S., Khakhria, R., Duck, D. & Lior, H. 1985. Molecular analysis confirms food source and simultaneous involvement of two distinct but related subgroups of *Salmonella typhimurium* bacteriophage type 10 in major interprovincial Salmonella outbreak. *Applied and Environmental Microbiology*, 50 (5): 1279-1284.
5. Bolster, C.H., Mills, A.L., Hornberger, G.M. & Herman, J.S. 1999. Spatial distribution of deposited bacteria following miscible displacement experiments in intact cores. *Water Resources Research*, 35 (6): 1797-1807.
6. Bradford, P.A. & Dean, C.R. 2008. Resistance of gram-negative bacilli to antimicrobials, In: Fong, I.W. &

Drlica, K. (eds) *Antimicrobial resistance and implications for the 21st century*, Springer, New York, NY, USA, 135 pp.

7. Burnham, C.A.D., Shokoples, S.E. & Tyrrell G.J. 2007. Invasion of Hela cells by group b *Streptococcus* requires the phosphoinositide-3-kinase signalling pathway and modulates phosphorylation of host-cell akt and glycogen synthase kinase-3. *Microbiology*, 153 (12): 4240-4252.

8. Cebrián, L., Rodríguez, J.C., Escribano, I. & Royo, G. 2005. Characterization of *Salmonella spp.* mutants with reduced fluoroquinolone susceptibility: Importance of efflux pump mechanisms. *Chemotherapy*, 51 (1): 40-43.

9. Centers for disease control and prevention (CDC) - *Salmonella* outbreaks. (http://www.cdc.gov/salmonella /outbreaks.html), (Date accessed 10 May 2018).

10. Centers for disease control and prevention (CDC). Investigation of outbreak of infections caused by *Salmonella typhimurium*. (http://www.cdc.gov/salmonella/typhimurium /map.html), (Date accessed 10 May 2018).

11. Chopra, I. & Roberts, M. 2001. Tetracycline antibiotics: Mode of action, applications, molecular biology, and epidemiology of bacterial resistance. *Microbiology and Molecular Biology Reviews*, 65 (2): 232-260.

12. Chu, C., Su, L.H., Chu C.H., Baucheron, S., Cloeckaert, A. & Chiu, C.H. 2005. Resistance to fluoroquinolones linked to gyra and parc mutations and overexpression of acrab efflux pump in *Salmonella enterica* serotype *Choleraesuis. Microbial Drug Resistance*, 11 (3): 248-253.

13. Clinical and Laboratory Standards Institute (CLSI) / National Committee for Clinical Laboratory, 2003. *Performance standards for antimicrobial disk and dilution susceptibility tests for bacteria isolated from animals*, 107 pp.

14. Crane, S.R. & Moore, J.A. 1984. Bacterial pollution of groundwater: A review. *Water, Air, & Soil Pollution*, 22 (1): 67-83.

15. Giraud, E., Cloeckaert, A., Kerboeuf, D. & Chaslus-Dancla, E. 2000. Evidence for active efflux as the primary mechanism of resistance to ciprofloxacin in *Salmonella enterica* serovar *Typhimurium. Antimicrobial Agents and Chemotherapy*, 44 (5): 1223-1228.

16. Hutson, S.H., Barber, N.L., Kenny, J.F., Linsey, K.S., Lumia, D.S. & Maupin, M.A. 2004. *Estimated use of water in the United States in 2000*, in *U.S. Geological Survey Circular*. U.S. Geological Survey, Virginia, USA, 52 pp.

17. Kumar, A & Schweizer, H.P. 2005. Bacterial resistance to antibiotics: Active efflux and reduced uptake. *Advanced Drug Delivery Reviews*, 57 (10): 1486-1513.

18. Kunihiko Nishino, T.L. & Groisman, E.A. 2006. Virulence and drug resistance roles of multidrug efflux systems of *Salmonella enterica* serovar *Typhimurium. Molecular Microbiology*, 59 (1): 126-141.

19. Lacroix, F.J., Cloeckaert, A., Grépinet, O., Pinault, C., Popoff, M.Y., Waxin, H. & Pardon, P. 1996. *Salmonella typhimurium* acrb-like gene: Identification and role in resistance to biliary salts and detergents and in murine infection. *FEMS Microbiology Letters*, 135 (2-3): 161-167.

20. Niesel, D.W. & Peterson, J.W. 1987. Calcium enhances *Salmonella typhimurium* invasion of Hela cells. *FEMS Microbiology Letters*, 41 (3): 299-304.

21. Nikaido, H., Basina, M., Nguyen, V. & Rosenberg, E.Y. 1998. Multidrug efflux pump acrab of *Salmonella typhimurium* excretes only those beta-lactam antibiotics containing lipophilic side chains. *Journal of Bacteriology*, 180 (17): 4686-4692.

22. Orth, P., Schnappinger, D., Hillen, W., Saenger, W. & Hinrichs, W. 2000. Structural basis of gene regulation by the tetracycline inducible Tet repressor-operator system. *Nature Structural & Molecular Biology*, 7 (3): 215-219.

23. Peterson, J.W. & Niesel, D.W. 1988. Enhancement by calcium of the invasiveness of *Salmonella* for Hela cell monolayers. *Reviews of Infectious Diseases*, 10(Supplement 2): 319-322.

24. Piddock, L.J.V., White, D.G., Gensberg, K., Pumbwe, L. & Griggs, D.J. 2000. Evidence for an efflux pump mediating multiple antibiotic resistance in *Salmonella enterica* serovar *Typhimurium. Antimicrobial Agents and Chemotherapy*, 44 (11): 3118-3121.

25. Poole, K. 2000. Efflux-mediated resistance to fluoroquinolones in gram-negative bacteria. *Antimicrobial Agents and Chemotherapy*, 44 (9): 2233-2241.

26. Quinn, T., O'Mahony, R., Baird, A.W., Drudy, D., Whyte, P. & Fanning, S. 2006. Multi-drug resistance in *Salmonella enterica*: Efflux mechanisms and their relationships with the development of chromosomal resistance gene clusters *Current Drug Targets*, 7 (7): 849-860.

27. Roberts, M. 1996. Tetracycline resistance determinants: Mechanisms of action, regulation of expression, genetic mobility, and distribution. *FEMS Microbiology Reviews*, 19 (1): 1-24.

28. Schmoll, O., Howard, G., Chilton, J. & Chorus, I. 2006. *Protecting groundwater for health*. IWA Publishing, Cornwall, UK, 698 pp.

29. Vugia, D.J., Samuel, M., Farley, M.M., Marcus, R., Shiferaw, B., Shallow, S., Smith, K. & Angulo, F.J. 2004. Invasive salmonella infections in the United States, FoodNet, 1996–1999: Incidence, serotype distribution, and outcome. *Clinical Infectious Diseases*, 38 (Supplement 3): 149-156.

30. Vulliet, E. & Cren-Olivé, C. 2011. Screening of pharmaceuticals and hormones at the regional scale, in surface and groundwaters intended to human consumption. *Environmental Pollution*, 159 (10): 2929-2934.

31. Yamaguchi, A., Kimura, T., Someya, Y. & Sawai, T. 1993. Metal-tetracycline/h+ antiporter of *Escherichia coli* encoded by transposon tn10. The structural resemblance and functional difference in the role of the duplicated sequence motif between hydrophobic segments 2 and 3 and segments 8 and 9. *Journal of Biological Chemistry*, 268 (9): 6496-6504.

32. Yamaguchi, S., Aizawa, S., Kihara, M., Isomura, M., Jones, C.J. & Macnab, R.M. 1986. Genetic evidence for a switching and energy-transducing complex in the flagellar motor of *Salmonella typhimurium. Journal of Bacteriology*, 168 (3): 1172-1179.

http://dergipark.gov.tr/trkjnat
Trakya University Journal of Natural Sciences, 20(1): 9-17, 2019
ISSN 2147-0294, e-ISSN 2528-9691
DOI: 10.23902/trkjnat.454020

Research Article

THE EFFECTS OF VITAMIN C ON GLYCIDAMIDE-INDUCED CELLULAR DAMAGE AND APOPTOSIS IN MOUSE LEYDIG CELLS

Banu ORTA YILMAZ

İstanbul University, Faculty of Science, Department of Biology, 34134, Vezneciler, İstanbul, TURKEY
ORCID ID: orcid.org/ 0000-0002-8006-1107, e-mail: banu.yilmaz@istanbul.edu.tr

Cite this article as:

Orta Yılmaz, B. 2019. The Effects of Vitamin C on Glycidamide-Induced Cellular Damage and Apoptosis in Mouse Leydig Cells. *Trakya Univ J Nat Sci*, 20(1): 9-17, DOI: 10.23902/trkjnat.454020

Received: 16 August 2018, Accepted: 21 December 2018, Online First: 03 January 2019, Published: 15 April 2019

Abstract: The aim of this study was to elucidate the role of vitamin C on glycidamide-induced cytotoxicity, oxidative damage and cell death in Leydig (TM3) cells. Leydig cells were exposed to glycidamide (1, 10, 100 and 1000 μM) and/or vitamin C (50 μM) for 24 h. After completion of the exposure time, cell viability, amount of lactate dehydrogenase enzyme, apoptosis-necrosis rates, levels of oxidative stress parameters such as hydroxyl radical, hydrogen peroxide and lipid peroxidation were determined in Leydig cells. The results showed that glycidamide administration decreased Leydig cell viability and increased cytotoxicity significantly at high concentration (1000 μM). In addition, glycidamide generated oxidative damage by significantly increasing the production of reactive oxygen species and lipid peroxidation. Exposure to glycidamide increased the formation of early apoptosis, apoptosis and necrosis in Leydig cells. Consequently, glycidamide has been shown to cause apoptosis due to lipid peroxidation and formation of reactive oxygen species in Leydig cells, and vitamin C has a therapeutic role against toxicity caused by glycidamide.

Key words: Glycidamide, cytotoxicity, apoptosis, oxidative stress, Vitamin C, Leydig cell.

Özet: Bu çalışmanın amacı, C vitamininin Leydig (TM3) hücrelerinde glisidamid kaynaklı sitotoksisite, oksidatif stres ve apoptoz üzerindeki rolünü ortaya çıkarmaktır. Leydig hücreleri 24 saat boyunca glisidamid (1, 10, 100 ve 1000 μM) ve / veya C vitamini (50 μM) ile muamele edilmiştir. Deney süresinin tamamlanmasından sonra, Leydig hücrelerinde hücre canlılığı, laktat dehidrogenaz enzimi miktarı, apoptoz-nekroz oranları, hidroksil radikali, hidrojen peroksit ve lipit peroksidasyonu gibi oksidatif stres parametrelerinin seviyeleri belirlendi. Sonuçlar glisidamid uygulamasının yüksek konsantrasyonda (1000 μM) önemli ölçüde Leydig hücre canlılığını azalttığını ve sitotoksisitenin arttığını gösterdi. Ayrıca, glisidamid reaktif oksijen türlerinin ve lipid peroksidasyonunun üretimini önemli ölçüde arttırarak oksidatif hasara yol açmıştır. Glisidamide maruz kalma, Leydig hücrelerinde erken apoptoz, apoptoz ve nekroz oluşumunu artırmıştır. Sonuç olarak, glisidamid lipit peroksidasyonuna ve Leydig hücrelerinde reaktif oksijen türlerinin oluşmasına bağlı apoptosise neden olmuş, C vitamininin ise glisidamidin neden olduğu toksisiteye karşı iyileştirici bir rolü olduğu gösterilmiştir.

Introduction

Acrylamide is produced when vegetal products with high carbohydrate and low protein content are exposed to elevated temperatures (e.g. 120°C and above) during thermal processes such as cooking (Mottram *et al*. 2002, Stadler *et al*. 2002). Food products are the leading sources of acrylamide, and the food with the highest acrylamide content are potato chips, fast food products (hamburgers, all fried sandwiches), fried potatoes, fried bread, biscuits, breakfast cereals, bakery products, instant soups and coffee (Friedman 2015). Acrylamide is used in the enhancement of drinking and wastewater, the production of adhesives in the cosmetic sector, as a filling substance in dentistry, and in the production of paper, photography film and polyester (Lingnert *et al*. 2002, Taeymans *et al*. 2004). Tobacco smoke also serves as a source of acrylamide (Vattem & Shetty 2003). Studies on various experimental organisms have led to acrylamide being classified as a chemical with a serious toxicity profile. The International Agency for Research on Cancer (IARC) classified acrylamide as a Group 2A compound, which refers to compounds with potential carcinogenic effects in humans (IARC 1994). The United Nations Food and Agriculture Organization (FAO) and the World Health Organization (WHO) also classify acrylamide as a toxic substance with potential carcinogenic and teratogenic effects on humans that can be absorbed through the skin and can cause harm in the nervous and reproductive systems (WHO 2002).

Acrylamide is metabolized in the body via the CYP2E1 enzyme and converted to glycidamide, an epoxide derivative. (Fennel *et al*. 2005). In terms of its chemical activity, glycidamide is a more reactive (70%) compound than acrylamide, showing a high level of interaction with hemoglobin, and particularly with DNA

molecule (Paulsson *et al*. 2002, Martins *et al*. 2006). Previous studies reported that glycidamide plays a leading role in the development of the effects of acrylamide on the reproductive system (Li *et al*. 2017, Yilmaz *et al*. 2017, Sun *et al*. 2018). Studies performed on males of various animal models suggested that acrylamide exposure caused an atrophy of the seminiferous tubules in the testes, multiple nuclei formation, vacuolization, apoptosis of cell, aberration of sperm chromosomes, decreased sperm viability and abnormal giant cell formation, as well as impairment in spermatogenesis (Wang *et al*. 2010, Hamdy *et al*. 2012, Sen *et al*. 2015, Wang *et al*. 2015). Although there are studies on the toxic mechanism of acrylamide on various cells in the testes and the reproductive system, studies on the glycidamide, an epoxide derivative known to be more toxic than acrylamide, are low in number. Therefore, the direct mechanism(s) by which glycidamide performs toxicity in the testes has not been fully understood.

Various antioxidants are required to minimize the negative health effects of exposure to different toxic compounds. Vitamin C is distributed around the body and has a strong antioxidant effect in the neutralization of free radicals (Baba *et al*. 2013). Vitamin C enters the body predominantly through diet, with natural vitamin C sources including citrus fruits, rosehip, green walnut, cabbage, tomato, red and green pepper and all green leaved vegetables (Levine *et al*. 1999). It has been reported that vitamin C has anti-oxidative, anti-proliferative and anti-inflammatory capacities (Padayatty *et al*. 2003). It also plays a protective role against oxidative stress, stimulates cell division and reproduction, protects sperm from harmful oxidative processes and improves fertility (Das *et al*. 2002, Chang *et al*. 2007, Orta & Erkan 2014).

Leydig cells, characterized by their high hormonal activity, are over-specialized somatic cells found in interstitial area of testes (Haider 2004). The main function of Leydig cells is to synthetize and release testosterone, and they are the target of toxic substances that affect the reproductive system. In the present study, Leydig cells were used as an *in vitro* model to investigate the direct mechanisms underlying the toxic effects of glycidamide in the testes. Therefore, we aimed to evaluate the toxicity caused by glycidamide on Leydig cells, focusing on the changes in cytotoxicity, oxidative damage and apoptosis/necrosis levels. We also investigated whether vitamin C played a protective role in this damage.

Materials and Methods

Cell Culture and Treatment

The TM3 Leydig cell line was obtained from the American Type Culture Collection (ATCC): The Global Bioresource Center and was grown *in vitro* conditions. A cell culture medium containing 50:50 DMEM-F12 (Dulbecco's Modified Eagle Medium, nutrient mix F12 Ham medium) supplemented with 5% horse serum, 2.5% fetal bovine serum, 2.5 mM l-glutamine, 0.5 mM sodium pyruvate, 1.2 g / L Sodium Bicarbonate, 15 mM HEPES and 1% penicillin-streptomycin-amphoterin mixture was used. Cells were incubated in sterile conditions at 37°C in an incubator with 5% CO_2 and 95% air. Glycidamide (GA, Sigma Chemical Company) was dissolved in medium containing 1% horse serum for administration to the cells to obtain a 10 mM stock solution. Different concentrations of glycidamide were prepared from this stock solution by diluting with medium containing 1% horse serum. In the experiments, the concentration of vitamin C was 50 μM, which is the average antioxidant concentration *in vitro*. The vitamin C (VitC) was dissolved in 1% horse serum and was prepared freshly.

Cytotoxicity

Cell Viability Assay

The 3-(4,5-dimethylthiazol-2-yl)-2,5-diphenyltetrazolium bromide (MTT) colorimetric assay (Roche Diagnostics GmbH, Mannheim, Germany) was used to determine the viability of the cells. The viability of the control cells not exposed to the test substance GA was accepted as 100%. After 24 h of incubation with GA, maximal inhibitor concentrations of 50% (IC_{50}) for cell number reduction were calculated. Based on the calculations, GA concentrations of 1, 10, 100 and 1000 μM were selected for use in further experiments.

Lactate Dehydrogenase (LDH) Assay

The amount of lactate dehydrogenase enzyme was determined using the Cytotoxicity Detection Kit (Roche Diagnostics GmbH, Mannheim, Germany) from cell supernatants of cells exposed with GA. The kit procedure was applied individually, and the results were measured with ELISA reader device at 492 nm. The cytotoxicity of the control cells not exposed with the test substance was accepted as 100%.

Measurement of Lipid Peroxidation and Reactive Oxygen Species

For biochemical experiments, cells were seeded to ($1x10^6$) six-well plates per well. After 24 hours of application of GA and vitamin C, the cells were sonicated in Tris-HCl buffer (pH: 7.2) with an ultrasonicator. After the resulting cell suspension was centrifuged at 14,000 g in a refrigerated centrifuge, the supernatants were collected and the lipid peroxidation, hydroxyl radical and hydrogen peroxide (H_2O_2) measurements were performed.

The amount of lipid peroxidation was measured according to the method of Devasagayam & Tarachand (1987). As is the case in this method, the formation of malondialdehyde (MDA) in the presence of thiobarbituric acid was calculated by measuring the absorbance with the spectrophotometer at 532 nm.

Levels of hydroxyl radical was determined according the method of Puntarulo & Cederbaum (1988). This method is based on the formation of a formaldehyde by hydroxyl radical. Formaldehyde gives an absorbance at 570 nm with trichloroacetic acid (TCA).

Holland & Storey (1981) method was used for determination of amounts of H_2O_2. The amounts of H_2O_2 resulting from the oxidation of the acidified ferrocytochrome c were measured with a spectrophotometer at 550 nm.

Detection of apoptosis and necrosis

Hoechst 33342 (HO342) was used to determine apoptosis in cells and Propidium iodide (PI) fluorescence labeling method was used to determine necrosis. HO342 fluorescent dye marks apoptotic cells in purple color, while PI fluorescent dye passes through the weak cell membrane of necrotic cells and marks the cell in red color. The combination of these dyes makes it possible to distinguish viable, early apoptotic, apoptotic and necrotic cell populations with fluorescence microscopy. Cells were seeded in culture well-plates as 10^4 cells per well. After 24 hours of glycidamide and vitamin C administration, the cells were washed with phosphate-buffered solution (PBS) and incubated with PI (1 mg/ml PI) and HO342 (1 mg/ml Hoechst 33342) solutions for 20 min at 37°C. When the experiment was completed, the cells were washed with PBS and examined under fluorescent microscope (Olympus IX71, New York, USA) equipped with UV filter and photographed in equal intervals with a digital camera (Olympus DP72, New York, USA). For each group, the fluorescence-emitting cells were counted separately, and the mean percentage values were calculated. For each group, viable, early apoptotic, apoptotic and necrotic cells were counted by screening 10-15 sites and 1000 cells in 12 wells in three different experiments.

Statistical analysis

All experimental data were analyzed with one-way ANOVA, followed by Tukey post-hoc test using the software program GraphPad Prism Version 5.0 (GraphPad Software, San Diego, CA, USA). All values were expressed as mean ± standard error mean. Shapiro-Wilk test was used as the normality test and the significance was accepted as $p<0.001$, $p<0.01$ and $p<0.05$.

Results

Effects of GA and GA+VitC on Cytotoxicity

The MTT test was carried out to determine the effects of ten different glycidamide concentrations on 24-hour cell viability of Leydig cells. Figure 1 (one-way ANOVA; $F_{0.95}(10,66)=267.1$; $p<0.001$) shows cell viability rates (%) in the control and experimental groups. When the MTT values of the experimental groups were compared with that of the control group, significant reductions were noted in the groups exposed to glycidamide at concentrations of 5 μM and higher ($p<0.05$, $p<0.01$ and $p<0.001$). Fifty percent inhibition concentration (IC_{50}) of glycidamide was calculated according to MTT results for 24 h and the IC_{50} value for glycidamide in Leydig cells was found to be 872.4 μM.

Glycidamide concentrations that reduced cell viability to 94.61% (1 μM GA), 92.29% (10 μM GA), 78.30% (100 μM GA) and 42.34% (1000 μM GA) were selected and treated with vitamin C (50 μM). The MTT value of the control group was compared with four different glycidamide concentration groups selected and the concentration groups formed with the addition of vitamin C (Fig. 2; one-way ANOVA; $F_{0.95}(9,70)=24.43$; $p<0.0001$). The comparisons revealed significant reduction in cell viability in the groups exposed to glycidamide at concentrations of 10 μM and above, and in combined groups of 100 and 1000 μM concentrations treated with vitamin C ($p<0.05$ and $p<0.001$). When the groups treated with vitamin C were compared only with the glycidamide groups, vitamin C was found to significantly increase cell viability at a glycidamide concentration of 1000 μM ($p<0.05$).

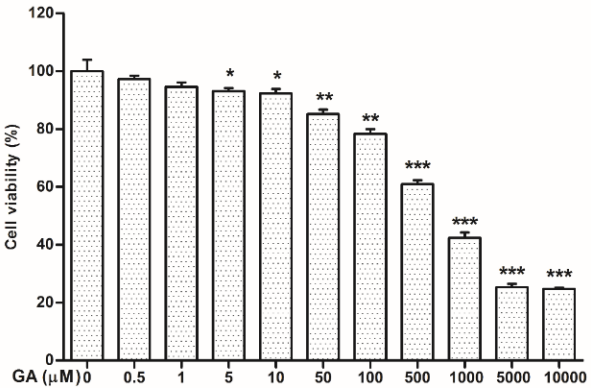

Fig. 1. The viability of TM3 Leydig cells exposed to various concentrations of GA. *p<0.05, **p<0.01 and ***p<0.001, (*) compared with control.

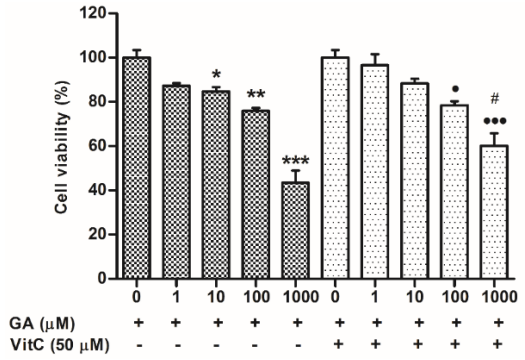

Fig. 2. Effects of glycidamide and vitamin C on cell viability of TM3 Leydig cells *in vitro*. *p<0.05, ** p<0.01 and ***p<0.001. (*) comparison with the control group, (•) comparison with Vit C combination and (#) comparison with glycidamide alone group.

Concentration-dependent changes in LDH levels in the control and experimental groups in TM3 Leydig cells are given in Fig. 3 (one-way ANOVA; $F_{0.95}(9,69)=22.21$; $p<0.0001$). When the LDH levels of the control group and the groups exposed to four different glycidamide concentrations were compared after 24 hours, a significant increase was noted at 1000 μM glycidamide concentration ($p<0.001$). On the other hand, the comparison of LDH levels of the control group with the groups formed with addition of Vitamin C revealed a

significant reduction only in the 1000 µM glycidamide concentration group ($p<0.001$).

Effects of GA and GA+VitC on Lipid Peroxidation and Reactive Oxygen Species

Figure 4A shows the lipid peroxidation values in TM3 Leydig cells of the control and experimental groups, as estimated after 24 hours through the use of spectrophotometric methods. The comparison of the MDA values of the control group with those of four different glycidamide concentration groups revealed significant increase for concentrations of 10 µM and above ($p<0.001$). In the groups treated with vitamin C, significant reductions were noted in glycidamide concentrations of 10 µM and above when compared to the groups not treated with vitamin C ($p<0.001$) (Fig 4A; one-way ANOVA; $F_{0.95}(9,69)=25.34$; $p<0.0001$).

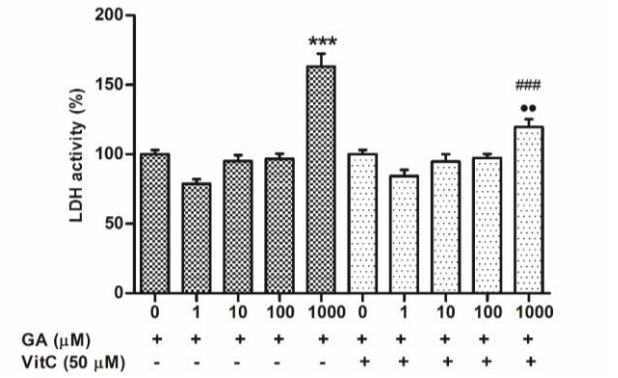

Fig. 3. Effects of glycidamide and vitamin C on lactate dehydrogenase activity of TM3 Leydig cells *in vitro*. *p<0.05, ***p<0.001. (*) comparison with the control group, (•) comparison with VitC addition and (#) comparison with glycidamide alone group.

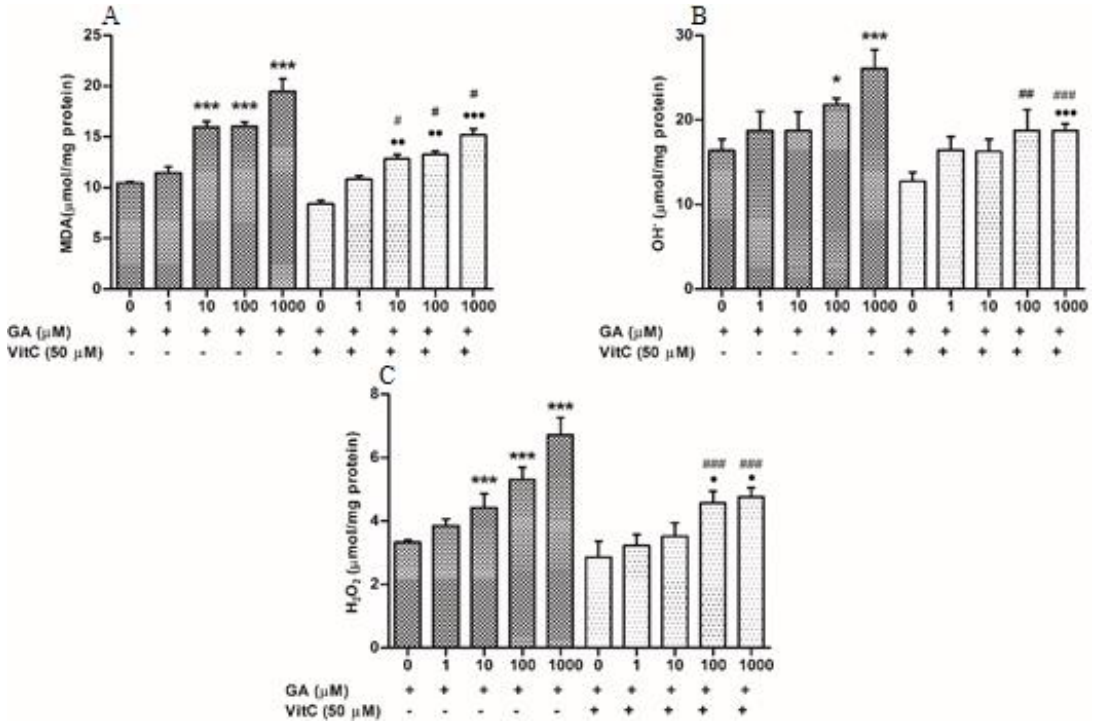

Fig. 4. Effects of glycidamide and vitamin C on lipid peroxidation (A), hydroxyl radical (B) and hydrogen peroxide (C) levels in TM3 Leydig cells *in vitro*. *p<0.05, **p<0.01 and ***p<0.001. (*) comparison with the control group, (•) comparison with VitC addition and (#) comparison with glycidamide alone group.

Table 1. Effects of GA and GA+VitC on viable cell, early apoptosis, apoptosis and necrosis of TM3 Leydig cells.

	Concentrations	Viable Cell	Early Apoptosis	Apoptosis	Necrosis
GA groups	**0**	97.4±0.4	1.6±0.3	0.7±0.1	0.3±0.01
	1 µM	90.3±0.7	8.3±0.6*	0.8±0.1	0.6±0.02
	10 µM	87.8±1.8**	10.3±1.5***	1.8±0.3***	0.1±0.3
	100 µM	75.9±0.4***	19.6±0.2***	4.2±0.1***	0.3±0.2
	1000 µM	42.3±2.0***	33.8±1.3***	10.2±0.5***	13.7±1.1***
GA+VitC groups	**0**	98.1±0.1	1.7±0.2	0.1±0.1	0.1±0.06
	1 µM	97.2±0.5 #	2.4±0.3 #	0.1±0.1	0.3±0.04
	10 µM	95.1±0.4 #	4.1±0.4• #	0.3±0.1#	0.5±0.06
	100 µM	84.3±1.1••• #	13.5±0.8••• #	1.8±0.3•• #	0.4±0.07
	1000 µM	64.5±2.0••• #	29.1±1.8••• #	4.1±1.0•• #	2.3±1.1• #

* p<0.05, **p<0.01, ***p<0.001. (*) comparison with the control group, (•) comparison with VitC addition and (#) comparison with glycidamide alone group. Viable cell (one-way ANOVA; $F_{0.95}(9,45)=58.31$; $p<0.0001$), early apoptosis (one-way ANOVA; $F_{0.95}(9,36)=15.33$; $p<0.0001$), apoptosis (one-way ANOVA; $F_{0.95}(9,45)=12.14$; $p<0.0001$) and necrosis (one-way ANOVA; $F_{0.95}(9,45)=8.822$; $p<0.0001$).

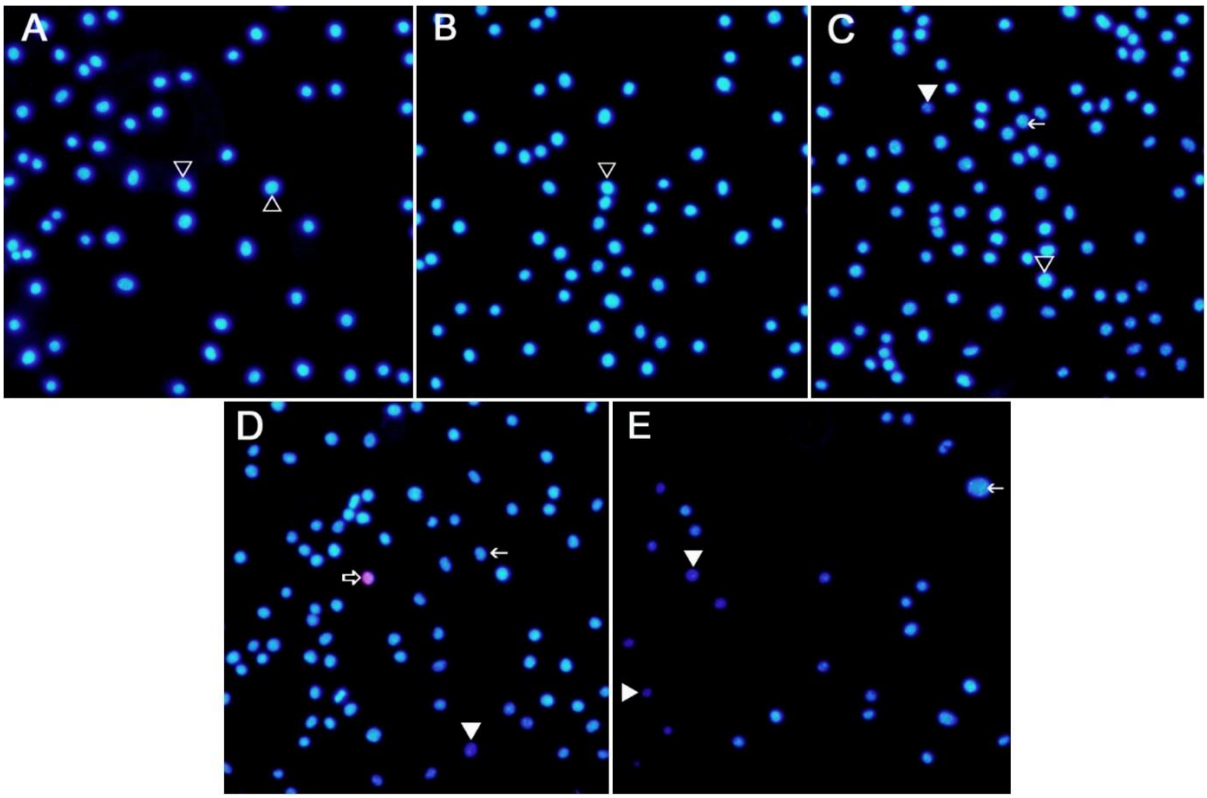

Fig. 5. Early apoptosis, apoptosis, necrosis findings in 24 h glycidamide exposure in TM3 Leydig cells. (A) Control, (B) 1 µM GA, (C) 10 µM GA, (D) 100 µM GA, (E) 1000 µM GA; ▽: viable cell, ←: early apoptosis, ▼: apoptosis, ⇨: necrosis. GA: Glycidamide. (10X magnification).

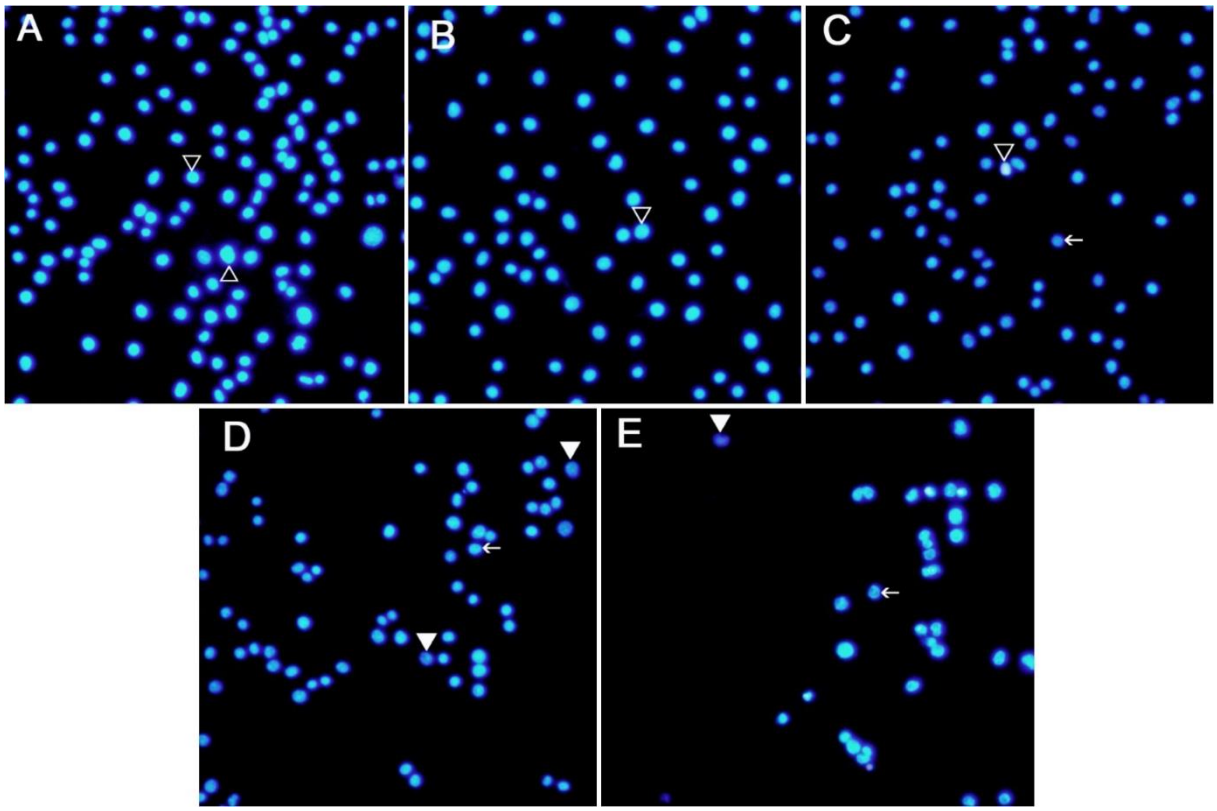

Fig. 6. Early apoptosis, apoptosis, necrosis findings in 24 h glycidamide and vitamin C exposure in TM3 Leydig cells. (A) Vitamin C, (B) 1 µM GA+VitC, (C) 10 µM GA+VitC, (D) 100 µM GA+VitC, (E) 1000 µM GA+VitC; ▽: viable cell, ←: early apoptosis, ▼: apoptosis, ⇨: necrosis. GA: Glycidamide, VitC: Vitamin C. (10X magnification).

When the levels of hydroxyl radicals in TM3 Leydig cells of the control and glycidamide groups were compared after 24 hours, significantly higher increases were noted in the glycidamide concentrations of 100 and 1000 μM ($p<0.05$ and $p<0.001$) (Fig.4B; one-way ANOVA; $F_{0.95}(9,81)=4.129$; $p<0.0002$). When the levels of hydroxyl radicals of the control group, four different glycidamide concentration groups and the groups treated with vitamin C were compared, significantly higher reductions were noted in the glycidamide concentrations of 100 and 1000 μM in vitamin C treated groups ($p<0.01$ and $p<0.001$).

Hydrogen peroxide levels in control and GA-exposed TM3 Leydig cells. were given in Fig. 4C. The comparison of hydrogen peroxide levels in the control and glycidamide groups after 24 hours showed significant increases in the concentration groups of 10 μM and above ($p<0.001$). When the hydrogen peroxide levels of the GA and GA+VitC groups were compared, significant decreases were detected in the 100 and 1000 μM glycidamide concentration groups treated with vitamin C ($p<0.001$) (Fig 4C; one-way ANOVA; $F_{0.95}(9,80)=9.125$; $p<0.0001$).

Apoptosis and necrosis rate in TM3 Leydig cells exposed to GA and GA+VitC

When the percentages of viable, early apoptotic, apoptotic and necrotic cells were compared, significant differences were observed in the glycidamide-treated groups when compared to the control groups (Table 1, Figs. 5-6). According to the results of fluorescence emission, the morphological changes observed in the experimental groups have the following characteristics: i) viable cells have highly organized nuclei and appear bright blue, ii) early apoptotic cells have nuclear condensation and appear blue, iii) apoptotic cells have highly nuclear condensation, fragmentation and appear dull blue to purple, iv) necrotic cells have no chromatin fragmentation and appear red.

Discussion

Studies on acrylamide showed that exposure is not solely related to diet, as it may also result from environmental sources. This has led to an increase in number of studies worldwide investigating acrylamide levels in both food and environmental sources. The direct or indirect intake of acrylamide into the body can cause various changes in cells which are known to be a highly dynamic system. Glycidamide, a major epoxide metabolite of acrylamide, possesses greater cytotoxicity and genotoxicity than acrylamide (Martins *et al*. 2006). Despite a limited number of studies conducted on acrylamide, there is still a need for more laboratory data concerning the toxicity of glycidamide. Thus, it has been demonstrated that glycidamide, a molecule that can enter the body via food, has a toxic effect on the functions of Leydig cells in the reproductive system, and this negative effect can be reduced with natural antioxidants.

Previous studies investigated the effects of acrylamide and glycidamide on viability of various cell lines. The administration of glycidamide on human breast epithelial cell line at concentrations of 1 mM, 2 mM, 3 mM and 4 mM for 24 hours was found to significantly reduce cell viability (Bandarra *et al*. 2013). Studies showed that acrylamide significantly reduced cell viability when applied to human astrocytoma cells and rat astrocyte cells at concentrations of 0.1 mM, 0.5 mM, 1 mM and 2 mM (Chen *et al*. 2013, Lee *et al*. 2014). Baum *et al.* (2005) conducted a study on V79 cells and human blood and determined that acrylamide was not cytotoxic at concentrations below 5000 μM, while glycidamide was cytotoxic at concentrations of 800 μM and above, with an LC_{50} concentration of 2000 μM for glycidamide. Another study investigating the toxic effects of glycidamide on RC2 Leydig cells found that glycidamide significantly reduced cell viability, with IC_{25}, IC_{50} and IC_{75} values being calculated as 0.635, 0.872 and 1.198 mM, respectively (Li *et al.* 2017). Many *in vivo* studies demonstrating the toxic effects of acrylamide on the male reproductive system also reported a significant reduction of Leydig cell viability as a result of administration of acrylamide on various laboratory animals (Yang *et al.* 2005, Ma *et al.* 2011, Camacho *et al.* 2012). Several antioxidants have been tested in studies to remove the toxic effects of acrylamide and glycidamide. In these studies, various antioxidants such as Vitamin C (Soliman *et al.* 2013), hesperetin (Shrivastava *et al.* 2018), L-carnitine (Zamani *et al.* 2017) and carnosic acid (Albalawi *et al.* 2017) were used to prevent acrylamide toxicity, and allicin (Wang *et al.* 2015) was used to prevent glycidamide toxicity. In the present study, the administration of glycidamide at concentrations of 5 μM and above significantly reduced Leydig cell viability, as in the case of acrylamide studies performed on other cell lines. However, glycidamide also reduced cell viability but at quite low concentrations in contrast to acrylamide. In addition, Vitamin C demonstrated a protective effect on cell viability at glycidamide concentrations as high as 1000 μM.

An increase in the cellular quantity of the lactate dehydrogenase enzyme, which is found in all tissues and cell cytoplasm, is an indication of cell cytotoxicity. Studies on various animals and cell lines/types showed that acrylamide and glycidamide exposure disrupted cell membrane integrity, causing a noticeable suppression of LDH activity (Chen *et al*. 2009, Zhang *et al.* 2013, Wang *et al.* 2015). In a recent study in which Leydig and Sertoli cells were exposed to 10 and 1000 μM acrylamide and 1 and 500 μM glycidamide, it was found that a significant increase was noted in lactate dehydrogenase levels in both cell lines for the applied concentrations (Yılmaz *et al.* 2017). The study of Yıldızbayrak and Erkan (2018) on Leydig cells revealed a significant increase in cell cytotoxicity at acrylamide concentrations of 100 μM and above. In a previous *in vivo* study measuring LDH levels in rats exposed to acrylamide, a significant increase was determined in enzyme levels when compared to the control group (Soliman 2013). The same study also administered Vitamin C to mitigate acrylamide-induced

cytotoxicity, resulting in a significant decrease in LDH levels (Soliman 2013). In another study with rats, glycidamide was found to increase LDH levels, while allicin, a natural antioxidant, was observed to reduce this cytotoxicity (Wang *et al.* 2015). In the light of these findings and given that the high glycidamide concentrations (1000 µM) applied in the present study led to a significant increase in LDH levels and that Vitamin C was found to reduce this form of cytotoxicity in former studies, it can be stated that excessive glycidamide exposure necessitates the use of antioxidants.

Reactive oxygen species (ROS) are metabolites that form naturally in cells during the conversion of nutrients into energy through the use of oxygen. Leydig cells can overcome the free radicals formed during normal energy metabolism by utilizing their antioxidant defense system (Sun *et al*. 2018), although an excess of reactive oxygen species that form in cells due to the presence of toxic substances can alter the oxidant-antioxidant balance, and the resulting reactive oxygen species may cause significant damage to nucleic acids, cell membranes and proteins (Zhang *et al.* 2010). Studies showed that acrylamide and glycidamide can cause toxicity, resulting in the formation, at a mitochondrial level, of excess ROS that are known to damage cellular components (Wang *et al.* 2015, Li *et al*. 2017, Sun *et al.* 2018). In the present study conducted with Leydig cells, glycidamide caused hydrogen peroxide formation at concentrations of 10 µM and above, and hydroxyl radical formation at concentrations of 100 µM and above. These findings are in parallel with studies suggesting that glycidamide triggers ROS formation *in vivo* and *in vitro* and demonstrate that glycidamide readily triggers oxidative stress in cells (Wang *et al*. 2015, Sun *et al*. 2018). The administration of Vitamin C in the present study reduced significantly, in a concentration-dependent manner, the formation of reactive oxygen species, indicating that Vitamin C may assume a protective role against glycidamide-induced oxidative stress. In addition, the release of these reactive oxygen species has an oxidizing effect on membrane lipids, disrupting membrane integrity through the formation of lipid peroxidation products (Lee *et al*. 2014). In the present study, glycidamide concentrations of 10 µM and above significantly increased levels of MDA – which is a final product of lipid peroxidation – when compared to the control, while groups administered with Vitamin C showed significantly lower MDA levels than the glycidamide-treated groups. These results are in parallel with studies demonstrating that acrylamide and glycidamide significantly increase MDA levels in various tissues, and that allicin (Wang *et al.* 2015), N-acetylcysteine (Alturfan *et al.* 2012) and garlic oil (Elghaffar *et al*. 2015), which are known as antioxidants, inhibit MDA levels.

Acrylamide and glycidamide were reported to generally trigger apoptotic signals and cause cell death through an increase in oxidative stress (Orta Yilmaz *et al.* 2017). This effect can be attributed to the increase in lipid peroxidation and mitochondrial membrane depolarization associated with oxidative stress (Lee *et al.* 2014). Acrylamide and glycidamide are known to trigger apoptosis in numerous cell lines and various laboratory animal tissues (Yousef & El-Demerdash 2006, Lee *et al*. 2014, Li *et al*. 2017, Kacar *et al.* 2018, Sun *et al*. 2018). In one such study, Li *et al.* (2017) applied glycidamide to R2C Leydig cells at concentrations of 0.635, 0.872 and 1.198 mM, and found, through a Comet test, that glycidamide induced cell apoptosis at an early phase. In a study performed on A549 human lung adenocarcinoma cell line, the ratio of apoptosis in cells exposed to 4.6 mM concentrations of acrylamide was reported as 64 percent (Kacar *et al.* 2018). Chen *et al.* (2013) found that acrylamide at 1 and 2 mM concentrations caused structural changes in the mitochondria of astrocytoma cells, along with mitochondria-dependent apoptosis. In their study with male rats, Yang *et al.* (2005) noted increased Leydig cell death in the testes of acrylamide-administered groups, as well as abnormal histopathological lesions containing apoptotic cells (Yang *et al.* 2005). In the present study, the glycidamide-administered groups of Leydig cells under *in vitro* conditions showed a concentration-dependent increase in apoptosis, accompanied by a significant increase in the ratio of cells in early apoptosis. It was also observed that Vitamin C suppressed apoptosis induced by glycidamide toxicity, and these results are supported by other *in vitro* studies conducted on various cell lines (Chen *et al.* 2013, Sun *et al*. 2018).

Conclusion

Since the mechanism of the effect of glycidamide on the male reproductive system has not yet been elucidated, this study can be relied upon as an *in vitro* model involving Leydig cells. Our findings showed that glycidamide has cytotoxic, anti-proliferative and apoptotic effects on Leydig cells, even at low concentrations. The results also revealed that Vitamin C could be a good antioxidant in preventing the harmful effects of glycidamide on male fertility.

References

1. Albalawi, A., Alhasani, R.H.A., Biswas, L., Reilly, J. & Shu, X. 2017. Protective effect of carnosic acid against acrylamide-induced toxicity in RPE cells. *Food and Chemical Toxicology*, 108: 543-553.

2. Alturfan, E.I., Beceren, A., Sehirli, A.O., Demiralp, Z.E., Sener, G. & Omurtag, G.Z. 2012. Protective effect of N-acetyl-L-cysteine against acrylamide induced oxidative stress in rats. *Turkish Journal of Veterinary and Animal Sciences*, 36(4): 438-445.

3. Baba, N.A., Raina, R., Verma, P.K., Sultana, M., Prawez, S. & Nisar, N.A. 2013. Toxic effects of fluoride and chlorpyrifos on antioxidant parameters in rats: protective effects of vitamin C and E. *Fluoride*, 46(2):73-9.

4. Bandarra, S., Fernandes, A.S., Magro, I., Guerreiro, P.S., Pingarilho, M., Churchwell, M.I., Gil, O.M., Batinić-Haberle, I., Gonçalves, S., Rueff, J., Miranda, J.P., Marques, M.M., Beland, F.A., Castro, M., Gaspar, J.F. & Oliveira, N.G. 2013. Mechanistic insights into the

cytotoxicity and genotoxicity induced by glycidamide in human mammary cells. *Mutagenesis*, 28(6): 721-729.

5. Baum, M., Fauth, E., Fritzen, S., Herrmann, A., Mertes, P., Merz, K., Rudolphi, M., Zankl, H. & Eisenbrand, G. 2005. Acrylamide and glycidamide: genotoxic effects in V79-cells and human blood. *Mutation Research/Genetic Toxicology and Environmental Mutagenesis*, 580(1): 61-69.
6. Camacho, L., Latendresse, J.R., Muskhelishvili, L., Patton, R., Bowyer, J.F., Thomas, M. & Doerge, D.R. 2012. Effects of acrylamide exposure on serum hormones, gene expression, cell proliferation, and histopathology in male reproductive tissues of Fischer 344 rats. *Toxicology Letters*, 211(2): 135-143.
7. Chang, I.S., Jin, B., Youn, P., Park, C., Park, J.D. & Ryu, D.Y. 2007. Arsenic-induced toxicity and the protective role of ascorbic acid in mouse testis. *Toxicology and Applied Pharmacology*, 218(2): 196-203.
8. Chen, J.H., Wu, K.Y., Chiu, M., Tsou, T.C. & Chou, C.C. 2009. Acrylamide-induced astrogliotic and apoptotic responses in human astrocytoma cells. *Toxicology in Vitro*, 23(5): 855-861.
9. Chen, J.H., Yang, C.H., Wang, Y.S., Lee, J.G., Cheng, C.H. & Chou, C.C. 2013. Acrylamide-induced mitochondria collapse and apoptosis in human astrocytoma cells. *Food and Chemical Toxicology*, 51: 446-452.
10. Das, U.B., Mallick, M., Debnath, J.M. & Ghosh, D. 2002. Protective effect of ascorbic acid on cyclophosphamide-induced testicular gametogenic and androgenic disorders in male rats. *Asian Journal of Andrology*, 4(3): 201-208.
11. Devasagayam, T.P. & Tarachand, U. 1987. Decreased lipid peroxidation in the rat kidney during gestation. *Biochemical and Biophysical Research Communications*, 145: 134-138.
12. Elghaffar, S.K.A., Fiedan, I.O., Ahmed, E.A. & Omar, H.E.D.M. 2015. Acrylamide Induced Testicular Toxicity in Rats: Protective Effect of Garlic Oil. *Biomarkers*, 1(1): 5.
13. World Health Organization. 2002. Health Implications of Acrylamide in Food: Report of a Joint FAO/ WHO Consultation WHO Headquarters. Geneva, Switzerland. PDF version available at: http://apps.who.int/iris/bitstream/10665/42563/1/9241562188.pdf. (Date accessed: May 2017).
14. Fennell, T.R., Sumner, S.C.J., Snyder, R.W., Burgess, J., Spicer, R., Bridson, W.E. & Friedman, M. 2005. Metabolism and hemoglobin adduct formation of acrylamide in human. *Toxicological Sciences*, 85: 447-59.
15. Friedman, M. 2015. Acrylamide: inhibition of formation in processed food and mitigation of toxicity in cells, animals, and humans. *Food & Function*, 6(6): 1752-1772.
16. Haider, S.G. 2004. Cell Biology of Leydig Cells in the Testis. *International Review of Cytology*, 233: 181-241.
17. Hamdy, S.M., Bakeer, H.M., Eskander, E.F. & Sayed, O.N. 2012. Effect of acrylamide on some hormones and endocrine tissues in male rats. *Human & Experimental Toxicology*, 31(5): 483-491.
18. Holland, M.K. & Storey, B.T. 1981. Oxygen metabolism of mammalian spermatozoa. Generation of hydrogen peroxide by rabbit epididymal spermatozoa. *Biochemical Journal*, 198: 273-280.
19. IARC. 1994. Acrylamide In IARC Monographs on the Evaluation of Carcinogenic Risk to Humans, International Agency for Research on Cancer, 60: 389-433.
20. International Agency for Research on Cancer (IARC). 1994. *Monographs on the Evaluation of Carcinogenic Risks to Humans.* Some Industrial Chemicals.IARC, Lyon, France.
21. Kacar, S., Vejselova, D., Kutlu, H.M. & Sahinturk, V. 2018. Acrylamide-derived cytotoxic, anti-proliferative, and apoptotic effects on A549 cells. *Human & experimental toxicology*, 37(5): 468-474.
22. Lee, J.G., Wang, Y.S. & Chou, C.C. 2014. Acrylamide-induced apoptosis in rat primary astrocytes and human astrocytoma cell lines. *Toxicology in Vitro*, *28*(4): 562-570.
23. Levine, M., Rumsey, S.C., Daruwala, R., Park, J.B. & Wang, Y. 1999. Criteria and recommendations for vitamin C intake. *Jama*, 281(15): 1415-1423.
24. Li, M., Sun, J., Zou, F., Bai, S., Jiang, X., Jiao, R. & Bai, W. 2017. Glycidamide inhibits progesterone production through reactive oxygen species-induced apoptosis in R2C Rat Leydig Cells. *Food and Chemical Toxicology*, 108: 563-570.
25. Lingnert, H., Grivas, S., Jägerstad, M., Skog, K., Törnqvist, M. & Åman, P. 2002. Acrylamide in food: mechanisms of formation and influencing factors during heating of foods. *Scandinavian Journal of Nutrition*, 46(4): 159-172.
26. Ma, Y., Shi, J., Zheng, M., Liu, J., Tian, S., He, X., Zhang, D., Li, G. & Zhu, J. 2011. Toxicological effects of acrylamide on the reproductive system of weaning male rats. *Toxicology and industrial health*, 27(7): 617-627.
27. Martins, C., Oliveira, N.G., Pingarilho, M., Gamboa da Costa, G., Martins, V., Marques, M.M., Beland, F.A., Churchwell, M.I., Doerge., D.R. & Gaspar, J.F. 2006. Cytogenetic damage induced by acrylamide and glycidamide in mammalian cells: correlation with specific glycidamide-DNA adducts. *Toxicological Sciences*, 95(2): 383-390.
28. Mottram, D.S., Wedzicha, B.L. & Dodson, A.T. 2002. Food chemistry: acrylamide is formed in the Maillard reaction. *Nature*, 419:448-449.
29. Orta, B. & Erkan, M. 2014. Effects of vitamin c on antioxidant systems and Steroidogenic enzymes in sodium fluoride exposed Tm4 sertoli cells. *Fluoride*, 47(2): 139-151.
30. Padayatty, S.J., Katz, A., Wang, Y., Eck, P., Kwon, O., Lee, J.H., Chen, S., Corpe, C., Dutta, A., Dutta, S.H. & Levine, M. 2003. Vitamin C as an antioxidant: evaluation of its role in disease prevention. *Journal of the American college of Nutrition*, 22(1): 18-35.
31. Paulsson, B., Grawé, J. & Törnqvist, M. 2002. Hemoglobin adducts and micronucleus frequencies in mouse and rat after acrylamide or N-methylolacrylamide treatment. *Mutation Research/Genetic Toxicology and Environmental Mutagenesis*, 516(1): 101-111.
32. Puntarulo, S. & Cederbaum, A.I. 1988. Effect of oxygen concentration on microsomal oxidation of ethanol and

generation of oxygen radicals. *Biochemical Journal*, 251: 787-794.

33. Sen, E., Tunali, Y. & Erkan, M. 2015. Testicular development of male mice offsprings exposed to acrylamide and alcohol during the gestation and lactation period. *Human & Experimental Toxicology*, 34(4): 401-414.

34. Shrivastava, S., Uthra, C., Reshi, M., Singh, A., Yadav, D. & Shukla, S. 2018. Protective effect of hesperetin against acrylamide induced acute toxicity in rats. *Indian Journal of Experimental Biology*, 56: 164-170.

35. Soliman, G.Z. 2013. Protective effect of *Solanum nigrum*, vitamin C or melatonin on the toxic effect of acrylamide on rats. *Journal of Pharmaceutical and Biological Sciences*, 5: 47-54.

36. Stadler, R.H., Blank, I., Varga, N., Robert, F., Hau, J., Guy, P.A., Robert, M.C. & Riediker, S. 2002. Food chemistry: acrylamide from Maillard reaction products. *Nature*, 419(6906): 449.

37. Sun, J., Li, M., Zou, F., Bai, S., Jiang, X., Tian, L., Ou, S., Jiao, R. & Bai, W. 2018. Protection of cyanidin-3-O-glucoside against acrylamide-and glycidamide-induced reproductive toxicity in leydig cells. *Food and Chemical Toxicology*, 119: 268-274.

38. Taeymans, D., Wood, J., Ashby, P., Blank, I., Studer, A., Stadler, R.H., Gondé, P., Eijck, P., Lalljie, S., Lingnert, H., Lindblom, M., Matissek, R., Müller, D., Tallmadge, D., O'brien, J., Thompson, S., Silvani, D. & Lindblom, M. 2004. A review of acrylamide: an industry perspective on research, analysis, formation, and control. *Critical Reviews in Food Science and Nutrition*, 44(5): 323-347.

39. Vattem, D.A. & Shetty, K. 2003. Acrylamide in food: a model for mechanism of formation and its reduction. *Innovative Food Science & Emerging Technologies*, 4(3): 331-338.

40. Wang, H., Huang, P., Lie, T., Li, J., Hutz, R.J., Li, K. & Shi, F. 2010. Reproductive toxicity of acrylamide-treated male rats. *Reproductive Toxicology*, 29(2): 225-230.

41. Wang, E.T., Chen, D.Y., Liu, H.Y., Yan, H.Y. & Yuan, Y. 2015. Protective effect of allicin against glycidamide-induced toxicity in male and female mice. *General Physiology and Biophysics*, 34(2): 177-187.

42. Yang, H.J., Lee, S.H., Jin, Y., Choi, J.H., Han, D.U., Chae, C., Lee, M.H. & Han, C.H. 2005. Toxicological effects of acrylamide on rat testicular gene expression profile. *Reproductive Toxicology*, 19(4): 527-534.

43. Yildizbayrak, N. & Erkan, M. 2018. Acrylamide disrupts the steroidogenic pathway in Leydig cells: possible mechanism of action. *Toxicological & Environmental Chemistry*, 100(2): 235-246.

44. Yilmaz, B.O., Yildizbayrak, N., Aydin, Y. & Erkan, M. 2017. Evidence of acrylamide-and glycidamide-induced oxidative stress and apoptosis in Leydig and Sertoli cells. *Human & Experimental Toxicology*, 36(12): 1225-1235.

45. Yousef, M.I. & El-Demerdash F.M. 2006. Acrylamide induced oxidative stress and biochemical perturbation in rats. *Toxicology*, 219: 133-141.

46. Zamani, E., Shokrzadeh, M., Ziar, A., Abedian-Kenari, S. & Shaki, F. 2017. Acrylamide attenuated immune tissues' function via induction of apoptosis and oxidative stress: Protection by l-carnitine. *Human & Experimental Toxicology*, 37(8): 859-869.

47. Zhang, J.X., Yue, W.B., Ren, Y.S. & Zhang, C.X. 2010. Enhanced fat consumption potentiates acrylamide-induced oxidative stress in epididymis and epididymal sperm and effect spermatogenesis in mice. *Toxicology Mechanisms and Methods*, 20(2): 75-81.

48. Zhang, L., Wang, E., Chen, F., Yan, H. & Yuan, Y. 2013. Potential protective effects of oral administration of allicin on acrylamide-induced toxicity in male mice. *Food & Function*, 4(8): 1229-1236.

http://dergipark.gov.tr/trkjnat
Trakya University Journal of Natural Sciences, 20(1): 19-26, 2019
ISSN 2147-0294, e-ISSN 2528-9691
DOI: 10.23902/trkjnat.508120

Research Article

MOLECULAR DYNAMICS STUDIES OF THE NOROVIRUS-HOST CELL INTERACTION MEDIATED BY H-TYPE 1 ANTIGEN

Abdülkadir KOCAK[1*], Muslum YILDIZ[2]

[1]Department of Chemistry, Gebze Technical University, Kocaeli, TURKEY
[2]Department of Molecular Biology and Genetics, Gebze Technical University, Kocaeli, TURKEY
*Corresponding author: ORCID ID: orcid.org/0000-0001-6891-6929, e-mail: kocak@gtu.edu.tr

Cite this article as:

Kocak A., Yildiz M. 2019. Molecular Dynamics Studies of the Norovirus-Host Cell Interaction Mediated by H-type 1 Antigen. *Trakya Univ J Nat Sci*, 20(1): 19-26, DOI: 10.23902/trkjnat.508120

Received: 04 January 2019, Accepted: 27 January 2019, Online First: 30 January 2019, Published: 15 April 2019

Abstract: Noroviruses are the main cause for acute gastroenteritis disease. They infect the host cell via interaction with HGBA receptors on the cell surface. Virus makes complex with cell surface receptors through its capsid protein VP1 to enter the cell. Although the protein has been successfully crystallized in the presence of some common glycans, the dynamic change in the protein structure when interacting with sugar moieties has yet to be fully elucidated. This is critically important since it leads to understanding the protein's recognition mechanism of HBGAs and develop therapeutic strategies against the gastroenteritis disease. Here, we computationally assessed the dynamic features of wild type VP1 envelope protein to get insights into the interactions that can be important for virus infectivity. We have found that the binding of sugar moiety does not cause noticeable dynamic changes in the binding region. However, interestingly, a drastic change occurs in a distant loop lying at the residue numbers of 395-400, which might be indication of an allosteric effect.

Key words: Norovirus, therapeutic antibody, HBGA blockage, molecular dynamics.

Özet: Akut gastroenterit hastalığının önemli nedenlerinden biri norovirüslerdir. Konakçı hücreye, hücre yüzeyindeki çoklu şeker halkalarından oluşan HGBA reseptörleri ile etkileşerek enfekte olurlar. Hücreye girmek için virüse ait kapsid proteini hücre yüzeyi reseptörleri ile kompleksleşir. Her ne kadar protein bazı ortak glikanların varlığında kompleks olarak başarılı bir şekilde kristalize edilmiş olsa da, şeker kısımlarının bağlanmasından kaynaklanan protein yapısındaki dinamik değişim henüz tam olarak aydınlatılamamıştır. Virüs proteinin HBGA'lara bağlanma mekanizmasını anlama ve gastroenterit hastalığına karşı tedavi stratejileri geliştirmesine yardımcı olması nedeniyle bu dinamik değişimi anlamak kritik derecede öneme sahiptir. Bu çalışmada, virüs enfeksiyonu için önemli olabilecek etkileşimler hakkında bilgi edinmek için yabanıl VP1 kapsit proteininin dinamik özelliklerini moleküler dinamik metotlarla hesapladık. Şeker kısmının bağlanmasının, bağlanma bölgesinde gözle görülür dinamik değişikliklere neden olmadığını tespit ettik. Bununla birlikte, ilginç bir şekilde, allosterik bir etkinin göstergesi olabilecek 395-400 numaralı sekansa ait amino asitlerinde ihmal edilemeyecek bir hareketlilik meydana geldiğini gözlemledik.

Introduction

Gastroenteritis disease is one of the greatest health problems among all infectious diseases. The annual number of people suffering from gastroenteritis worldwide is about 90 million of which the number of deaths is close to 2.5 million (Kotloff *et al.* 2013, Belliot *et al.* 2014, Kambhampati *et al.* 2015). The disease is also the major reason for deaths of 1.8 million children and infants every year (Hoa Tran *et al.* 2013, Karst *et al.* 2014, Rocha-Pereira *et al.* 2014). All populations are susceptible to the causing virus, but elders and children constitute the highest risk group. The infection mostly starts with the ingestion of contaminated food and water and can also be transmitted from person to person during outbreaks. The virus specifically binds to the antigens on the surfaces of red blood cells (erythrocytes) and epithelial cells in the gastrointestinal tract. This binding initiates the infection in these cells. The infectivity of noroviruses is responsible for sporadic gastroenteritis and severe childhood diarrhea. Despite the tremendous scientific efforts, an approved vaccine or an effective antiviral drug has not been developed yet (Tan & Jiang 2014, Aliabadi *et al.* 2015).

Noroviruses are classified in six genogroups (GI-GVI) and each group contains several genotypes. The notation used to categorize Norwalk viruses (NV) is given by "GI.1", where "G" stands for genogroup, "I" refers to the 1st genogroup, and "1" to genotype 1. The GI, GII and GIV are principal groups that are responsible for infecting human (Patel *et al.* 2009, White 2014).

The entrance of Human Noroviruses (HuNoVs) into the cell is initiated by the interaction of the virus protein's domain 1 (VP1) and histo-blood group antigens (HBGAs) (Caddy *et al.* 2014, Shanker *et al.*

2014, de Graaf *et al.* 2016). This has attracted great scientific attention to develop therapeutics that will block the interaction between VP1 and HBGAs as a cure for virus infection (Lochridge *et al.* 2005, Garaicoechea *et al.* 2015, Sapparapu *et al.* 2016, Tamminen *et al.* 2016). Thus, several crystal structures that show atomic details of interactions among residues residing in the complex interface are solved (Choi *et al.* 2008, Kubota *et al.* 2012, Shanker *et al.* 2014). Even though the crystal structures have rich information about the interaction, they lack the dynamic features of this interaction. Moreover, so far studies have shown that the interaction is rather weak and binding regions of HBGAs are varied (Ishida 2018).

Here, in order to understand the dynamic properties of residues on the VP1-HGBA complex, we computationally investigated the interaction of an H-type HBGA antigen with VP1. We probed dynamic changes in the VP1 capsid protein that may be visible upon sugar binding. Given the fact that the manipulation of the possible changes can be harnessed for designing new therapeutic agents, our findings can offer opportunity for opening new avenue for treatment of norovirus dependent gastroenteritis disease.

Materials and Methods

MD Preparation

The starting structures of the wild type unliganded (VP1) and liganded (VP1 HBGA complex) were retrieved from the Protein Data Bank (PDB id=2ZL5 and 2ZL6, respectively) (Choi *et al.* 2008). The protein preparation wizard utility of Maestro (Schrödinger 2015) was used to add the H atoms, assign bond orders, remove steric clashes and optimize hydrogen-bonding network. The protonation states of acidic and basic amino acids were calculated using Propka 3.1 (Olsson *et al.* 2011) at pH=7. According to that, negatively charged side chains of Asp and Glu (unprotonated) and positively charged side chains of Arg and Lys (protonated) residues were presumed. The amber99sb-ildn (Lindorff-Larsen *et al.* 2010) force field was used for the VP1 protein. The pentasaccharide ligand was first optimized using G09 software at B3LYP/6-311++G(d,p) level by freezing the heavy atoms at the x-ray coordinates. Then, the RESP charges and GAFF parameters were generated using antechamber software (Wang *et al.* 2004, Wang *et al.* 2006).

Simulation Protocol

The molecular dynamics simulations were carried out using Gromacs 5.1 software package (Abraham *et al.* 2015). The system (either containing unliganded or liganded VP1) is placed in the center of a dodecahedron box and solvated in a water box of ~1500 nm^3 with the TIP3P model (Toukan & Rahman 1985) with a cell margin distance of 14 Å for each dimension. Each system consisting of ~145,000 atoms was neutralized and salted by 0.15 M NaCl. Bonds with hydrogen atoms were restrained to their equilibrium length with LINCS algorithm.

As in our former studies (Kocak *et al.* 2016, Kocak & Yildiz 2017), the system was very gently energy minimized within 13 steps, each consisting of 5000 cycles of two subsequent integrators, Steepest Descent and Conjugate Gradient. In the first step, only hydrogen atoms were relaxed while keeping all heavy atoms including water at 4000 $kJ.mol^{-1}.nm^{-2}$. In the second step, the water molecules were relaxed. Next, the side chains were gradually relaxed by reducing the force constants in the order of 4000, 2000, 1000, 500, 200, 50 and 0 $kJ.mol^{-1}.nm^{-2}$. At the last step of the minimization process, the backbone atoms were also released in the same gradual order.

After minimization, each system was equilibrated within six steps. The first step is a 5 ns of canonical ensemble. At this step, the system was heated to 310 K (with time constant of 0.1) with a simulated annealing fashion. This temperature was reached in the first 500 ps by linearly heating and kept constant for the next 4.5 ns. The V-rescale thermostat was used as the temperature-coupling group separately for the protein-ligand complex and surroundings. In the subsequent steps, the system was equilibrated to 1 atm pressure in a stepwise isobaric-isothermal ensemble. During this stage, the heavy atoms were smoothly and progressively released. MD simulations were run for ~70 ns at constant pressure using Langevin Dynamics.

Results and Discussion

The comparison of molecular dynamics simulations belonging to unliganded (bare VP1) and liganded (complexed VP1) P domain structures reflect the nature of the interaction between the VP1 and HBGA, along with dynamic changes upon binding. Thus, we investigated the RMSD and radius of gyration values of bare and complexed VP1 over time course of MD simulation. These values are lower in complexed VP1 and shows different trend from the complexed structure (Fig. 1), suggesting that the dynamic feature of VP1 varies when the HBGA is attached to it. In order to pin down the specific dynamic variations due to ligand binding, we specifically monitored the distances and fluctuations among residues in the interaction region that were already observed in the crystal structure.

According to the x-ray structures, the residues Gln342, Asp344, His329, Ser377, Asp327, Pro378 and Trp375 are involved in the interaction with H-type 1 pentasaccharide receptor. Among these, the first three residues interact with α-fucose and the remaining with β-Galactose (Fig. 2). The last three sugar moieties are not involved in the interaction. Although the sugar moieties have high degrees of freedom due to multiple torsions, the residues in the interacting region maintain in a stable state throughout the MD simulation. The structures from x-ray and MD simulations were superimposed in Fig. 3. The weak binding nature of the receptor to the VP1 protein does not perturb the rigid structures of the residues in this region.

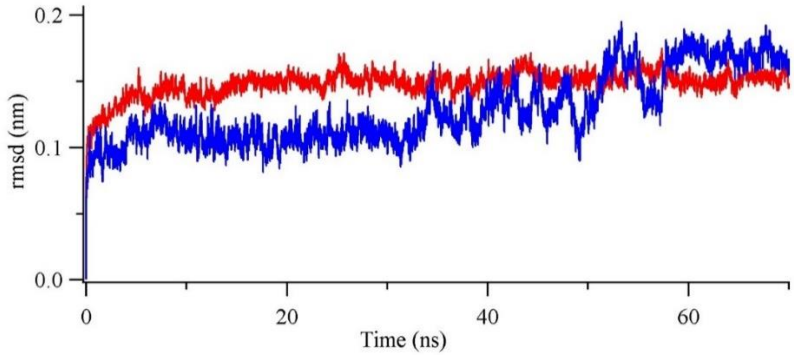

Fig. 1. The RMSD of Calpha atoms in liganded (blue) and unliganded (red) VP1 protein. The unliganded values are steadier and less fluctuated.

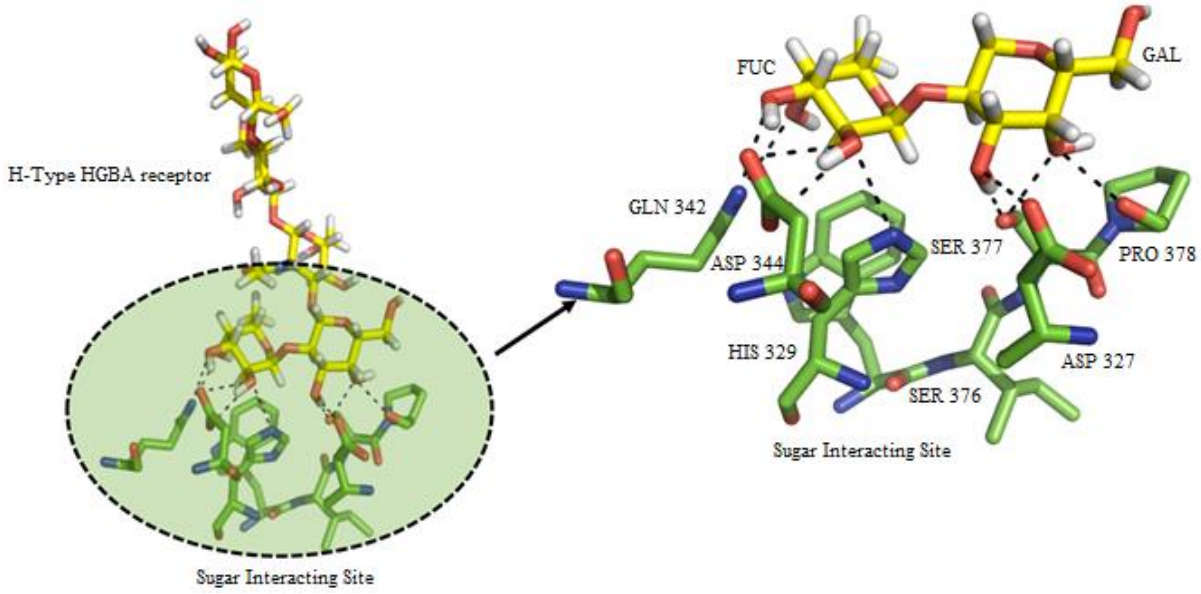

Fig. 2. Interacting pairs with residues labeled in the complex interface. The residues Gln342, Asp344, His329 interact with α-fucose and Ser377, Asp327, Pro378 and Trp375 with β-Galactose of the ligand.

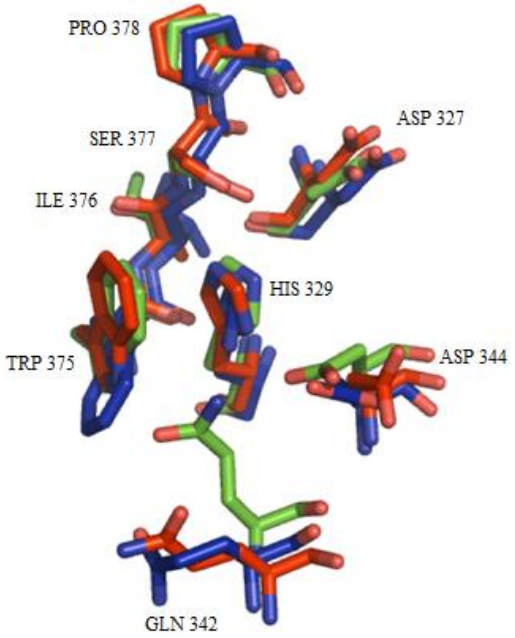

Fig. 3. Superimposed residues in the binding region for x-ray crystal structure (green) along with the most populated MD clusters of liganded (blue) and unliganded (red) VP1.

The distances among proximal residues in the interaction region and fluctuations of these residues showed no significant changes upon ligand binding. This impose the fact that the presence of some other dynamic entities is involved in the variations of the RMSD values of VP1 upon sugar binding. Fig. 4a-f shows some of the change of the selected pair distances among the residues in the interaction region throughout MD simulations. Almost all the distances monitored showed similar pattern of a steady H-bonding interaction with < 3.5 Å. There is only one exception to this on the pairs of 327OD2-380OG where the distance in unliganded VP1 is too large for H-bonding (Fig. 4b).

Not only the distances among the pairs in the interaction region, the fluctuations of those residues also showed no significant changes upon pentasaccharide binding (Fig. 5). On the other hand, the RMSF of the residues in the 395-405 region showed dramatic change upon binding. This is interesting given the fact that the ligand binding site is quite away from these residues. This cannot be simply explained by random loop motions.

The covariance analysis (also called principal component analysis, PCA) is a useful tool for investigating correlated dynamic movements in macromolecules.

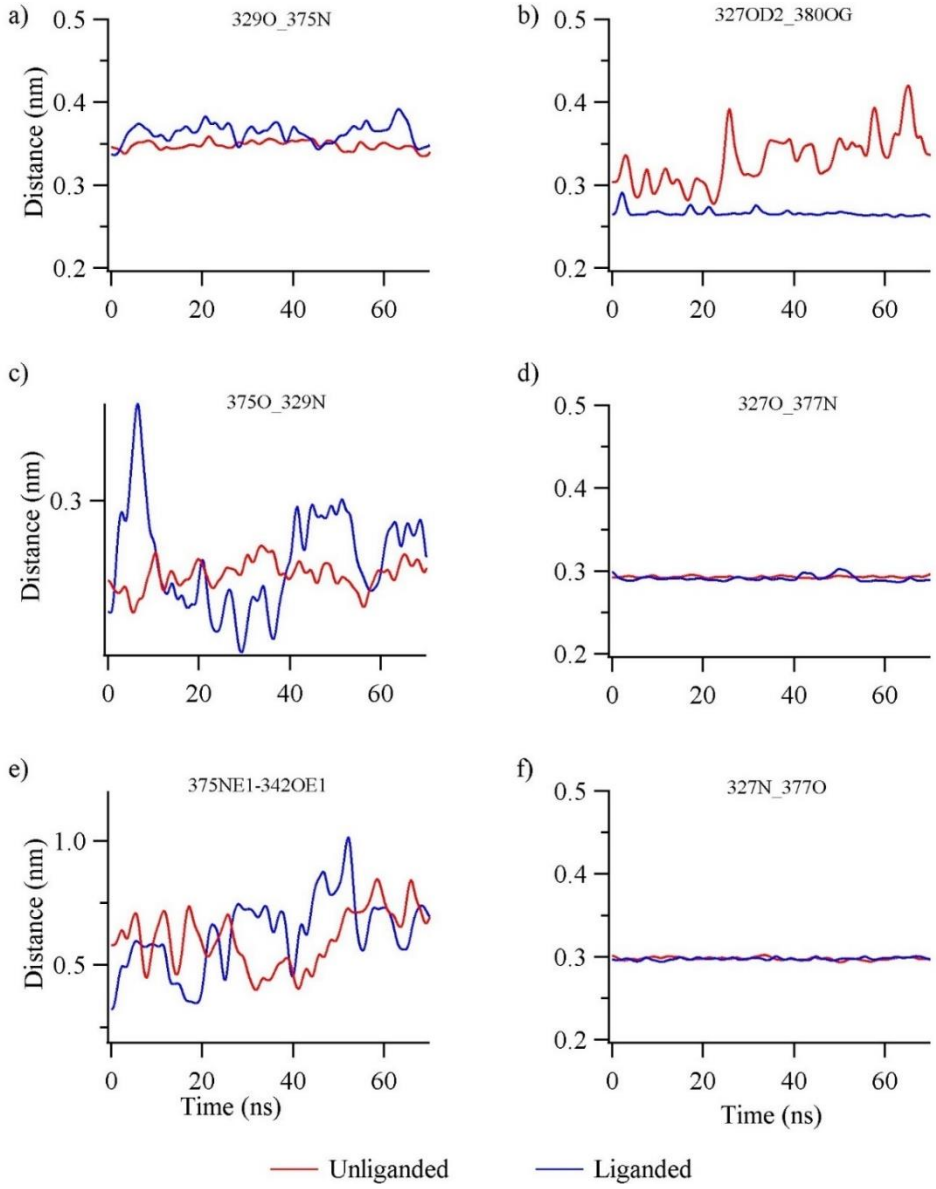

Fig. 4. Critical distances among residues in the sugar binding site for liganded (blue) and unliganded (red) VP1 protein. The notation in distance is as follows: the first 3 digits show the residue number, rest shows the atom name in that residue (e.g, 375NE1 refers to Nε1 atom of 375th residue). All data were smoothed using a Gaussian smoothing function of 10k fold.

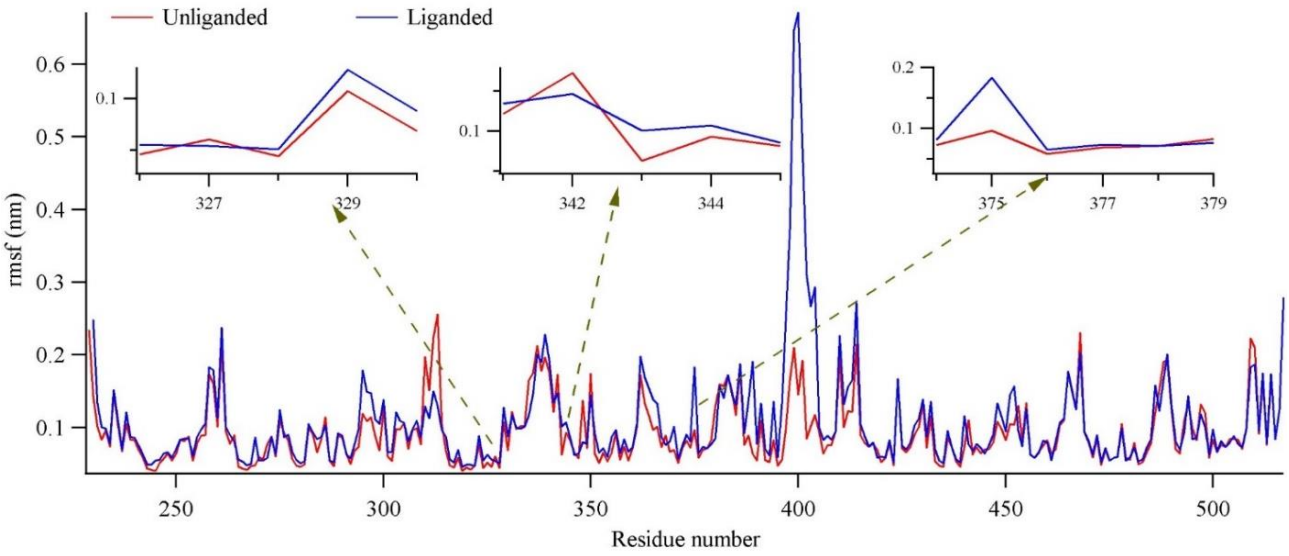

Fig. 5. The RMSF of liganded (blue) and unliganded (red) VP1 residues. The insets are the zoomed of the residues in the sugar binding site. Data show no noticeable rmsf difference at the binding site. The dashed arrows are not part of the data and only meant to show the location of zoomed insets (sugar binding site).

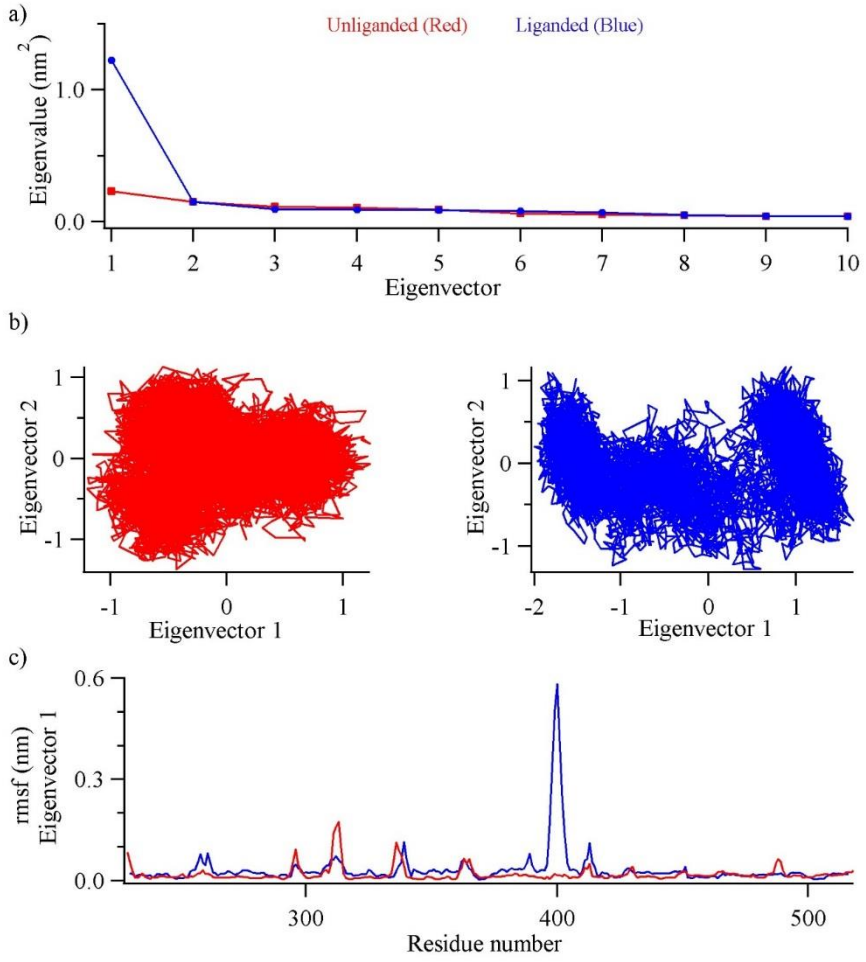

Fig. 6. Principal component analysis of unliganded (red) and liganded (blue) proteins for correlated motions. a) The first 10 eigenvalues showing two proteins differ in only eigenvector 1. b) The 2D projection of the trajectories on the first two eigenvectors (the most dominant collective motions) and c) RMSF of residues involved in the most dominant collective motion (eigenvector 1).

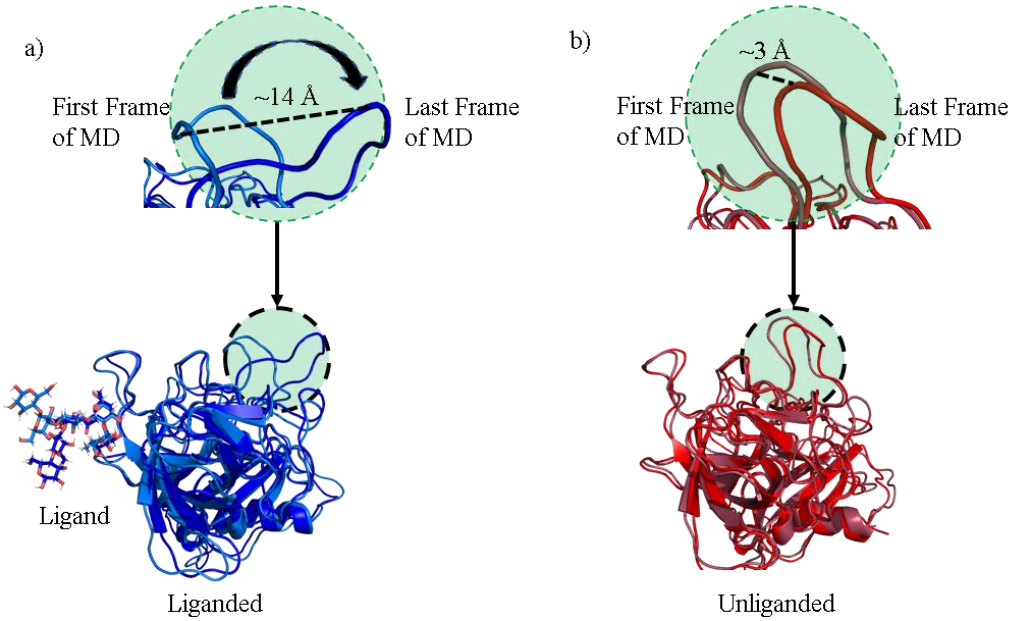

Fig. 7. The significant loop motion upon ligand binding is evident in the comparison of the first and last frame of MD simulations belong to liganded and unliganded structures.

Eigenvectors sorted by descending eigenvalues from a covariance matrix provide the essential collective motions. Therefore, the first eigenvector with the greatest eigenvalue shows the most dominant correlated motion.

Thus, we further dissected changes in the collective motion of VP1 by means of PCA. The first eigenvector for liganded spans over 1 nm^2 space whereas it is only 0.25 nm^2 for unliganded structure (Fig. 6a). The rest of the eigenvectors follow the same trend with the same values. The two-dimensional (2D) projection of the first two eigenvectors is very compact and mostly centers around a single cluster for unliganded while it is distributed (less-compact) and another distinct cluster starts to appear for the liganded structure (Fig. 6b). The RMSF value corresponding to the eigenvector 1 shows drastic changes in the 395-405 region of VP1 upon ligand binding (Fig. 6c). The overall analysis clearly shows that a significant motion become more visible and dominant upon ligand binding in VP1 protein structure**.** Since this motion is very far from the binding region, an allosteric effect might be involved in ligand binding mechanism. However, this needs to be validated by further experimental studies.

We also explored the structural changes that is suggested by covariance analysis with superimposing the last and first frames of MD simulation for both liganded and unliganded VP1. We have found that the ligand binding triggers a substantial mobility in the 395-405 loop that is distant to sugar binding site. The loop moves by 14 Å in liganded VP1(Fig. 7a) while it moves only 3 Å in unliganded VP1, (Fig. 7. The significant loop motion upon ligand binding is evident in the comparison of the first and last frame of MD simulations belong to liganded and unliganded structures. The significant loop motion upon ligand binding is evident in the comparison of the first and last frame of MD simulations belong to liganded and unliganded structures over the course of MD simulations. This motion is not random as the repetitive MD simulations showed the same loop movements. The drastic motion of the loop upon ligand binding is clearly visible in compared representative structures of the first and last frame of MD simulations for liganded and unliganded structures. This data may be an indication of a cross talk between the sugar binding site and this loop which suggests an allosteric effect.

Conclusion

In this study, we investigated the dynamic changes occurred on the structure of wild type VP1 capsid protein upon binding to an H-type 1 HBGA antigen by means of molecular dynamic simulations. The data suggested very little dynamic changes in the binding region. This is in complete agreement with the experimental studies which showed the weak binding nature of the sugar. Data also showed a very interesting loop movement at a distal location from the ligand binding region, suggesting an allosteric communication between sugar binding site and this loop. Further experimental tests would be complementary and confirmative to this study. In addition to the experimental studies, molecular dynamics simulations could be extended to the interaction between VP1 and other antigen receptors such as A-type HBGA.

Acknowledgement

The numerical calculations reported in this paper were partially performed at TUBITAK ULAKBIM, High Performance and Grid Computing Center (TRUBA resources). This research did not receive any specific grant from funding agencies in the public, commercial, or not-for-profit sectors.

References

1. Abraham, M.J., Murtola, T., Schulz, R., Páll, S., Smith, J.C., Hess, B. & Lindahl, E. 2015. GROMACS: High performance molecular simulations through multi-level parallelism from laptops to supercomputers. *SoftwareX*, 1-2: 19-25. https://doi.org/10.1016/j.softx.2015.06.001
2. Aliabadi, N., Lopman, B.A., Parashar, U.D. & Hall, A.J. 2015. Progress toward norovirus vaccines: considerations for further development and implementation in potential target populations. *Expert Review of Vaccines*, 14(9): 1241-1253. https://doi.org/10.1586/14760584.2015.1073110
3. Belliot, G., Lopman, B.A., Ambert-Balay, K. & Pothier, P. 2014. The burden of norovirus gastroenteritis: an important foodborne and healthcare-related infection. *Clinical Microbiology and Infection*, 20(8): 724-730. https://doi.org/10.1111/1469-0691.12722
4. Caddy, S., Breiman, A., le Pendu, J. & Goodfellow, I. 2014. Genogroup IV and VI canine noroviruses interact with histo-blood group antigens. *Journal of Virology*, 88(18): 10377-10391. https://doi.org/10.1128/JVI.01008-14
5. Choi, J.-M., Hutson, A.M., Estes, M.K. & Prasad, B.V.V. 2008. Atomic resolution structural characterization of recognition of histo-blood group antigens by Norwalk virus. *Proceedings of the National Academy of Sciences*, 105(27): 9175-9180. https://doi.org/10.1073/pnas.0803275105
6. de Graaf, M., van Beek, J., & Koopmans, M.P. 2016. Human norovirus transmission and evolution in a changing world. *Nature Reviews: Microbiology*, 14(7): 421-433. https://doi.org/10.1038/nrmicro.2016.48
7. Garaicoechea, L., Aguilar, A., Parra, G.I., Bok, M., Sosnovtsev, S.V., Canziani, G., Green, K.Y., Bok, K. & Parreno, V. 2015. Llama nanoantibodies with therapeutic potential against human norovirus diarrhea. *PLoS One*, 10(8): e0133665. https://doi.org/10.1371/journal.pone.0133665
8. Hoa Tran, T.N., Trainor, E., Nakagomi, T., Cunliffe, N.A. & Nakagomi, O. 2013. Molecular epidemiology of noroviruses associated with acute sporadic gastroenteritis in children: global distribution of genogroups, genotypes and GII.4 variants. *Journal of Clinical Virology*, 56(3): 185-193. https://doi.org/10.1016/j.jcv.2012.11.011
9. Ishida, T. 2018. Computational analysis of carbohydrate recognition based on hybrid QM/MM modeling: a case study of norovirus capsid protein in complex with Lewis antigen. *Physical Chemistry Chemical Physics*, 20(7): 4652-4665. https://doi.org/10.1039/C7CP07701G
10. Kambhampati, A., Koopmans, M. & Lopman, B.A. 2015. Burden of norovirus in healthcare facilities and strategies for outbreak control. *Journal of Hospital Infection*, 89(4): 296-301. https://doi.org/10.1016/j.jhin.2015.01.011
11. Karst, S.M., Wobus, C.E., Goodfellow, I.G., Green, K.Y. & Virgin, H.W. 2014. Advances in norovirus biology. *Cell Host Microbe*, 15(6): 668-680. https://doi.org/ 10.1016/j.chom.2014.05.015
12. Kocak, A., Erol, I., Yildiz, M. & Can, H. 2016. Computational insights into the protonation states of catalytic dyad in BACE1-acyl guanidine based inhibitor complex. *Journal of Molecular Graphics and Modeling*, 70: 226-235. https://doi.org/10.1016/j.jmgm.2016.10.013
13. Kocak, A. & Yildiz, M. 2017. Docking, molecular dynamics and free energy studies on aspartoacylase mutations involved in Canavan disease. *Journal of Molecular Graphics and Modeling*, 74: 44-53. https://doi.org/ 10.1016/j.jmgm.2017.03.011
14. Kotloff, K.L., Nataro, J.P., Blackwelder, W.C., Nasrin, D., Farag, T.H., Panchalingam, S., Wu, Y., Sow, S.O., Sur, D., Breiman, R.F., Faruque, A.S., Zaidi, A.K., Saha, D., Alonso, P.L., Tamboura, B., Sanogo, D., Onwuchekwa, U., Manna, B., Ramamurthy, T., Kanungo, S., Ochieng, J.B., Omore, R., Oundo, J.O., Hossain, A., Das, S.K., Ahmed, S., Qureshi, S., Quadri, F., Adegbola, R.A., Antonio, M., Hossain, M.J., Akinsola, A., Mandomando, I., Nhampossa, T., Acacio, S., Biswas, K., O'Reilly, C.E., Mintz, E.D., Berkeley, L.Y., Muhsen, K., Sommerfelt, H., Robins-Browne, R.M. & Levine, M.M. 2013. Burden and aetiology of diarrhoeal disease in infants and young children in developing countries (the Global Enteric Multicenter Study, GEMS): a prospective, case-control study. *Lancet*, 382(9888): 209-222. https://doi.org/10.1016/S0140-6736(13)60844-2
15. Kubota, T., Kumagai, A., Ito, H., Furukawa, S., Someya, Y., Takeda, N., Ishii, K., Wakita, T., Narimatsu, H. & Shirato, H. 2012. Structural basis for the recognition of Lewis antigens by genogroup I norovirus. *Journal of Virology*, 86(20): 11138-11150. https://doi.org/10.1128/JVI.00278-12
16. Lindorff-Larsen, K., Piana, S., Palmo, K., Maragakis, P., Klepeis, J.L., Dror, R.O. & Shaw, D.E. 2010. Improved side-chain torsion potentials for the Amber ff99SB protein force field. *Proteins*, 78(8): 1950-1958. https://doi.org/10.1002/prot.22711
17. Lochridge, V.P., Jutila, K.L., Graff, J.W. & Hardy, M.E. 2005. Epitopes in the P2 domain of norovirus VP1 recognized by monoclonal antibodies that block cell interactions. *Journal of General Virology*, 86(Pt 10): 2799-2806. https://doi.org/10.1099/vir.0.81134-0
18. Olsson, M.H., Sondergaard, C.R., Rostkowski, M. & Jensen, J.H. 2011. PROPKA3: Consistent Treatment of Internal and Surface Residues in Empirical pKa Predictions. *Journal of Chemical Theory and Computation*, 7(2): 525-537. https://doi.org/10.1021/ct100578z
19. Patel, M.M., Hall, A.J., Vinje, J. & Parashar, U.D. 2009. Noroviruses: a comprehensive review. *Journal of Clinical Virology*, 44(1): 1-8. https://doi.org/10.1016/j.jcv.2008.10.009
20. Rocha-Pereira, J., Neyts, J. & Jochmans, D. 2014. Norovirus: targets and tools in antiviral drug discovery. *Biochemical Pharmacology*, 91(1): 1-11. https://doi.org/10.1016/j.bcp.2014.05.021
21. Sapparapu, G., Czako, R., Alvarado, G., Shanker, S., Prasad, B.V., Atmar, R.L., Estes, M.K. & Crowe, J.E., Jr. 2016. Frequent Use of the IgA Isotype in Human B Cells Encoding Potent Norovirus-Specific Monoclonal Antibodies That Block HBGA Binding. *PLoS Pathog*, 12(6): e1005719. https://doi.org/10.1371/journal.ppat.1005719

22. Schrödinger, L. 2015. *Maestro*. New York, NY: Schrödinger, LLC.

23. Shanker, S., Czako, R., Sankaran, B., Atmar, R.L., Estes, M.K. & Prasad, B.V. 2014. Structural analysis of determinants of histo-blood group antigen binding specificity in genogroup I noroviruses. *Journal of Virology*, 88(11): 6168-6180. https://doi.org/10.1128/JVI.00201-14

24. Tamminen, K., Malm, M., Vesikari, T. & Blazevic, V. 2016. Mucosal Antibodies Induced by Intranasal but Not Intramuscular Immunization Block Norovirus GII.4 Virus-Like Particle Receptor Binding. *Viral Immunology*, 29(5): 315-319. https://doi.org/10.1089/vim.2015.0141

25. Tan, M. & Jiang, X. 2014. Vaccine against norovirus. *Hum Vaccin Immunother*, 10(6): 1449-1456. https://doi.org/ 10.4161/hv.28626

26. Toukan, K. & Rahman, A. 1985. Molecular-dynamics study of atomic motions in water. *Physical Review B: Condensed Matter and Materials Physics*, 31(5): 2643-2648.

27. Wang, J., Wolf, R.M., Caldwell, J.W., Kollman, P.A. & Case, D.A. 2004. Development and testing of a general amber force field. *Journal of Computational Chemistry*, 25(9): 1157-1174. https://doi.org/10.1002/jcc.20035

28. Wang, J., Wang, W., Kollman, P.A. & Case, D.A. 2006. Automatic atom type and bond type perception in molecular mechanical calculations. *Journal of Molecular Graphics and Modelling*, 25(2): 247-260. doi: https://doi.org/10.1016/j.jmgm.2005.12.005

29. White, P.A. 2014. Evolution of norovirus. *Clinical Microbiology and Infection*, 20(8): 741-745. https://doi.org/10.1111/1469-0691.12746

http://dergipark.gov.tr/trkjnat
Trakya University Journal of Natural Sciences, 20(1): 27-34, 2019
ISSN 2147-0294, e-ISSN 2528-9691
DOI: 10.23902/trkjnat.448851

Research Article

BIOPRODUCTION OF γ-POLY(GLUTAMIC ACID) USING FEATHER HYDROLYSATE AS A FERMENTATION SUBSTRATE

Müslüm ALTUN

Adıyaman University, Department of Material Engineering, Adıyaman, TURKEY
ORCID ID: orcid.org/0000-0003-2697-7370, e-mail: muslumaltun@hotmail.com

Cite this article as:

Altun M. 2019. Bioproduction of γ-Poly(glutamic acid) using feather hydrolysate as a fermentation substrate. *Trakya Univ J Nat Sci*, 20(1): 27-34, DOI: 10.23902/trkjnat.448851

Received: 29 July 2018, Accepted: 04 March 2019, Online First: 07 March 2019, Published: 15 April 2019

Abstract: Polyglutamic acid (PGA) is water-soluble and biodegradable polymer with high production cost. For feasible PGA production, feather hydrolysate (FH) was used as fermentation substrate. 30L fermentation of native feather was realized to obtain keratinase enzyme using *Streptomyces pactum* DSM 40530. Fermentation broth was concentrated by cross-flow filtration where the enzyme activity increased by 8.75-fold and $8\times10^{3}UL^{-1}d^{-1}$ of enzyme activity was the optimum for achieving 75% degradation per gram of feather. 40g/L of FH was used with different media compositions to produce PGA using *Bacillus licheniformis* 9945a. Among four different cultivation where L-glutamate, tri-sodium citrate and glycerol were used as the constituents of Medium E, highest yields of γ-PGA and cell dry matter (CDM) were obtained from cultivation-1, at 5.4±0.4 and 8.6±0.5g/L, respectively, despite the culture media did not contain glutamic acid. In cultivation-2, which was not only missing glutamate but also citrate, the γ-PGA and CDM yielded 3.2±0.2 and 7.8±0.4g/L, respectively whereas it was only 1.9±0.2 and 4.2+0.4g/L when FH was used as the sole substrate in cultivation-3. When cultivation-4 was adopted where only glycerol was missing, the γ-PGA and CDM yields slightly increased to 2.3±0.2 and 5.5±0.3g/L, respectively. This is the first study that achieved the production of γ-PGA from FH.

Key words: γ-Poly(glutamic acid), γ-PGA, feather hydrolysate, keratinolytic activity, feather.

Özet: Poliglutamik asit (PGA) yüksek üretim maliyeti olan, suda çözünen ve biyobozunabilir bir polimerdir. Bu çalışmada, fizıbıl PGA üretimi için tavuk tüyü hidrolizatları (TH) fermantasyon substratı olarak kullanılmıştır. Keratinaz enzimi eldesi için, *Streptomyces pactum* DSM 40530 ile doğal tavuk tüyleri fermente (30L) edilmiştir. Fermantasyon çözeltisindeki enzim aktivitesi, çapraz akışlı filtrasyon ünitesi kullanılarak 8,75 kat deriştirilmiştir. Enzim aktivitesi ($8\times10^{3}UL^{-1}gün^{-1}$), gram tavuk tüyü başına %75'lik bozunma için optimum değer olarak belirlenmiştir. PGA üretimi için *Bacillus licheniformis* 9945a kullanılmış ve 40g/L TH kullanılarak farklı kompozisyonlarda besiyeri çözeltileri hazırlanmıştır. Besiyeri-E bileşenleri olan L-glutamat, sodyum sitrat ve gliserol kullanılarak dört farklı kompozisyonda besiyeri hazırlanmıştır. Bunlar arasında en fazla PGA ve kuru hücre maddesi (KHM) üretimi, glutamik asit içermeyen bir numaralı kültürde, sırasıyla 5,4±0,4 and 8,6±0,5g/L olarak gerçekleşmiştir. Glutamik asitin yanı sıra sitrik asitin de olmadığı iki numaralı kültürde PGA ve KHM değerleri sırasıyla 3,2±0,2 ve 7,8±0,4g/L olurken, sadece TH'nin substrat olarak kullanıldığı üç numaralı kültürde yalnızca 1,9±0,2 ve 4,2+0,4g/L değerleri elde edilmiştir. Sadece gliserolün kullanılmadığı dört numaralı kültürde ise PGA ve KHM değerleri bir miktar yükselmiş ve sırasıyla 2,3±0,2 ve 5,5±0,3g/L değerlerini almıştır. Yapılan çalışma PGA üretiminin TH kullanılarak yapıldığı İlk çalışma olmuştur.

Introduction

Polyglutamic acid (PGA) is a biodegradable, protease-resistant, non-immunogenic and unusual anionic homopolyamide that is made of D- and L-glutamic acid units with nylon-like properties upon esterification of its carboxyl side chains. PGA is attracting attention due to its multi-functionality in numerous fields including wastewater treatment, medicine, food industry, cosmetics, agriculture and some special applications of gene delivery, antibacterial activity, inhibition of virus, sensors and treatment of xerostomi (dry mouth) (Ben-Zur & Goldman 2007, Wang *et al.* 2008, Kubota *et al.* 1995, Kurosaki *et al.* 2009, Inbaraj *et al.* 2011, Ogata *et al.* 2009, Uotani *et al.* 2012). PGA can be divided into two isforms, α-PGA and γ-PGA, depending on the attachment of the carboxy group. γ-PGA has been produced extensively using especially *Bacillus* species. It can either be in the form of only L-glutamic acid residues or D-glutamic acid residues. γ-PGA is a ribosome-independent synthesized protein since glutamate is polymerized inside the cell via the γ-amide linkages which results in eliminating the inhibiting effect of substances like chloramphenicol during protein translation. γ-PGA can be in the water-soluble free acid or salt form with a variety of cations

such as Na^+, Mg^{2+}, K^+, NH^{4+} or Ca^{2+} where the latter is completely soluble (Ashiuchi *et al.* 2006, Ogunleye *et al.* 2015). A big obstacle for γ-PGA production and application is its relatively high cost and low productivity which is also recognized for any biotechnologically produced industrial good. Apart from some biopolymers such as polylactic acid and cellulose, many others suffer from high production cost for a successful commercialization (Bajaj & Singhal 2011). One option for cost-efficient production of biopolymers is valorization of renewable resources or wastes, including byproducts of agriculture, horticulture and food industry as low-cost substrates. Among others, feathers could be promising due to their production in large amounts as a waste by-product at poultry processing plants throughout the world. Feathers are composed of over 90% keratin, which is a fibrous and insoluble protein. Highly cross-linked nature of feather with disulfide and other bonds hinders their degradation by commonly known proteolytic enzymes like trypsin, pepsin and papain. Despite the recalcitrance structure of keratin, it can be degraded efficiently by certain bacteria by means of their keratinolytic proteases or keratinases. While established methods such as steam pressure cooking requires high-energy input and the resulted feather meal is deficient in methionine and histidine which restricts to be used as animal feed, hydrolysis of keratinous waste by keratinolytic activity represents an attractive method for its bioconversion and improved nutritional value (Kornillowicz-Kowalska & Bohacz 2011).

Growth substrate costs often constitute the major part of the production cost for microorganisms and bioproducts. Nitrogen sources are usually the most expensive medium compenent. Peptones, as organic nitrogen sources are one of the most important elements for cultivation of microorganisms. On the other hand, these protein hydrolysates (peptones) could be produced from feather keratin and known as feather hydrolysates (FH) (Vasileva-Tonkova *et al.* 2007). This study was performed to demonstrate and evaluate for the first time the use of enzymatically produced FH for the production γ-PGA using biotechnological approaches. In the first step, the native goose feather was used as the sole carbon and nitrogen source to produce keratinolytic enzyme via 30-L fermentation. Then, the lyophilized crude enzyme was utilized to degrade feather to produce FH, and lastly the generated FH was used as a cheap and renewable medium to evaluate the production of γ-PGA in combination with different media compositions.

Materials and Methods

Bacterial strains and cultivation conditions

The bacterial strain used for keratinolytic enzyme production, *Streptomyces pactum* DSM 40530, was grown from spores in GYM medium [glucose (4.0g/L), yeast extract (4.0g/L), malt extract (10.0g/L)]. Agar (12.0g/L) and $CaCO_3$ (2.0g/L) were added for solid medium. The flasks were incubated on a Pilotshake RC-4/6-W horizontal shaker (Kühner AG, Birsfelden, Switzerland) at 30°C, 130rpm and 24-h cultures were used as inocula (5%, v/v). The medium used for keratinolytic enzyme production contained the following (in g/L): goose feather (5.0), K_2HPO_4 (0.1), KH_2PO_4 (0.3), $MgSO_4{\cdot}7H_2O$ (0.3), and 10 mL of trace element solution containing (in mg/L) $CaCl_2$ (3969.5), Fe(III) citrate (979.8), $MnSO_4$ (219.7), $ZnCl_2$ (95.4), $CuSO_4$ (25.5), $CoCl_2$ (40.5), Na_2MoO_4 (24.2) and $Na_2B_4O_7$ (99.2). *S. pactum* was cultivated for 4 days at pH 7 and 30 °C after the medium was autoclaved at 121°C for 20 minutes. Whole goose feathers were obtained from a local company and were used without any pre-treatment procedure for the enzyme production process (Böckle & Müller 1997).

The γ-PGA producer *Bacillus licheniformis* 9945a was grown in Standard I medium or Medium E with 15g/L agar at 37°C for 20h. Strong γ-PGA producers were selected by visual inspection for mucoid colonies by repeated (3 times) restreaking (Leonard *et al.* 1958). Pre-cultures of *B. licheniformis* 9945a were grown overnight in Medium E at 30°C and 130rpm and were used as inocula (2%, v/v). For flask-based γ-PGA production experiments, four different modified versions of Medium E were used with supplementation of FH. The modified media were prepared from the following compounds (in g/L); FH (40.0), L-glutamate (25.6), tri-sodium citrate dihydrate (18.7), glycerol (50.0), K_2HPO_4 (0.5), $MgSO_4{\cdot}7H_2O$ (0.5), $FeCl_3{\cdot}6H_2O$ (0.04), $MnSO_4{\cdot}H_2O$ (0.1), $CaCl_2{\cdot}2H_2O$ (0.2) and 1mL of trace element solution SL-6; $ZnSO_4{\cdot}7H_2O$ (0.1), $MnCl_2{\cdot}4H_2O$ (0.03), H_3BO_3 (0.3), $CoCl_2{\cdot}6H_2O$ (0.2), $CuCl_2{\cdot}2H_2O$ (0.01), $NiCl_2{\cdot}6H_2O$ (0.02), $Na_2MoO_4{\cdot}2H_2O$ (0.03). For different trials, required compounds were added to FH solution separately after autoclaving. The pH of the medium was adjusted to 6.5 with 1N HCl or 5N NaOH as required, and the experiments were performed at 30°C, 130rpm. The flow diagram of the γ-PGA production process is shown in Fig. 1. All experiments were performed in duplicate and the results are presented as the mean values of the duplicates during the course of study.

Keratinolytic enzyme production: 30L-scale fermentation

A Biostat UD30 stainless steel reactor (B. Braun Biotech International, Melsungen, Germany) with a working volume of 30L was connected to a digital control unit capable of controlling fermentation parameters such as temperature, anti-foaming, pH, agitation, and pO_2 level. Foaming was controlled either by mechanical means or by addition of antifoam agent (1%, v/v) Struktol SB2121 (Schill & Seilacher "Struktol" GmbH, Hamburg, Germany) as required. The UD30 fermenter containing the keratinolytic enzyme production medium as described above was autoclaved in situ at 121 °C for 20 min. The pO_2 value in the medium was kept at or above 15% saturation by controlling the agitation rate between 150 and 600rpm at an aeration rate of 0.5vvm (volume per volume per minute). The pH of the medium was held at

7.5±0.1 using 4N of either HCl or NaOH. 10mL of a 24h-old inoculum (prepared in 100-mL flasks) were added to 190mL (prepared in 1L flasks) of fresh GYM medium and cultured for another 24h. Sabsequently, 7 inoculum flasks were combined and transferred to the bioreactor. Samples taken from the bioreactor were analyzed for soluble protein and enzyme activity assays every 24h. After cultivation, the biomass was separated from the broth using a CEPA type Z61 continuous centrifuge (Carl Padberg Zentrifugenbau GmbH, Lahr, Germany) and subsequently the supernatant was passed through a cross-flow filtration unit (Sartoflow, Sartorius) with a 10-kDa molecular weight cut-off in order to increase the enzyme concentration in the retentate. Finally, the retentate was freeze-dried using a BETA 1-16 freeze-drier (Christ, Osterode, Germany) to obtain concentrated crude lyophilizate containing keratinolytic enzyme.

Production of feather hydrolysates by enzymatic degradation

Freeze-dried lyophilizate enriched in keratinases was obtained from the concentrated supernatant of the 30L fermentations where native whole feather was used as the only carbon and nitrogen source, without any further enzyme purification. A set amount of lyophilizate was used for the degradation of feather using screw-cap bottles at 50°C, pH 8.0 and 250rpm for 24h. Unlike the 30L fermentations, a pre-treatment step was applied to the feathers for enzymatic feather degradation experiments. Pre-treatment of feathers was done by degreasing with a methanol-chloroform (1:1) mixture using a Soxhlett apparatus with a 30cm of glass extraction filter. Whole feathers were then suspended in a solution of 10mM Na_2SO_3 (1g feather per 100mL of solution) and autoclaved at 121°C for 20 minutes, followed by an extensive washing step with tap water followed by distilled water. Lastly, feathers were air-dried and stored in the laboratory at room temperature. After incubation of the feathers with lyophilizate without using buffer solution, the resulting media was centrifuged (5000×*g*, 15 minutes) and subsequently filtered using Whatman no. 1 filter paper. After incubation, the residual feather material was washed several times with distilled water and then air-dried at 70°C until a constant weight was obtained. The obtained filtrate served as a source of FH and was stored at +4°C after autoclaving until use as the main carbon, energy and nitrogen source for γ-PGA production (Altun *et al.* 2018). Since the hydrolysate is highly complex and has an undefined composition, the concentration of total FH was calculated by the amount of degraded feather on weight basis. The FH solution was diluted to the desired concentration with distilled water if necessary.

Enzyme activity assay

An enzyme activity assay was adapted to determine the amount of lyophilizate necessary for hydrolyses of pre-treated feather and to ensure the standardisation of the enzyme content of the lyophilizate produced from different cultivations. For this purpose, 120µL of enzyme solution (0.2mg lyophilizate/mL) was added to 480µL of an azocasein solution (10mg/mL) in 100mM phosphate at pH 7.0. The mixture was incubated at 50°C for 30 minutes, and the reaction was stopped by adding 600µL of 10% (w/v) trichloroacetic acid and incubating the preparation on ice for 30 minutes. The mixture was then centrifuged at 10 000×*g* for 10 minutes at 4°C and 800µL of the supernatant was added to 200µL of NaOH (1.8M). One unit of enzyme activity was defined as the amount of enzyme that resulted in an increase of one unit absorbance at 440nm under the assay conditions (Thys *et al.* 2004).

Fig. 1. The flow chart of γ-PGA production process using feather as substrate.

Production and isolation of γ-PGA

The γ-PGA production was realized using 50mL (in 250mL flasks) of variations of Medium E at 30°C and 130rpm with supplementation of 40.0g/L FH as described above. Isolation and purification of γ-PGA was done according to a previously reported method (Troy 1973). Briefly, after the cultures reached stationary phase, half of the culture medium was mixed with an equal volume of ice and blended. After the ice thawed, the cells were separated from the culture broth by centrifugation (60 minutes, 3000×*g*, 4°C) and the resulting pellets were lyophilized after washing with distilled water for cell dry matter (CDM) calculations. The supernatant was mixed with 4 volumes of ice-cold ethanol and incubated for 24h at -20°C. The precipitated γ-PGA was separated from the supernatant by careful decanting and dried for several hours under a stream of compressed air. The crude precipitate was dissolved in 20mL of water, centrifuged to remove insoluble materials, and dialysed against 5.0L of water using dialysis membrane tubing (Spectra/Por®) that had been boiled in 2% $NaHCO_3$ before use. The resultant solution was lyophilized to obtain pure γ-PGA, which was then weighed for yield calculation.

The statistical analysis of the data was performed by using SPSS Version 15.0 software (SPSS Inc., USA). Normality was assessed with the Shapiro–Wilk test and Levene's test was used for homogeneity of variances. One-way analysis of variance (ANOVA) was conducted, followed by pair-wise comparisons of each group using independent sample post hoc tukey test. Significance was designated at $p < 0.05$ for all data analyzed.

Analytical methods

The cell dry matter was determined by weighing the lyophilized cells. The soluble protein concentration of FH was measured by the Bradford method (Bradford 1976). The L-glutamic acid content of the FH and the amino acid constituents of the isolated γ-PGA were determined by high-performance liquid chromatography (HPLC) using a Waters B801 (300- by 4-mm) column (Aboulmagd *et al.* 2000, Steinle *et al.* 2009). Pre-column OPA derivatization was done using a Smartline Autosampler 3900 as described in the manual (Knauer GmbH, Berlin, Germany). Calibration was done with samples from a reference kit for L-glutamic acid (Kollektion AS-10 from Serva Feinbiochemica, Heidelberg, Germany). γ-PGA was hydrolyzed in 6M HCl (100µl/mg γ-PGA) at 95°C overnight, neutralized, and lyophilized before analysis.

Results and Discussion

Keratinolytic enzyme production: 30L scale fermentation

Streptomyces pactum was used for the 30L fermentation for the keratinases production because it is able to use native whole feather as a carbon and nitrogen source without treatment. This eliminates the use of expensive carbon and nitrogen sources such as peptones. The fermentation process was carried out over 4 days as the highest enzyme activity and highest soluble protein content was obtained at 96h, when almost all of the feathers had been degraded (Fig. 2). Further cultivation of the bacteria decreased the soluble protein concentration whereas the enzyme activity did not change dramatically for another 2 days (results are not shown).

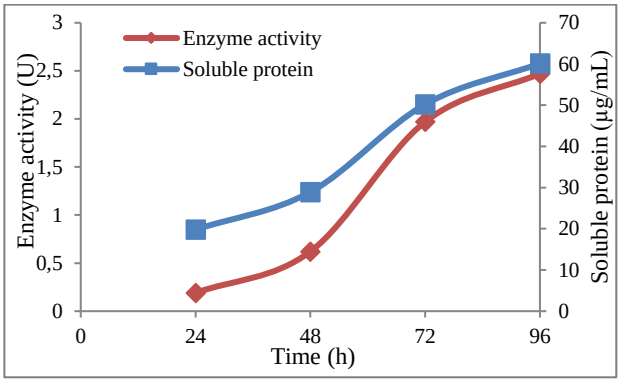

Fig. 2. Changes in enzyme activity and soluble protein during the course of the 30L scale fermentation using *S. pactum*; autoclaved for 20min at 121°C before cultivation, the pO_2 value was kept above 15% saturation by controlling the agitation rate between 150 and 600rpm, aeration rate: 0.5vvm, pH 7.5±0.1.

The pO_2 level, which dropped below 20% during the second day of process, reached 99% saturation after 96h of cultivation, proving that the bacterial metabolism had diminished. Flask experiments (data not shown) also gave similar results, but with a much lower feather degradation rate (up to 60%), most probably because of the unfavorable aeration, mixing, and pH control.

A recent study used feather as a carbon and peptone source for cyanophycin biopolymer production, which is a bacterial storage polymer that is of increasing interest to the scientific community and has applications in various fields of industry (Altun *et al.* 2018). During this study, one of the main problems was that the lyophilized fermentation broth that contained extracellular enzyme also contained substances that had no effect on bacterial growth but lowered the feather degradation performance of keratinases. In the present study, in order to avoid these problems, following the centrifugation an additional step was adopted to wash out such substances from the fermentation broth retentate by using cross-flow filtration which resulted in concentrated crude enzyme. When the total volume of the fermentation broth retentate was decreased by a factor of 15, the washing process increased the volumetric enzyme activity by 8.75-fold. The enzyme activity recovery rate after cross-flow filtration was 58.3%. The protein content of the permeate (below 10kDa in size) accounts for only 2.9% of total protein which shows efficiency of the filtrating process.

Enzymatic feather hydrolysate production

Lyophilization of the concentrated crude enzyme offered many advantages over the liquid form, such as ease of storage, handling, and preservation of enzyme activity over the course of the study (Altun *et al.* 2018). Since one of the goals of the study was to establish a method of producing γ-PGA in a simple, cost- and time-

effective manner, the lyophilizate was not subjected to further processing or purification steps. Production of FH by enzymatic treatment was performed by the addition of lyophilizate containing keratinases to glass screw-cap bottles containing the required amount of pre-treated feathers. Since feather keratin is a recalcitrant material that shows resistance to proteolytic degradation because of its extensively cross-linked structure, e.g. via disulfide bonds, hydrogen bonds, and salt bridges, a single keratinolytic protease is not sufficient for complete keratine hydrolysis. Extensive cystine bridges, which are structural features of feather, prevent the enzymatic degradation of keratine (Sangali & Brandelli 2000, Ramani *et al.* 2005, Kunert 1992, Böckle *at al.* 1995). Therefore, a reducing agent is required to disrupt disulfide bonds and make the feather material susceptible to enzymatic hydrolysis. Experiments from a previous study of our group suggested that Na_2SO_3 was the best candidate among others (cysteine, glutathione, mercaptoethanol and dithioerythritol) because of the relatively cheaper cost, non-toxcicity and efficient disulfide cleavage rate with a concentration of 10mM. An enzyme activity of 8×10^3U per $g^{-1}L^{-1}d^{-1}$ of feather was the optimum value for achieving up to 75% feather degradation. In both cases, further increase of Na_2SO_3 or enzyme concentration did not affect feather degradation performance dramatically. This result is in good accordance with the literature, where the best result (82% feather degradation) was obtained when 10g/L of pre-treated feather (using dithioerythritol as a reductant) was used. For optimum enzyme activity and satisfactory feather degradation rate, an incubation temperature of 50°C at pH 8.0 was appropriate (Böckle *at al.* 1995). Using lyophilizate of the concentrated enzyme obtained by cross-flow filtration greatly increased feather degradation from 43.8% to 73.4%, where the former result was obtained with the lyophilizate from unconcentrated crude enzyme at same activity. According to HPLC analysis, the FH generated by keratinase activity also contained free amino acids such as aspartic acid, serine, arginine, alanin, valine, isoleucine, leucine, lysine, methionine and glutamic acid. Among others, glutamic acid plays an important role in γ-PGA biosynthesis and had a concentration of 15mg per g FH used.

Production of γ-PGA using FH

γ-PGA is up to a hundred-fold more expensive than its conventional alternatives, and a reduction of the production cost seems to be the only option to solve the problem (Sung *et al.* 2005). In order to contribute to the cost-effective γ-PGA production, FH derived from enzymatic hydrolysis of feather was used to produce biopolymer using different media compositions as depicted in Table 1.

Bacillus licheniformis 9945a, the most widely used bacterium for γ-PGA production, was chosen as a model microorganism. As shown in Table 1, while FH, salts and micro nutrients were used in all cultivations, L-glutamate, sodium citrate and glycerol were used interchangeably in four cultivations in order to observe the effect of substrate composition on bacterial growth and γ-PGA production.

Table 1. Chemical composition of different cultivations for γ-PGA production.

Substances	Cltv 1	Cltv 2	Cltv 3	Cltv 4
FH	+	+	+	+
L-glutamate	—	—	—	+
tri-sodium citrate dihydrate	+	—	—	+
Glycerol	+	+	—	—
K2HPO4, MgSO4·7H2O, FeCl3·6H2O MnSO4·H2O, CaCl2·2H2O SL-6 solution	+	+	+	+

Cltv: Cultivation.

Fig. 3 represents the OD_{600} measurements for all cultivations. Cultivation-1 (without L-glutamate) and -2 (without L-glutamate and tri-sodium citrate dihydrate) reached the stationary phase at 60 h and exhibited substantial growth, whereas cultivation-3 (without L-glutamate, tri-sodium citrate dehydrate and glycerol) and -4 (without glycerol) reached stationary phase much earlier, approximately at 30h.

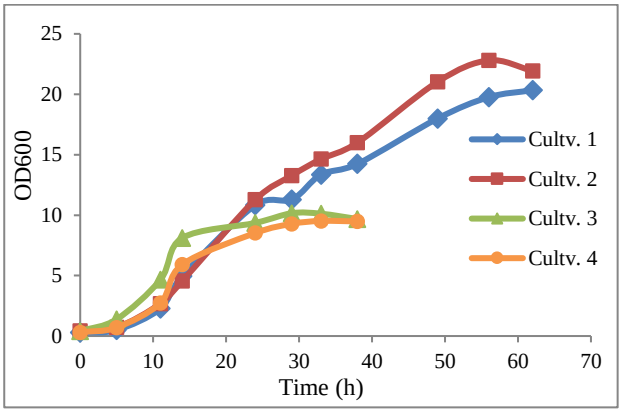

Fig. 3. Changes in OD_{600} values for varied culture compositions during γ-PGA production in flasks; 30°C, 130rpm, inocula: 2% (v/v), pH 6.5, (Erlenmeyer flasks (volume 250ml) contained 50ml of the combined media).

The γ-PGA and CDM yields of cultivations-1 and -2 are much higher than those of cultivations-3 and -4 due to the supplementation of the culture media with glycerol (Table 2.). This result is in good accordance with the literature since glycerol is also reported to encourage PGA production in most studied strains in addition to its favorable effect on bacterial growth. Troy (1973) proposed that glycerol could stimulate polyglutamyl synthetase, which catalyses the polymerization of glutamic acid to PGA and it is also responsible for a decrease of PGA chain length, which lowers the viscosity of the culture broth and increases the uptake rate of substrates, and consequently leads to improved cell growth and PGA production.

As shown in Table 2, the highest yields of 5.4±0.4 and 8.6±0.5g/L were obtained from cultivation-1 for γ-PGA and CDM, respectively, despite the culture media did not contain glutamic acid, an essential precursor for γ-PGA production.

Table 2. γ-PGA yield (g/L) and CDM (g/L) measurement of cultivations in flasks (30°C, 130rpm, inocula: 2% (v/v), pH 6.5).

CDM[a] / γ-PGA[b]		CDM		γ-PGA	
Cultivations	**Mean ± Std. Error**	**Cultivations**	**Mean ± Std. Error**	**Cultivations**	**Mean ± Std. Error**
Cultv-1	8.6 ± 0.5[a] 5.4 ± 0.4[b]	**Cultv-3**	4.2 ± 0.4*	**Cultv-2**	3.2 ± 0.2*
		Cultv-4	5.5 ± 0.3*	**Cultv-3**	1.9 ± 0.2*
				Cultv-4	2.3 ± 0.2*
Cultv-2	7.8 ± 0.4[a] 3.2 ± 0.2[b]	**Cultv-3**	4.2 ± 0.4*	**Cultv-1**	5.4 ± 0.4*
		Cultv-4	5.5 ± 0.3*		
Cultv-3	4.2 ± 0.4[a] 1.9 ± 02[b]	**Cultv-1**	8.6 ± 0.5*	**Cultv-1**	5.4 ± 0.4*
		Cultv-2	7.8 ± 0.4*		
Cultv-4	5.5 ± 0.3[a] 2.3 ± 0.2[b]	**Cultv-1**	8.6 ± 0.5*	**Cultv-1**	5.4 ± 0.4*
		Cultv-2	7.8 ± 0.4*		

This shows that either use of FH and/or presence of citric acid could compensate absence of glutamic acid to some degree during cultivation-1 which should be elaborated with further experiments. In cultivation-2, γ-PGA yield decreased to 3.2±0.2g/L, while CDM yield (7.8±0.4g/L) did not change dramatically. The sharp decrase of γ-PGA yield could be from the fact that this culture was not only missing glutamic acid but also citric acid, which is another crucial precursor and affects γ-PGA production significantly. The lowest values were obtained by cultivation-3, which was included to observe the effect of FH as the sole substrate on CDM and γ-PGA yield, without the use of glycerol and precursors. When the results of cultivation-3 are compared with cultivation-4, it was observed that there is a slight increase in both CDM and γ-PGA yields when glutamic and citric acids were added to the culture medium though the difference was not statistically significant ($p>0.05$) according to the one-way ANOVA with Tukey test. Also, a comparison of cultivations-3 and -2 reveals the significance of glycerol, which increased CDM and γ-PGA yields by 1.9 and 1.7-fold, respectively, however the latter was also not different statistically ($p>0.05$). The present results showed that the effect of glycerol on CDM yield is much higher than that on γ-PGA production and supplementation of FH to the medium is encouraging microbial growth rather than γ-PGA production. In all cultivations, HPLC analysis of extracted γ-PGA showed the high purity of the biopolymer.

Cromwick *et al.* (1996) obtained 15g/L of γ-PGA using *B. licheniformis* 9945a and Medium E in 2L batch fermentations (pH 6.5, 250rpm, 96h), which provides better aeration and pH control than that of flask-based experiments, resulting in increased polymer yield. When the effect of aeration was examined by increasing the agitation speed (250 to 800rpm) and aeration rate (0.5 to 2.0L/min) at pH 6.5, both the γ-PGA and CDM yields increased from 2.0 to 4.0g/L and 6.3 to 23g/L in 48h, respectively. Although the CDM content of cultivation-1 is higher (2 to 4.3-fold) than that of the study of Cromwick *et al.* (1996), the γ-PGA yield is lower (4.3-fold). It is assumed that the media composition used in the present study mostly favored bacterial growth rather than γ-PGA production. Also, the lower γ-PGA yield could be attributed to the unfavorable conditions in flasks, such as inadequate aeration and lack of pH control. Cultivations-1 and -2 were terminated once they reached stationary phase at 60h. It may be assumed that longer cultivation times would be required for enhanced γ-PGA production, as studies with much longer cultivation times are reported in the literature (Hoppensack *et al.* 2003, Goto and Kunioko 1992). Also, the media composition could be another reason, as the strain *B. licheniformis* 9945a is a strictly L-glutamic-acid-dependent microorganism, and an increase in glutamic acid concentration in the medium leads to an enhanced γ-PGA yield (Buescher & Margaritis 2007). Qiu *et al.* (2017) used Jerusalem artichoke as a substrate for γ-PGA production using strain *B. amyloliquefaciens* NX-2S. After one-step fermentation without glutamate supplementation the strain produced 6.85±0.2g/L of γ-PGA whereas exogenous glutamate greatly affected the yield (39.4±0.4g/L).

On the other hand, glutamic acid is also a relatively costly material and therefore directly affects the production cost of PGA. Hence, glutamate-independent producers are more desirable for industrial γ-PGA production because of their low cost of production and ease of operation in fermentations (Cromwick *et al.* 1996, Du *et al.* 2005, Cao *et al.* 2011). Murao *et al.* (1971) reported that *B. subtilis* 5E did not require glutamic acid in the medium, and among the amino acids tested, proline was preferred for efficient polymer production. Proline is also one of the amino acids already exist in culture medium after enzymatic feather degradation (Jeong *et al.*

2010). Moreover, mixtures of hydrolysates obtained from different keratinous sources, like wool, could also create synergy and increase nutritional value for better γ-PGA production. Using carbon sources other than glycerol, such as fructose or glucose together with supplementation of FH could also increase γ-PGA production (Ko & Gross 1998). Thus, it could be envisaged that efficient bioconversion of FH to γ-PGA could be achieved using microorganisms that would not require glutamic and/or citric acid.

Although using keratinolytic enzymes is a promising approach for feather bioconversion, more efficient enzyme production and disulfide cleavage methods are required for economically feasible FH bioproduction. Results of the present study, which was designed as proof of principle suggest that further in-depth investigation of improved culture media compositions with supplementation of FH and use of glutamate and citrate independent strains could lead to an efficient γ-PGA production.

Conclusion

The aim of the present study was to show the biotechnological perspective of the use of enzymatically produced FH as a fermentation substrate for γ-PGA production as a model process. The use of FH as fermentation substrate not only ensures the efficient disposal of feather, which is also classified as a hazardous material creating serious environmental problems worldwide, but also contributes to the valorization of feather with respect to its potential for future applications with biorefinery concept.

Acknowledgement

The author gratefully acknowledges the contribution made by Dr. Martin Krehenbrink from CYSAL GmbH (Münster, Germany) and Prof. Dr. Alexander Steinbüchel (Institute of Molecular Microbiology and Biotechnology, Westfalische Wilhelms-Universitat Muenster, Germany).

References

1. Aboulmagd, E., Oppermann-Sanio, F.B. & Steinbüchel, A. 2000. Molecular characterization of the cyanophycin synthetase from *Synechocystis* sp. strain PCC 6308. *Archives of Microbiology*, 174: 297-306.
2. Altun, M., Wiefel, L. & Steinbüchel, A. 2018. Cyanophycin production from feather hydrolysate using biotechnological methods. *Preparative Biochemistry and Biotechnology*, https://doi.org/10.1080/10826068.2018.1476881.
3. Ashiuchi, M., Shimanouchi, K., Horiuchi, T., Kamei, T. & Misono, H. 2006. Genetically engineered poly-γ-glutamate producer from *Bacillus subtilis* ISW1214. *Bioscience, Biotechnology, and Biochemistry*, 70(7): 1794-1797.
4. Bajaj, I. & Singhal, R. 2011. Poly(glutamic acid) – An emerging biopolymer of commercial interest. *Bioresource Technology*, 102: 5551-5561.
5. Ben-Zur, N. & Goldman, D.M. 2007. γ-Poly glutamic acid: a novel peptide for skin care. *Cosmetics and toiletries*, 122: 65-74.
6. Böckle, B. & Müller, R. 1997. Reduction of disulfide bonds by *Streptomyces pactum* during growth on chicken feathers. *Applied and Environmental Microbiology*, 63(2): 790-792.
7. Böckle, B., Galunsky, B. & Müller, R. 1995. Characterization of a keratinolytic serine proteinase from *Streptomyces pactum* DSM 40530. *Applied and Environmental Microbiology*, 61(10): 3705-3710.
8. Bradford, M.M. 1976. A rapid and sensitive method for the quantitation of microgram quantities of protein utilizing the principle of protein-dye binding. *Analytical Biochemistry*, 72: 248-254.
9. Buescher, J.M. & Margaritis, A.M. 2007. Microbial biosynthesis of polyglutamic acid biopolymer and applications in the biopharmaceutical, biomedical and food industries. *Critical Reviews in Biotechnology*, 27: 1-19.
10. Cao, M., Geng, W., Liu, L., Song, C., Xie, H., Guo, W., Jin, Y. & Wang, S. 2011. Glutamic acid independent production of poly-γ-glutamic acid by *Bacillus amyloliquefaciens* LL3 and cloning of pgsBCA genes. *Bioresource Technology*, 102: 4251-4257.
11. Cromwick, A.M., Birrer, G.A. & Gross, R.A. 1996. Effects of pH and aeration on γ-poly(glutamic acid) formation by *Bacillus licheniformis* in controlled batch fermentor cultures. *Biotechnology and Bioengineering*, 50: 222-227.
12. Du, G., Yang, G., Qu, Y., Chen, J. & Lun, S. 2005. Effects of glycerol on the production of poly(γ-glutamic acid) by *Bacillus licheniformis*. *Process Biochemistry*, 40: 2143-2147.
13. Goto, A. & Kunioka, M. 1992. Biosynthesis and Hydrolysis of Poly(γ-glutamic acid) from *Bacillus subtilis* IF03335. *Bioscience, Biotechnology, and Biochemistry*, 56(7): 1031-1035.
14. Hoppensack, A., Oppermann-Sanio, F.B. & Steinbüchel, A. 2003. Conversion of the nitrogen content in liquid manure into biomass and polyglutamic acid by a newly isolated strain of *Bacillus licheniformis*. *FEMS Microbiology Letters*, 218: 39-45.
15. Inbaraj, B.S., Kao, T.H., Tsai, T.Y., Chiu, C.P., Kumar, R. & Chen, B.H. 2011. The synthesis and characterization of poly(γ -glutamic acid)-coated magnetite nanoparticles and their effects on antibacterial activity and cytotoxicity. *Nanotechnology*, 22(7): 075101.
16. Jeong, J.H., Kim, J.N., Weeb, Y.J. & Ryu, H.W. 2010. The statistically optimized production of poly(γ-glutamic acid) by batch fermentation of a newly isolated *Bacillus subtilis* RKY3. *Bioresource Technology*, 101: 4533-4539.
17. Ko, Y.H. & Gross, R.A. 1998. Effects of glucose and glycerol on γ -poly(glutamic acid) formation by *Bacillus licheniformis* ATCC 9945a. *Biotechnology and Bioengineering*, 57(4): 430-437.
18. Korniłłowicz-Kowalska, T. & Bohacz, J. 2011. Biodegradation of keratin waste: theory and practical aspects. *Waste Management*, 31: 1689-1701.

19. Kubota, H., Nambu, Y. & Endo, T. 1995. Convenient esterification of poly(γ-glutamic acid) produced by microorganism with alkyl halides and their thermal properties. *Journal of Polymer Science*, 33: 85-88.

20. Kunert, J. 1992. Effect of reducing agents on proteolytic and keratinolytic activity of enzymes of *Microsporum gypseum*. *Mycoses*, 35: 343-348.

21. Kurosaki, T., Kitahara, T., Fumoto, S., Nishida, K., Nakamura, J., Niidome, T., Kodama, Y., Nakagawa, H., To, H. & Sasaki, H. 2009. Ternary complexes of pDNA, polyethylenimine, and γ-polyglutamic acid for gene delivery systems. *Biomaterials*, 30: 2846-2853.

22. Leonard, C.G., Housewright, R.D. & Thorne, C.B. 1958. Effects of metallic ions on glutamyl polypeptide synthesis by *Bacillus subtilis*. *Journal of Bacteriology*, 76: 499-503.

23. Murao, S., Murakawa, T. & Omata, S. 1971. Polyglutamic acid fermentation: Culture condition for the production of polyglutamic acid by *Bacillus subtilis* no. 5E, effects of amino acids and glucose. Part II. *Nippon Nogeikagaku Kaishi*, 45: 118-123.

24. Ogata, M., Hidari, K.I., Murata, T., Shimada, S., Kozaki, W., Park, E.Y., Suzuki, T. & Usui, T. 2009. Chemoenzymatic synthesis of sialoglycopolypeptides as glycomimetics to block infection by avian and human influenza viruses. *Bioconjugate Chemistry*, 20: 538-549.

25. Ogunleye, A., Bhat, A., Irorere, V.U., Hill, D., Williams, C. & Radecka, I. 2015. Poly-γ-glutamic acid: production, properties and applications. *Microbiology*, 161: 1-17.

26. Qiu, Y., Sha, Y., Zhang, Y., Xu, Z., Li, S., Lei, P., Xu, Z., Feng, X. & Xu, H. 2017. Development of Jerusalem artichoke resource for efficient one-step fermentation of poly-(γ-glutamic acid) using a novel strain *Bacillus amyloliquefaciens* NX-2S. *Bioresource Technology*, 239: 197-203.

27. Ramani, P., Singh, R. & Gupta, R. 2005. Keratinolytic potential of *Bacillus licheniformis* RG1: structural and biochemical mechanism of feather degradation. *Canadian Journal of Microbiology*, 51(3): 191-196.

28. Sangali, S. & Brandelli, A. 2000. Feather keratin hydrolysis by a *Vibrio* sp. strain kr2. *Journal of Applied Microbiology*, 89: 735-743.

29. Steinle, A., Bergander, K. & Steinbüchel, A. 2009. Metabolic engineering of *Saccharomyces cerevisiae* for production of novel cyanophycins with an extended range of constituent amino acids. *Applied and Environmental Microbiology*, 75: 3437-3446.

30. Sung, M.H., Park, C., Kim, C.J., Poo, H., Soda, K. & Ashiuchi, M. 2005. Natural and edible biopolymer poly- γ -glutamic acid: synthesis, production, and applications. *Chemical Record*, 5: 352-366.

31. Thys, R.C.S., Lucas, F.S., Riffel, A., Heeb, P. & Brandelli, A. 2004. Characterization of a protease of a feather degrading *Microbacterium* species. *Letters in Applied Microbiology*, 39: 181-186.

32. Troy, F.A. 1973. Chemistry and biosynthesis of the poly(γ-D-glutamyl) capsule in *Bacillus licheniformis*. I. Properties of the membrane mediated biosynthesis reaction. *Journal of Biological Chemistry*, 248: 306-315.

33. Uotani, K., Hidetoshi, K., Endou, H. & Tokita, F. 2012. Sialogogue, oral composition and food product containing the same. *US Patent 7910089 B2*.

34. Vasileva-Tonkova, E., Nustorova, M. & Gushterova, A. 2007. New protein hydrolysates from collagen wastes used as peptone for bacterial growth. *Current Microbiology*, 54: 54-57.

35. Wang, Q., Chen, S., Zhang, J., Sun, M., Liu, Z. & Yu, Z. 2008. Co-producing lipopeptides and poly- γ -glutamic acid by solid-state fermentation of *Bacillus subtilis* using soybean and sweet potato residues and its biocontrol and fertilizer synergistic effects. *Bioresource Technology*, 99: 3318-3323.

http://dergipark.gov.tr/trkjnat
Trakya University Journal of Natural Sciences, 20(1): 35-46, 2019
ISSN 2147-0294, e-ISSN 2528-9691
DOI: 10.23902/trkjnat.493928

Research Article

Rheocricotopus (s. str.) *costai* sp. n. AND *R.* (s. str.) *pyrenaeus* sp. n., TWO RELICT SPECIES FROM GLACIAL RHEOCRENES AND STREAMS IN CORSICA AND THE EASTERN PYRENEES (DIPTERA: CHIRONOMIDAE, ORTHOCLADIINAE)

Joel MOUBAYED-BREIL[1*], Patrick ASHE[2]

[1] Freshwater & Marine biology, 10 rue des Fenouils, F-34070 Montpellier, FRANCE
[2] 33 Shelton Drive, Terenure, Dublin 12, D12 PK68, IRELAND
* Corresponding author: ORCID ID: orcid.org/0000-0002-6793-5746, e-mail: jm.aquabiol@free.fr

Cite this article as:

Moubayed-Breil, J. & Ashe, P. 2019. *Rheocricotopus* (s. str.) *costai* sp. n. and *R.* (s. str.) *pyrenaeus* sp. n., two relict species from glacial rheocrenes and streams in Corsica and the eastern Pyrenees (Diptera: Chironomidae, Orthocladiinae). *Trakya Univ J Nat Sci*, 20(1): 35-46, DOI: 10.23902/trkjnat.493928

Received: 10 December 2018, Accepted: 4 March 2019, Online First: 13 March 2019, Published: 15 April 2019

Abstract: Two new species of the genus *Rheocricotopus* subgenus *Rheocricotopus* (*R. costai* sp. n. and *R. pyrenaeus* sp. n.) are diagnosed and described, based on material collected in some glacial rheocrenes and streams located in the high mountains of Corsica and the Eastern Pyrenees. *Rheocricotopus costai* sp. n. is described as male and pupal exuviae, while *R. pyrenaeus* sp. n. is described as male and female adults and pupal exuviae. *Rheocricotopus costai* sp. n. is known from both western Corsica and the Eastern Pyrenees, while the geographical distribution of *R. pyrenaeus* sp. n. is restricted to the protected area of the Mantet Nature Reserve (Eastern Pyrenees). Larvae of both *R. costai* sp. n. and *R. pyrenaeus* sp. n. are exclusively rheophilic being confined to lotic habitats located at high altitude (crenal and rhithral). Apart from the presence of an additional median circular small patch of spinules on tergite III of the exuviae, *R. costai* sp. n. directly keys into the *effusus*-group on the basis of several specific characters found in the male adult. Nevertheless, *R. pyrenaeus* sp. n. keys near both of *R. reduncus* Sæther & Schnell, 1988 (known from Finland, Norway and Russian Far East) and *R. tchernovskii* Makarchenko & Makarchenko, 2005 (known from Russian Far East), based in particular, on the unusual shape of the superior volsella which is inwardly markedly turned over distally. The genus *Rheocricotopus* is currently represented by 10 species in continental France and by 8 species in Corsica (Moubayed-Breil 2016). Consequently, the description of *R. costai* sp. n. and *R. pyrenaeus* sp. n. increases the total number in the genus to 12 for continental France and to 9 for Corsica. Taxonomic remarks, discussion and comments on the ecology and geographical distribution of the two new species are given.

Key words: *Rheocricotopus* (*s. str.*), new species, Diptera Chironomidae, glacial rheocrenes, Corsica, continental France, conservation.

Özet: Bu çalışmada, Korsika ve Pireneler'deki yüksek dağlarda yer alan glasiyal rheokrenler ve akarsulardan toplanmış materyal incelenmiş ve *Rheocricotopus* cinsine ait iki yeni tür (*R. costai* sp. n. and *R. pyrenaeus* sp. n.) tanımlanmıştır. *Rheocricotopus costai* sp. n. erkek birey ve pupal kılıf ile tanımlanırken *R. pyrenaeus* sp. n. yetişkin erkek ve dişi bireyler ve pupal kılıf ile tanımlanmıştır. *Rheocricotopus costai* sp. n. hem Batı Korsika'dan hem de Pireneler'in doğusundan elde edilirken *R. pyrenaeus* sp. n.'nın coğrafik dağılımı Doğu Pirenler'de bir koruma alanı olan Mantet doğa koruma alanı ile sınırlıdır. Hem *R. costai* sp. n. hem de *R. pyrenaeus* sp. n. larvaları yüksek rakımlardaki lotik habitatlarda sınırlı olduklarından reofilik özelliktedirler. *Rheocricotopus costai* sp. n., pupal kılıfın 3. tergiti üzerinde medyan alanda yer alan küçük dairesel spinül yamasına ek olarak yetişkin erkeklerdeki çeşitli spesifik karakterleri ile *effusus*-grubu içinde yer almaktadır. *Rheocricotopus pyrenaeus* sp. n. ise özellikle distalde içe doğru dönük olan superior volsellanın olağan olmayan şekli bakımından Finlandiya, Norveç ve Uzak Doğu Rusyası'ndan bilinen *R. reduncus* Sæther & Schnell, 1988 ile Uzak Doğu Rusyası'ndan bilinen *R. tchernovskii* Makarchenko & Makarchenko, 2005'e benzemektedir. *Rheocricotopus* cinsi Fransa'da 10, Korsika'da ise 8 tür ile temsil edilmekteydi (Moubayed-Breil 2016). Sonuç olarak, *R. costai* sp. n. and *R. pyrenaeus* sp. n.'nın tanımlanması ile cinsin Fransa'daki tür sayısı 12'ye, Korsika'daki tür sayısı ile 9'a çıkmıştır. İki yeni türün ekolojileri ve coğrafik dağılımları ile ilgili taksonomik notlar, görüşler ve değerlendirmeler verilmiştir.

Introduction

Data on the taxonomy and geographical distribution of the known *Rheocricotopus* species from Europe and some neighbouring areas (Brundin 1956, Lehmann 1969, Chaudhuri & Sinharay 1983, Sæther 1986, Sæther & Schnell 1988, Coffman *et al*. 1986, Langton 1991, Wang & Zheng 1989, Bhattacharyay *et al*. 1991, Wang 1995, Wang & Sæther 2001, Makarchenko & Makarchenko 2005, Langton & Pinder 2007, Ashe & O'Connor 2012, Ree 2013, Sæther & Spies 2013, Liu *et al*. 2014a, 2014b, Moubayed-Breil 2016) shows that there are currently about 77 valid species and subspecies worldwide of which only 13 are reported from Europe. Members of the genus

Rheocricotopus Thienemann & Harnisch, 1932 consist of exclusively rheophilic species which are encountered in lotic habitats extended from the upper reaches of streams (crenal, rhithral and peat bogs) to the lower reaches of rivers (potamal).

The genus *Rheocricotopus* has been revised and divided into two subgenera (*Psilocricotopus* and *Rheocricotopus*) by Sæther (1985), who recognised and created three different groups within each subgenus: *godavarius*-group, *chalybeatus*-group and *atripes*-group for *Psilocricotopus* subgenus; *effusus*-group, *fuscipes*-group and *tuberculatus*-group for *Rheocricotopus* subgenus.

Rheoccricotopus costai sp. n. and *R. pyrenaeus* are diagnosed and described based on material collected in some glacial rheocrenes and streams located in the high mountains of Corsica and the Pyrenees. *Rheoccricotopus costai* sp. n. is described as male adult and pupal exuviae, while *R. pyrenaeus* sp. n. is described as male and female adults and pupal exuviae.

The two new described species directly key into the *effusus*-group created by Sæther (1986) for known *Rheocricotopus* species (Nearctic, Palaearctic and Oriental Regions), on the basis of the following characters found in the male adult and pupal exuviae: humeral pit reduced or ellipsoid with smaller separate ellipsoid pit below; superior volsella rounded or right-angled with distal short or long pronounced projection; gonostylus with or without long crista dorsalis; frontal setae present on frontal apotome; median circular patch of spines/or strong spinules present on tergites IV-VI. Meanwhile the male adult and pupal exuviae of *R. costai* sp. n. show some morphological affinities with some members of the *effusus*-group, those of *R. pyrenaeus* sp. n. keys near both *R. reduncus* Sæther & Schnell, 1988 and *R. tchernovskii* Makarchenko & Makarchenko, 2005 on the basis, in particular, of the unusual shape of the superior volsella which is markedly turned over inwards distally. Moreover, *R. costai* sp. n. seems to belong to a local 'Pyreneo-corsican element', based on the presence of an additional small median patch of spinules on tergite III of the exuviae. Consequently, a fourth additional group within the subgenus *Rheocricotopus*, the '*reduncus*-group', could be created which would include, *R. reduncus*, *R. tchernovskii* and *R. pyrenaeus* sp. n.

According to Moubayed-Breil (2016), there are 13 valid *Rheocricotopus* species known from Europe, of which 10 are reported from France: *R. atripes* (Kieffer, 1913); *R. chalybeatus* (Edwards, 1929); *R. gallicus* Lehmann, 1969; *R. glabricollis* (Meigen, 1830); *R. meridionalis* Moubayed-Breil, 2016; *R. subacutus* Caspers & Reiss, 1989; *R. thomasi* Moubayed-Breil, 2016; *R. tirolus* Lehmann, 1969; *R. effusus* (Walker, 1856) and *R. fuscipes* (Kieffer, 1909). Consequently, the description here of *R.* (*R.*) *costai* sp. n. and *R.* (*R.*) *pyrenaeus* sp. n. currently increases the total number of species in the genus *Rheocricotopus* to 12 from France and to 15 in Europe.

In this paper, *R. costai* sp. n. (known from western Corsica and France) and *R. pyrenaeus* sp. n. (known from south western France) are diagnosed and described based on material collected in glacial springs and streams at high altitude. *Rheocricotopus costai* sp. n. is identical with '*R.* (*Rh.*) sp. 1' in Moubayed-Breil & Ashe (2012), while *R.* (*Rh.*) *pyrenaeus* sp. n. is the same as '*R.* (*Rheocricotopus*) sp. 1' in Moubayed-Breil & Ashe (2016). The first new species (*R. costai*) is described as male adult and pupal exuviae, the second (*R. pyrenaeus*) as male and female adults and pupal exuviae.

Materials and Methods

The examined material was collected using some standard methods: Surber net for the benthos (larvae and pupae); Brundin drift nets for pharates, pupae and drifted pupal exuviae; troubleau net for individuals floating on the surface of the water and a sweep net for flying adults. Male adults were preserved in 80% Ethanol, then cleared of musculature in 90% lactic acid (head, thorax, abdomen and anal segment) for about 60 to 80 minutes, but can be left overnight at room temperature without any detrimental effect or damage. The specimens were checked under a binocular microscope after 20 minutes in lactic acid to determine how the clearing was progressing. When clearing was complete the specimens were washed in two changes of 70% Ethanol to ensure that all traces of lactic acid were removed.

The studied material was mounted in polyvinyl lactophenol. Before the final slide mountings (dorsally) of the male holotype and paratype material, the hypopygium including the IXth tergum, the anal point, the gonocoxite and the gonostylus, were viewed ventrally and laterally to examine and draw from both sides all the necessary details of each species. In particular, the ventral view of the hypopygium was illustrated when the anal point and tergite IX were removed.

Part of the abdomen and the halters of the male adults were preserved in 85% ethanol for an eventual DNA analysis. Morphological terminology and measurements follow that of Sæther (1980, 1985) and Langton & Pinder (2007) for the adults and Sæther (1980) and Langton (1991) for the pupal exuviae. Taxonomic remarks on some related species from Europe and neighbouring geographical areas, as well as discussion and comments on the ecology and geographical distribution of the two new species are provided.

Descriptions

Rheocricotopus (*Rheocricotopus*) *costai* sp. n.

LSID:urn:lsid:zoobank.org:act:D1B65F1D-6893-4B49-ACDF-A3A15F618046

Material examined

Holotype. **Corsica**. 1 male adult, leg. J. Moubayed-Breil, glacial stream, upper basin of the Asco River at the locality of 'High-Asco', (42° 27' 13" N, 09° 01' 57" E), altitude 1550-1800 m, 05.VI.2015.

Paratype (all, leg. J. Moubayed-Breil). **Corsica**. 1 male pharate adult, same locality and data as for holotype. **Continental France** (Eastern Pyrenees, biogeographical zone 8a, as given in Moubayed-Breil & Ashe (2016), 1 male pharate adult and 2 female pharate adults, glacial springs and streams, upper basin of the River Tech, (42.428° N, 2.361° E), alt. 1800-2000 m, 03.VI.2005. 1 male adult, glacial springs and streams, Pic Carlit (42.57° N, 1.93° E), alt. 2000 m, 05.VI.2001. Environmental data of aquatic habitat: crystalline water, conductivity 35-40 µS/cm, pH 5.5-5.7; temperature 8-12°C.

The Holotype (male adult, on one slide) is deposited in the collections of the National Museum of Ireland, Kildare Street, Dublin 2, Ireland. Remaining paratypes are deposited in the senior author's collection.

Type material was preserved in 80% ethanol, and later mounted in polyvinyl lactophenol. For each adult, the head, thorax and abdomen were cleared in 90% lactic acid, then washed in 70% ethanol before mounting on slides.

Etymology: The new species is named *"costai"* in honour of Jacques Costa (president of the Nature Regional Park of Corsica), who is actively contributing to preserving the environment and species associated with all aquatic habitats occurring in the protected areas of Corsica.

Diagnostic characters

Apart from the presence of an additional median small patch of spinules on tergite III of exuviae, *R. costai* sp. n. belongs to the *effusus*-group based on some other characters found in the male adult: humeral pit elongate ellipse-like, superior volsella with a pronounced distal projection. However, this new species can be distinguished from other related members of the *effusus*-group in having:

- male adult. Coronal area with 2 coronals (1 seta on each side); lobes of antepronotum not gaping and thinner medially; tarsomere ta_5 of PI, PII and PIII entirely blackish; sensilla chaetica present on tarsomeres ta_4-ta_5 of PI, PII and PIII; humeral pit extremely elongate ellipsoid, narrowing distally, with a distinct smaller separate oval pit below; tergite IX with a weak hump medially, which is clearly visible in lateral view; anal point with 12-14 lateral setae, apex unusually rounded; superior volsella broadly bent downwards, nose-like apically, distal part short and distinctly projecting downwards; inferior volsella long, finger-like in shape, dorsal side large and lobe-like, ventral side triangular; posterior side of gonostylus swollen medially and abruptly narrowing apically, anterior side with 2 rows of setae at obtuse angle; crista dorsalis short, tooth-like, only visible when viewed laterally and at right-angle, located distally and occupying 20 to 30% of the total length of the gonostylus.

- pupal exuviae. Frontal apotome weakly covered with wrinkles; thoracic horn finger-like and strongly toothed on one side. Circular median patch of spines and spinules present on tergites III-VI; patch on tergite III smaller and armed with short spinules; patches on tergites IV-VI are subequal, more extensive and armed with much bigger and longer spines.

Male imago

(n = 3: 1 male adult and 2 male pharate adults; Figs. 1-5, 9, 12, 14-16, 19-21, 31)

= "*R.* (*Rh.*) sp. 1" in Moubayed-Breil & Ashe (2012)

Large sized species (among the largest species of *Rheocricotopus* s. str.). Total length 3.45-3.55 mm. Wing length 1.60-1.65 mm. General colouration variable from dark brown to blackish. Head, antenna and halters dark brown. Thorax dark brown with blackish mesonotal stripes; humeral pit brownish. Legs dark brown, tarsomeres ta_5 of PI, PII and PIII blackish (Fig. 5). Abdominal tergites and anal segment dark brown. **Head**. Eyes hairy, elongated vertically. Coronal area (Fig. 31) with 2 coronals (1 seta on each side); Temporal setae 10, including 5 inner, 3 outer verticals and 2 postorbitals. Palp 5-segmented, length (µm) of palpomeres 1-5: 45, 30, 85, 95, 105; distal part of third palpomere (Fig. 1) with 3 sensilla clavata and 4 sensilla coeloconica (Fig. 2). Clypeus (Fig. 3) semicircular, bearing 12 setae in 3 rows. Antenna 970 µm long, last flagellomere 520 µm long, distinctly clubbed distally, bearing a brush of curved sensilla chaetica apically; antennal groove reaching flagellomeres 2-3. AR 1.15. **Thorax**. Lobes of antepronotum not gaping with dome-like median area; lateral anteprotonotals 7 including 5 located distally and 2 vestigial located medially; acrostichals 18 in 1 row; dorsocentrals 9-10 in 1 row; prealars 3, supraalars absent. Humeral pit (Fig. 9) strongly elongate, ellipsoidal with narrowed distal part, a distinct smaller separate oval pit is located below. Scutellum with 8 uniserial setae. Wing. Brachiolum with 3 setae. Distribution of setae on veins: R, 7-8; R_1, 0-1; R_{4+5}, 1-2; other veins bare. Squama with 7 setae in 1 row. Legs. Length (µm) of tibial spurs of: PI, distinctly spiniforme, 60; PII, 25 and 35; PIII, 65 and 30; longest seta of tibial comb 65 µm long. Sensilla chaetica present in low number (proximally and distally) on tarsomeres ta_1-ta_5 of PI, PII and PIII. Length (µm) and proportions of prothoracic (PI), mesothoracic (PII) and metathoracic (PIII) legs as in Table 1.

Abdomen. Hypopygium in dorsal and ventral view (Figs. 14-15). Tergite IX nearly semicircular, with a weak median hump, which is clearly visible in lateral view (Fig. 12). Anal point about 45 µm long, triangular, large at base, uniformly narrowed distally and ending with a distinct rounded apex; 12-14 setae are present laterally (6-7 on each side). Latero-sternite IX with 5 setae. Transverse sternapodeme and phallapodeme as in Figs. 15-16. Virga absent. Gonocoxite about 250 µm long, maximum width 25-30 µm, distinctly truncate apically. Superior volsella (Figs. 15-16) widely projecting downwards and ending with a rounded apex; inferior volsella large and lobe-like dorsally with a long finger-like apex, ventral side triangle-like. Gonostylus in dorsal, lateral and ventral view (Figs. 14, 19-21) 85 µm long, 25 µm maximum width, posterior margin swollen medially and abruptly narrowing apically, anterior surface with 2 rows of setae clearly visible at obtuse angle; crista dorsalis located distally close to the megaseta, short tooth-like and only visible in right-angle view (Figs. 20-21).

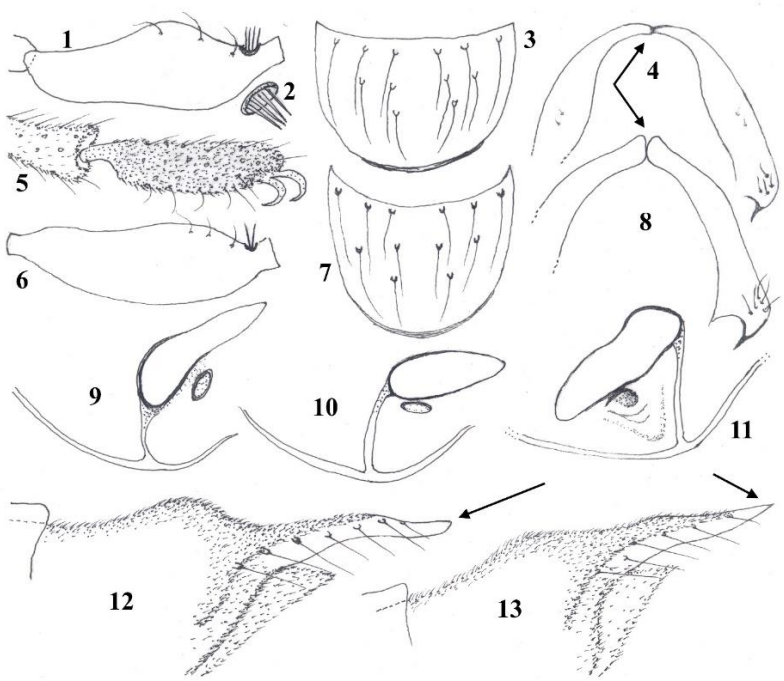

Figs. 1-13. Male imago of *Rheocricotopus* (*s. str.*) spp. *R. costai* sp. n.: palpomere 3 (1); with details of sensilla coeloconica (2); clypeus (3); lobes of antepronotum (4); apex of tarsomeres 4 and 5 (5). *Rheocricotopus effusus*: palpomere 3 (6); clypeus (7); lobes of pronotum (8). Humeral pit of: *R. costai* sp. n., holotype (9); *R. effusus* (10); *R. pyrenaeus* sp. n. (11). Lateral view of tergite IX and anal point of: *R. costai* sp. n. (12); *R. effusus* (13).

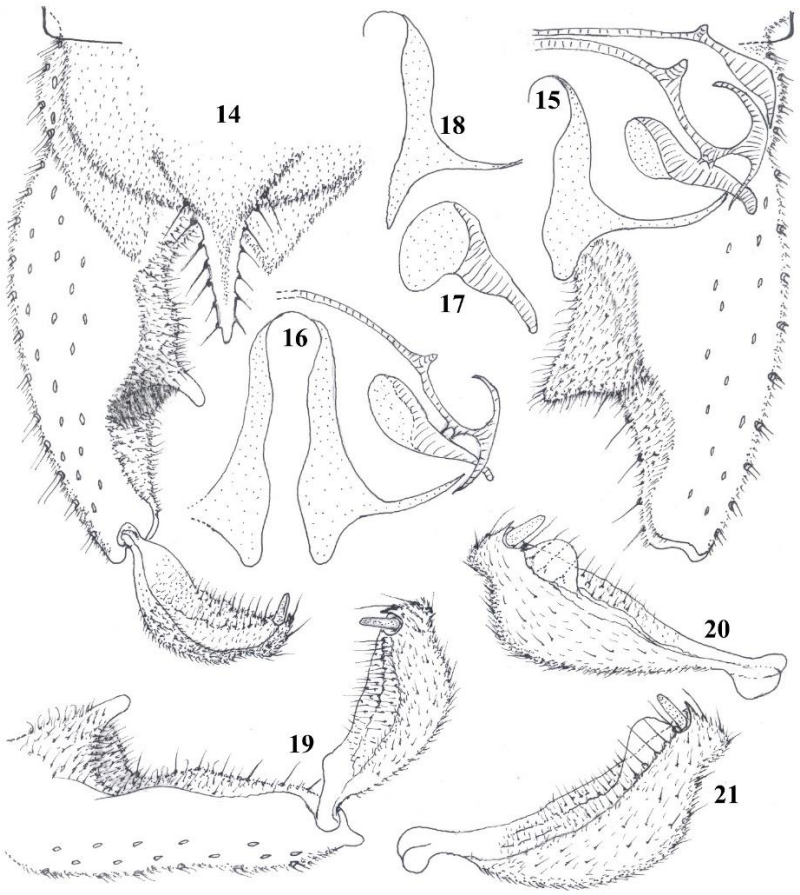

Figs. 14-21. Male imago of *Rheocricotopus* (*s. str.*) spp. *R. costai* sp. n.: hypopygium in dorsal (14) and ventral view (15), with tergite and anal point removed); superior volsella, sternapodeme and phallpodeme (16). *R. effusus*: phallapodeme (17); superior volsella (18). *R. costai* sp. n.: gonocoxite and gonostylus in lateral view (19); gonostylus (right angle, dorsal, 20 and ventral, 21).

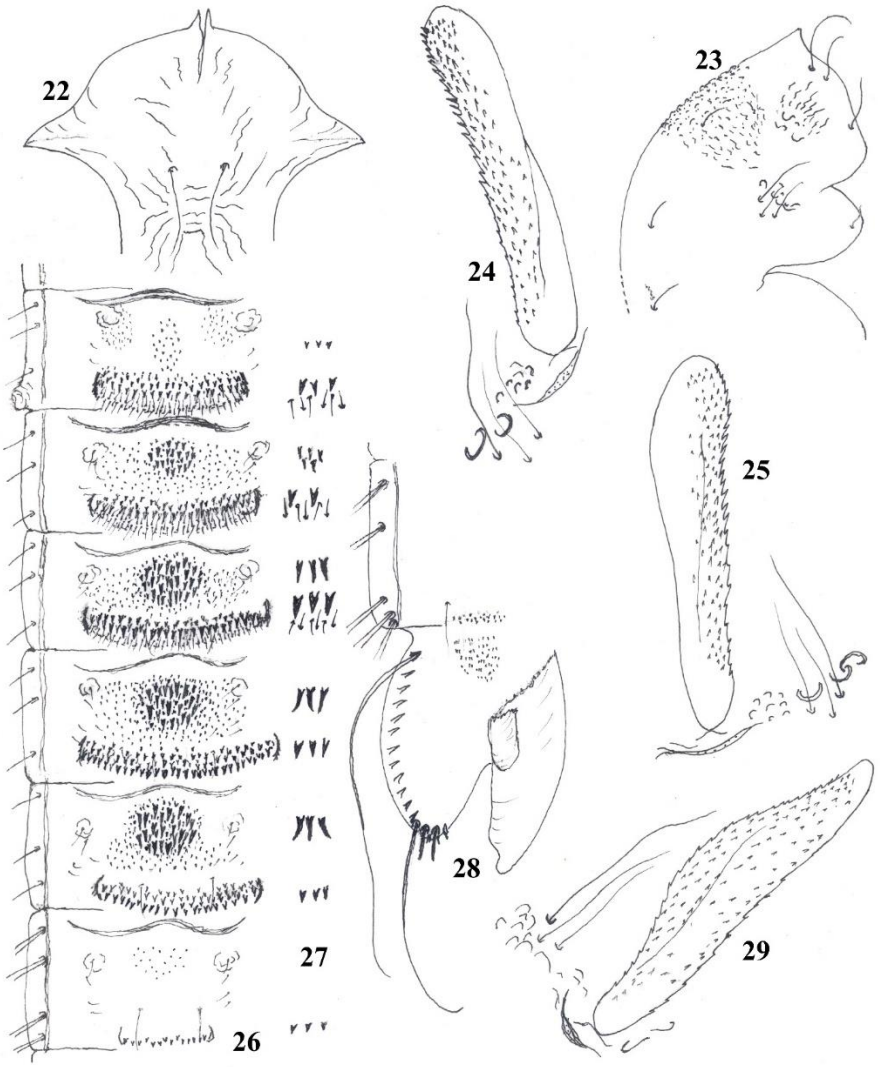

Figs. 22-29. Pupal exuviae of *Rheocricotopus* (*s. str.*) spp. *R. costai* sp. n.: frontal apotome (22); cephalothorax (23); two aspects of thoracic horn (24-25); distribution pattern of armament and chaetotaxy of abdominal segments II-VII (26); details of armament on tergites II-VII and conjunctives (27); tergite VIII and anal segment (28). *R. effusus*: thoracic horn (29).

Pupal exuviae

(n = 4: 2 males and 2 females; Figs. 22-28)

Total length 3.60-3.65 mm. Colouration brownish in general. Frontal apotome brown and weakly wrinkled. Anterio-median area of cephalothorax including the thoracic suture markedly rugulose and wrinkled; blackish shading present near the base of thoracic horn and wing sheath; outer and inner margin of antennal sheath brownish. Abdomen brown yellowish, lateral margin of segments I-VIII dark brown. Anal lobe and genital sac brown yellowish. Cephalothorax as in Figs. 22-23. Frontal apotome (Fig. 22) broadly semicircular, lateral margin with a distinct triangular expansion, frontal setae 95-100 µm long, distance between frontal setae 25 µm. **Thorax**. Median antepronotals are nearly subequal (160 and 155 µm long), 1 lateral antepronotal 105 µm long; prealars, 1 vestigial seta; precorneals 190, 180 and 125 µm long, inserted long distance from base of thoracic horn. Thoracic horn (Figs. 24-25) about 320-330 µm long, maximum width 40-50 µm, finger-like, linearly elongated and strongly toothed on one side, teeth becoming gradually larger towards apex. Dorsocentrals Dc_1-Dc_4 (Fig. 23) include: 3 sub-equal setae (Dc_1, Dc_2 and Dc_4 = 55 µm long), Dc_3 20 µm long; distance (µm) between: Dc_1 to Dc_2 185, Dc_2 to Dc_3 130, Dc_3 to Dc_4 15.

Abdomen. Armament, chaetotaxy, distribution pattern of shagreen and details of armament on tergites II-VII as in Figs. 26-27. All pleurae and tergite I bare. Pedes spurii A present on sternites IV-VI, pedes spurii B present only on segment II. Caudal transverse rows of posteriorly projecting stout spines (3-4 rows) present on tergites II-VI, those on tergites IV-V are the widest (350-400 µm); caudal transverse rows (2-3) of orally and posteriorly directed pins are restricted to conjunctives of tergites II-IV, those on tergite IV are the widest (390 µm); caudal transverse rows of short spines and spinules (about 120-150 µm wide) are present on tergites VII-VIII.

Table 1. Male adult of *Rheocricotopus costai* sp. n. Length (µm) and proportions of prothoracic (PI), mesothoracic (PII) and metathoracic (PIII) legs.

	fe	ti	ta_1	ta_2	ta_3	ta_4	ta_5	LR	BV	SV	BR
PI	585	690	535	275	225	160	115	0.78	2.34	2.38	2.10
PII	735	685	365	175	145	105	90	0.53	3.47	3.89	2.60
PIII	1190	1360	730	265	215	125	95	0.54	4.69	3.49	3.40

LR = Length of tarsomere ta_1 divided by length of tibia (ti); BV = Combined length of femur (fe), tibia and ta_1 divided by combined length of tarsomeres ta_2-ta_5; SV = Ratio of femur plus tibia to tarsomere ta_1; BR = Ratio of longest seta of ta_1 divided by minimum width of ta_1, measured one third from apex.

Distribution pattern, shape and size of circular median patch of stout spines on tergites IV-VI as in Figs. 26-27: those on tergites V-VI are subequal in size, more extensive and armed with much larger spines, longest spines 18-20 µm long; median patch on tergite III is smaller and armed with short spinules, longest one 10-12 µm long; caudal transverse rows (1-2) of short spines present on tergites VII-VIII (maximum width 120-150 µm). Number and distribution pattern of lateral setae and lamelliform setae (taeniae) on segments I-VIII as in Fig. 26: lateral setae on segments I-VI (1, 3, 3, 3, 3, 3); taeniae on segments VII-VIII (4, 5). Anal segment (Fig. 28): anal lobe 225 µm long, 250 µm maximum width, fringe with 15-17 taeniae; genital sac 190-200 µm long, overreaching apical margin of anal lobe by 35-40 µm; macrosetae 310-325 µm long, curved and pointed apically.

Larva

Known but not described.

***Rheocricotopus* (*Rheocricotopus*) *pyrenaeus* sp. n.**

LSID:urn:lsid:zoobank.org:act:3875E849-80A2-4710-AE18-551F2D573119

Material examined

Holotype. **Continental France**. 1 male pharate adult, leg. J. Moubayed-Breil, Mantet Nature Reserve (Eastern Pyrenees), upper basin of 'Font des Soques', glacial springs and stream, altitude 2000 m, (42° 28' 38" N, 02° 18' 26" E), 05.08.2010. Environmental data of aquatic habitat: crystalline water, conductivity 30-40 µS/cm, pH 5.5-5.7; temperature 6-12°C.

Paratypes (all leg. J. Moubayed-Breil). 3 pharate adults (1 male and 2 females), 1 pupal exuviae, same locality and data as for holotype. Callau acid springs and peat bogs at Mantet Nature Reserve, 1 male adult and 1 male pharate adult, alt. 2000-2300 m, 05.08.2010. Environmental data of aquatic habitat: crystalline water, conductivity 20-30 µS/cm, pH 5.5-5.7; temperature 6-12°C.

Holotype (male adult + its pupal exuvie, on 1 slide) is deposited in the collections of the National Museum of Ireland, Kildare Street, Dublin 2, Ireland. Paratypes are deposited in the senior author's collection.

Type material was preserved in 80% ethanol, and later mounted in polyvinyl lactophenol. For each adult, the head, thorax and abdomen were cleared in 90% lactic acid, then washed in 70% ethanol before mounting on slides.

Etymology: The new species is named *'pyrenaeus'* after the Pyrenees mountains where its geographical distribution is currently restricted to the protected area of the 'Mantet Nature Reserve', (located in the Eastern Pyrenees of France), which covers glacial springs, peat bogs and pristine cold streams.

Diagnostic characters

Rheocricotopus pyrenaeus sp. n. directly keys near both *R. reduncus* (Finland, Norway and Russian Far East) and *R. tchernovskii* (Russian Far East) in the *effusus*-group based, on the following two main imaginal and pupal characters: distal part of superior volsella markedly turned over and curved inwards; median circular patch of spinules on tergite IV much smaller than those on tergites V-VI. However, this new species can be separated from other related members of the *effusus*-group in having:

- male adult. Coronal area with 4 coronals (2 setae on each side); lobes of antepronotum thick and widely gaping medially; distal half of tarsomere ta_5 of PI, PII and PIII blackish; humeral pit ellipsoidal, moderately elongate, larger in proximal part with a distinct smaller half oval-like pit below; tergite IX bearing a distinct hump medially, which is clearly visible in lateral view; apex of anal point sharply pointed; superior volsella broad, nose-like apically, distal part distinctly projecting and turned over inwards; dorsal side of inferior volsella triangular with large thumb-like apex, ventral side triangular; posterior side of gonostylus swollen medially in both lateral view and at right-angles, distal part constricted near the apex; crista dorsalis clearly visible in lateral and at right-angles, widely extended distally from mid-distance till apex, semicircular and occupying 70 to 80 % of the total length of gonostylus.

- pupal exuviae. Frontal apotome nearly semicircular, anterior half covered with faint and fine wrinkles; thoracic horn markedly clubbed and toothed on one side. Circular median patch of spines present on tergites IV-VI; patch on tergite IV distinctly smaller and armed with short spinules; patches on tergites V-VI are subequal, more extensive and armed with much longer and larger spines.

Male imago

(n = 3: 1 male adult and 2 male pharate adults; Figs. 30, 32-46)

= "*R.* (*Rh.*) sp. 1" in Moubayed-Breil & Ashe (2016)

Large sized species, slightly larger than *R. costai* sp. n. Total length 3.60-3.65 mm. Wing length 1.80-1.85 mm. Colouration variable from dark brown to blackish in general, especially on the thorax, legs and tergites. Head, antenna and halters dark brown. Thorax dark brown; mesonotal stripes blackish and distinct; humeral pit

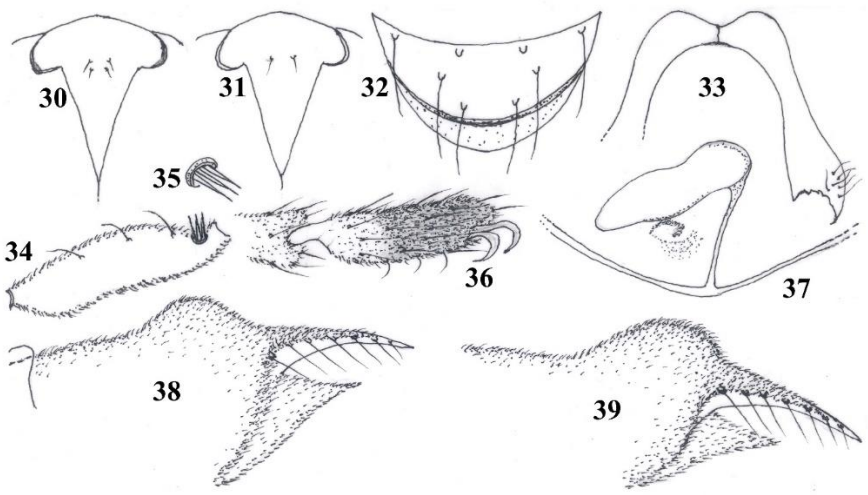

Figs. 30-39. Male imago of *Rheocricotopus* (*s. str.*) spp. vertex with coronal area of: *R. pyrenaeus* sp. n. (30); *R. costai* sp. n. (31). *R. pyrenaeus* sp. n.: clypeus (32); lobes of antepronotum (33); palpomere 3 (34) with details of sensilla coeloconica (35); tarsomere 5 of PI (36); humeral pit, holotype (37); two aspects of tergite IX and anal point in lateral view (38-39).

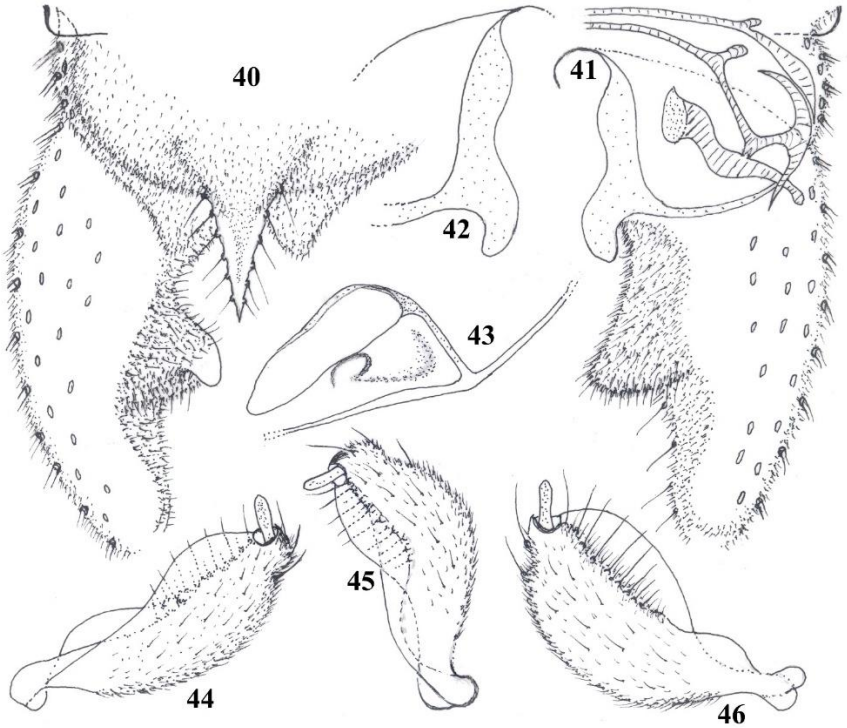

Figs. 40-46. Male imago of *Rheocricotopus* (*s. str.*) *pyrenaeus* sp. n.: hypopygium in dorsal (40) and ventral view (41 with tergite and anal point removed); superior volsella (42); humeral pit, paratype (43); gonostylus in dorsal (44), lateral (45) and ventral view (46).

brownish. Legs dark brown, distal half of tarsomeres ta_5 of PI, PII and PIII distinctly blackish. Abdominal tergites and anal segment dark brown. **Head**. Eyes hairy, elongated vertically. Coronal area (Fig. 30) with 4 coronals (2 setae on each side); Temporal setae 7, including 5 inner and 2 outer verticals, postorbitals absent. Clypeus (Fig. 32) semicircular, bearing 8 setae in 3 rows. Palp 5-segmented, length (µm) of palpomeres 1-5: 30, 55, 80, 105, 115; third palpomere (Fig. 34) with 3 sensilla clavata and 3 sensilla coeloconica (Fig. 35) located distally. Antenna 855 µm long; last flagellomere 390 µm long, distinctly clubbed distally, apex with a brush of curved sensilla chaetica; segments 6-10 subequal (about 45 µm long); length (µm) of segments: 70, 75, 30, 30, 35, 45, 45, 45, 45, 45, 390; antennal groove reaching segments 2-3. AR 0.84. Thorax. Lobes of antepronotum (Fig. 33) gaping and widely separated; lateral antepronotals 6 located distally; acrostichals 25-27 in 1-2 rows, reaching half of thorax; dorsocentrals 13-15 in 1-2 rows; prealars and supraalars absent. Humeral pit (Figs. 37, 43) moderately elongate, ellipsoid with broadened proximal part, a distinct smaller separate half oval-like pit is located below. Scutellum with 8 uniserial setae. **Wing**. Brachiolum with 2 setae. Distribution of setae on veins:

Table 2. Male adult of *Rheocricotopus pyrenaeus* sp. n. Length (µm) and proportions of prothoracic (PI), mesothoracic (PII) and metathoracic (PIII) legs.

	fe	**ti**	**ta_1**	**ta_2**	**ta_3**	**ta_4**	**ta_5**	**LR**	**BV**	**SV**	**BR**
PI	565	615	445	280	185	125	100	0.72	2.36	2.65	1.78
PII	640	590	325	170	140	75	75	0.55	3.38	3.78	2.00
PIII	665	695	390	220	180	90	90	0.56	3.02	3.49	2.40

R, 7-8; R_1, 2; R_{2+3}, 2; remaining veins bare. Squama with 5-7 setae in 1 row. **Legs**. Tarsomere ta_5 (Fig. 36) of PI, PII, PIII blackish in its distal half; tarsomeres ta_4 and ta_5 of PII and PIII are equal in size (respectively: 75 and 90 µm long). Length (µm) of tibial spurs of: PI, distinctly spiniforme, 40; PII, 25 and 20; PIII, 50 and 25; longest seta of tibial comb 55 µm long. Sensilla chaetica present in low number (proximally and distally) on tarsomeres ta_1-ta_5 of PI, PII and PIII. Length (µm) and proportions of prothoracic (PI), mesothoracic (PII) and metathoracic (PIII) legs as in Table 2.

Abdomen. Hypopygium in dorsal and ventral view (Figs. 40-41). Tergite IX semicircular, with a distinct rounded median hump, which is clearly visible in lateral view (Figs. 38-39). Anal point about 45-50 µm long, triangular and slightly curved downwards, large at base and uniformly narrowed distally with a sharp pointed apex; 12 setae are present laterally (6 on each side). Latero-sternite IX with 6 setae. Transverse sternapodeme and phallapodeme as in Fig. 41. Virga absent. Gonocoxite about 265 µm long, maximum width 50-55 µm, apex rounded. Superior volsella (Figs. 41-42) broadly projecting downwards and inwardly turned over distally, apex distinctly rounded. Inferior volsella large, lobe-like dorsally, with a large thumb-like apex, ventral side triangle-like. Gonostylus in dorsal, lateral and ventral view (Figs. 44-46) 85 µm long, 33 µm maximum width, posterior margin swollen medially and abruptly narrowing apically; crista dorsalis clearly visible in both lateral and right-angle views, starting at mid-distance and widely extended distally till apex of gonostylus, semicircular and occupying 70 to 80 % of the total length of gonostylus.

Female imago

(n = 2: 1 adult and 1 pharate adult; Figs. 47-55)

Large sized species. Total length 3.70-3.75 mm. Wing length 1.85-1.90 mm. Colouration dark brown to blackish including head, antenna, thorax and tergites. Head and halters dark brown; antenna dark brown, last flagellomere blackish (Fig. 49); thorax dark brown, mesonotal stripes blackish and distinct; humeral pit brownish. Legs brown to dark brown, distal half of tarsomeres 5 of PI, PII and PIII blackish. Abdominal tergites and anal segment dark brown to blackish. **Head**. Eyes hairy, elongated vertically. Coronal area, as in the male, with 4 coronals (2 setae on each side); Temporal setae 9, including 7 inner and 2 outer verticals, postorbitals absent. Palp 5-segmented, length (µm) of palpomeres 1-5: 45, 75, 105, 125, 165; distal part of third palpomere (Fig. 47) with 3 sensilla clavata, sensilla coeloconica absent. Clypeus (Fig. 48) semicircular, bearing 12 setae in 3 rows. Antenna 305 µm long; last flagellomere 120 µm long, proximal part slightly clubbed, distal part narrowing, surface including apex with numerous sensilla chaetica, antennal groove reaching segment 4. AR 0.65. **Thorax**. Lobes of antepronotum (Fig. 50) gaping and widely separated as in the male; lateral antepronotals 5 located distally; acrostichals 14 in 1-2 rows, reaching half of thorax; dorsocentrals 12-13 in 1-2 rows; prealars 4, supraalars absent; humeral pit (Fig. 51) moderately elongate, ellipsoid with broadened proximal part, a distinct smaller separate oval pit is located below. Scutellum with 8 uniserial setae. **Wing**. Brachiolum with 1 seta. Distribution of setae on veins: R, 12; R_1, 13; R_{4+5}, 20-25; remaining veins bare. Squama with 9-13 setae in 1 row. Legs. Distal half of tarsomere ta_5 of PI, PII and PIII blackish; tarsomere ta_4 and ta_5 of PIII are equal in size (135 µm long). Length (µm) of tibial spurs of: PI, distinctly spiniforme, 45; PII, 30 and 25; PIII, 90 and 30; longest seta of tibial comb 65 µm long. Sensilla chaetica present in low number on tibia and tarsomeres ta_1-ta_5 of PI, PII and PIII. Length (in µm) and proportions of prothoracic (PI), mesothoracic (PII) and metathoracic (PIII) legs as in Table 3.

Genitalia in dorsal and ventral view as illustrated in Fig. 52. Notum 130-135 µm long. Gonapophysis VIII including ventrolateral, dorsomesal and apodeme lobe (Figs. 52-54): apodemelobe (Fig. 53) inversed S-like, base crotchet-like; dorsomesal lobe (Fig. 54) conspicuous, proximal part slightly swollen, distal part linear; ventrolateral lobe (Fig. 52) projecting inwards apically. Sternite VIII with 22 setae (11 on each side of gonapophysis VIII). Seminal capsules (Fig. 52) 125 µm long, 85 µm wide, pearl-like, sclerotized part occupying basal, lateral and apical part, ducts with loops and separate openings. Tergite IX and gonocoxite (Fig. 55): gonocoxite weakly swollen with 9-10 setae; tergite IX nearly semicircular with convex anterior margin, distinctly divided in 2 oval lobes, bearing 20-22 setae (10-11 on each side), posterior margin concave. Cercus 70-80 µm long.

Pupal exuviae

(n = 4: 2 males and 2 females; Figs. 60-66)

Total length 3.65-3.75 mm. General colouration brownish. Frontal apotome brown, anterior half covered with fine wrinkles. Anterio-median area of cephalothorax and suture of thorax markedly rugulose and wrinkled; base of thoracic horn and wing sheath with blackish shading; outer and inner margin of antennal sheath brownish. Abdomen brown yellowish, lateral margin of segments I-VIII brownish. Anal lobe and genital sac

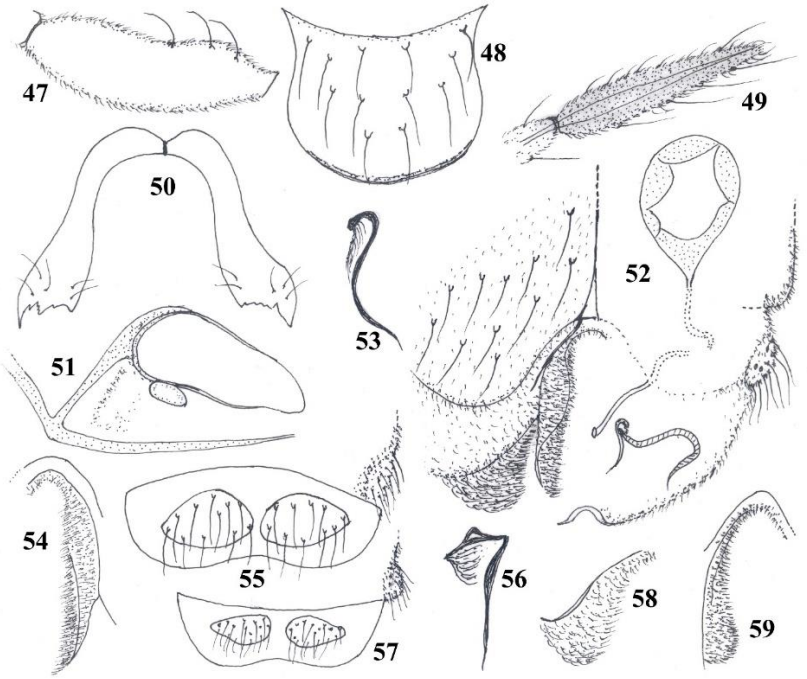

Figs. 47-59. Female imago of *Rheocricotopus* (*s. str.*) spp. *R. pyrenaeus* sp. n.: tarsomere 3 (47); clypeus (48); last flagellomere of antenna (49); lobes of antepronotum (50); humeral pit (51); genitalia, dorsal and ventral view (52) including gonapophysis VIII, sternite VIII, seminal capsule and right gonocoxite; apodeme lobe (53); dorsomesal lobe (54); tergite IX (55). *R. effusus*: apodeme lobe (56); tergite IX (57); ventrolateral lobe (58); dorsomesal lobe (59).

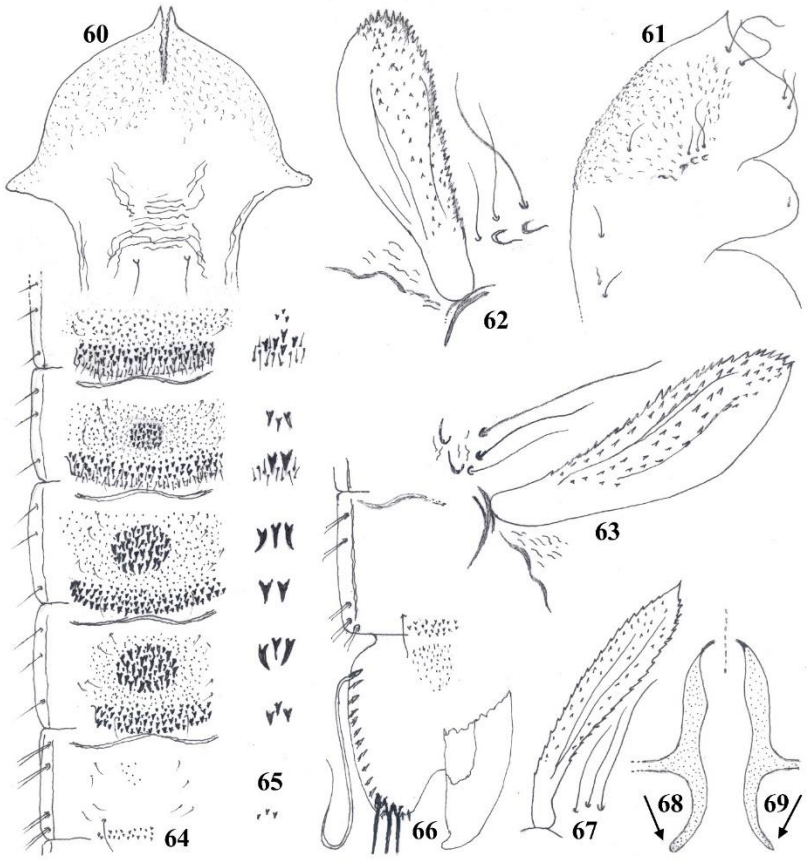

Figs. 60-69. Pupal exuviae of *Rheocricotopus* (*s. str.*) spp. *R. pyrenaeus* sp. n.: frontal apotome (60); cephalothorax (61); two aspects of thoracic horn (62-63); distribution pattern of armament and chaetotaxy of abdominal segments III-VII (64); details of armament on tergites III-VII and conjunctives (65); tergite VIII and anal segment (66). Thoracic horn of *R. tchernovskii* (67, after Makarchenko & Makarchenko 2005). Superior volsella of *R. reduncus* (68, after Sæther & Schnell 1988) and *R. tchernovskii* (69, after Makarchenko & Makarchenko 2005).

Table 3. Female adult of *Rheocricotopus pyrenaeus* sp. n. Length (µm) and proportions of prothoracic (PI), mesothoracic (PII) and metathoracic (PIII) legs.

	fe	ti	ta_1	ta_2	ta_3	ta_4	ta_5	LR	BV	SV	BR
PI	1025	1150	695	400	290	200	140	0.60	2.79	3.13	2.67
PII	1080	1225	720	410	285	175	150	0.59	2.97	3.20	2.00
PIII	1010	1030	460	270	210	135	135	0.45	3.33	4.43	2.00

brown yellowish. Cephalothorax as in Figs. 60-61. Frontal apotome (Fig. 60) semicircular, lateral margin bearing a distinct triangular expansion, frontal setae 80-85 µm long, distance between frontal setae 20 µm. Thorax. Median antepronotal nearly subequal (170 and 165 µm long), 2 lateral antepronotals each 105 µm long; prealars, vestigial; precorneals 195, 165 and 85 µm long. Thoracic horn (Figs. 62-63) about 300 µm long, maximum width 20-25 µm, distinctly clubbed and toothed on one side. Dorsocentrals Dc_1-Dc_4 (Fig. 61) consist of: 3 sub-equal setae (Dc_1, Dc_2 and Dc_4 = 55-60 µm long), Dc_3 25 µm long; distance (µm) between: Dc_1 to Dc_2 110, Dc_2 to Dc_3 40-50, Dc_3 to Dc_4 15-20.

Abdomen. Armament, chaetotaxy and distribution pattern of shagreen with details of armament on tergites III-VII as in Figs. 64-65. All pleurae and tergite I bare. Pedes spurii A present on sternites IV-VI, pedes spurii B present only on segment II. Caudal transverse rows of posteriorly projecting stout spines (3-4 rows) present on tergites II-VI, those on tergites IV-V are the widest (360-400 µm); caudal transverse rows (2-3) of orally and posteriorly directed pins are restricted to conjunctives of tergites II-IV, those on tergite IV are the widest (380 µm); caudal transverse rows of short spines and spinules (about 120-150 µm wide) are present on tergites VII-VIII. Distribution pattern, shape and size of circular median patch of stout spines on tergites IV-VI as in Figs. 64-65: those on tergites V-VI are subequal in size, more extensive and armed with much larger spines, longest spines 18-20 µm long; median patch on tergite IV is smaller and armed with short spines and spinules, longest one 10-12 µm long; caudal transverse rows (1-2) of short spines present on tergites VII-VIII (maximum width 120-150 µm). Number and distribution pattern of lateral setae and lamelliform setae (taeniae) on segments I-VIII as in Fig. 64: lateral setae on segments I-VI (1, 3, 3, 3, 3, 3); taeniae on segments VII-VIII (4, 5). Anal segment (Fig. 66): anal lobe 250 µm long, 285 µm maximum width, fringe with 14-16 taeniae; genital sac 190-200 µm long, overreaching apical margin of anal lobe by 40 µm; macrosetae 315-325 µm long curved and pointed apically.

Larva

Known but not described.

Taxonomic position

Though *R. costai* sp. n. apparently shows a closely phylogenetic relationships with the *effusus*-group (shape of the humeral pit and gonostylus), some other relevant specific characters found in the male adult and exuviae (lobes of antepronotum thin; apex of anal point rounded; distal part of superior volsella short and widely projecting downwards; tergite III of exuviae bearing a distinct median circular patch of spinules) allowed us to consider this new species as a separate local 'Pyreneo-corsican element'. Nevertheless, due to some specific characters found in the male adult and exuviae of *R. pyrenaeus* sp. n. (distal part of superior volsella markedly inwardly turned over distally; circular median patch of spines on tergite IV distinctly smaller than those on tergites V-VI), this new species keys near both *R. reduncus* (known from Norway) and *R. tchernovskii* (known from Far East Russia), based in particular, on the elongate distal part of the superior volsella which is markedly turned over inwards. Therefore, a fourth additional group within the subgenus *Rheocricotopus*, the '*reduncus*-group', could be created to include the three following species: *R. reduncus*, *R. tchernovskii* and *R. pyrenaeus* sp. n.

However, the specific characters found in the male and female adults and pupal exuviae will separate the two new described species from other related known members of the *effusus*-group, on the basis of the following combination of characters.

***R. costai* sp. n.**

- Male adult. Palpomere 3 with 3 sensilla coeloconica (Fig. 1), but only 2 in *R. effusus* (Fig. 6); clypeus and lobes of antepronotum (Figs. 3-4) are differently figured in *R. effusus* (Figs. 7-8); humeral pit (Fig. 9) is distinctly elongate and narrowed distally, which is broad ellipse-like in *R. effusus* (Fig. 10; Lehmann 1969, Fig. 13a); lateral view of both tergite IX and anal point (Fig. 12) clearly reveals the presence of a distinct rounded hump on tergite IV and anal point with rounded apex, while a lower hump and a sharply pointed apex are observed in *R. effusus* (Fig. 13); distal part of superior volsella not narrowing, short and broadly projecting downwards with a rounded apex (Figs. 15-16), is projecting outwards in *R. tamahumeralis* Sasa, 1981, which is only known from Japan (Sasa 1981, Fig. 19I), or moderately longer, gradually narrowing and bearing a pointed apex in *R. effusus* (Fig. 18; Albu 1968, Fig. 9; Lehmann 1969, Fig. 5; Langton & Pinder 2007, Fig. 189C; Makarchenko & Makarchenko 2005, Figs. 11-14); inferior volsella with a distinct rounded apex, while is notched apically in *R. tamahumeralis* (Sasa 1981, Fig. 19J); phallpodeme (Fig. 15) is differently shaped in *R. effusus* (Fig. 17); crista dorsalis (Figs. 20-21) short, tooth-like and located close to the megaseta, is lower and much wider in *R. effusus* (Lehmann 1969, Fig.5; Langton & Pinder 2007, Figs. 72D, 189C).

- Pupal exuviae. Frontal apotome (Fig. 22) semicircular, is nearly triangular in *R. effusus* (Coffman *et al.* 1986, Fig. 9.59A); thoracic horn finger-like and toothed on one side

(Figs. 24-25), is differently illustrated in both *R. tamahumeralis* (Sasa 1981, Fig. 20A) and *R. effusus* (Fig. 29; Coffman *et al*. 1986, Fig. 9.59C; Langton 1991, Fig. 45c); small circular median patch of spinules distinctly present on tergite III (Fig. 26), is apparently lacking in (almost) all members of the *effusus*-group (Lehmann 1969, Fig. 21b; Coffman *et al*. 1986, 9.59D; Langton 1991, Figs. 45b) except in *R. tamahumeralis* (species only known from Japan) which bears a 'weakly-defined' median patch of spinules on tergite III (Sasa 1981, Fig. 20B).

***R. pyrenaeus* sp. n.**

Male and female adults and pupal exuviae of this new species can be separated from its two closely related species *R. reduncus* and *R. tchernovskii*, and other members of the *effusus*-group by a combination of differentiating characters.

- Male adult. Clypeus and lobes of antepronotum (Figs. 32-33) are differently figured in *R. effusus* (Figs. 7-8); humeral pit (Figs. 11, 37, 43) is strongly reduced in both *R. reduncus* and *R. tchernovskii* and differently figured in *R. effusus* (Fig. 10); tergite IX and anal point in lateral view (Figs. 38-39) are differently shaped in *R. effusus* (Fig. 13); distal part of superior volsella short and broadly turned over inwards with a rounded apex (Figs. 41-42), while is much longer and gradually narrowing in both *R. reduncus* and *R. tchernovskii* (Figs. 68-69; Makarchenko & Makarchenko 2005, Figs. 21-22; Sæther & Schnell 1988, Fig. 1D); crista dorsalis largely extended (Figs. 44-46), is much shorter and lower in *R. effusus* (Lehmann 1969, Fig. 5) and entirely absent in both *R. reduncus* and *R. tchernovskii* (Makarchenko & Makarchenko 2005, Fig. 22; Sæther & Schnell 1988, Fig. 1D).

- Female adult. Lobes of antepronotum (Fig. 50) are similarly shaped as in the male adult; distal part of the apodeme lobe inversed S-like in shape (Fig. 53), while is linear in *R. effusus* (Fig. 56; Sæther 1986, Fig. 22E); dorsomesal and ventrolateral lobes (Figs. 52, 54) are differently figured in *R. effusus* (Figs. 58-59; Sæther 1986, Fig. 22E); gonocoxite and tergite IX (Figs. 52, 55) are differently illustrated in *R. effusus* (Fig. 57; Sæther 1986, Fig. 22D).

- Pupal exuviae. Thoracic horn (Figs. 62-63) club-like and toothed on one side, while is linearly elongated and toothed on each side in both *R. reduncus* (Sæther & Schnell 1988, Fig. 2C) and *R. tchernovskii* (Fig. 67; Makarchenko & Makarchenko 2005, Fig. 24); small circular median patch of spines on tergite IV (Fig. 64), similarly present in both *R. reduncus* (Sæther & Schnell 1988, Fig. 2E) and *R. tchernovskii* (Makarchenko & Makarchenko 2005, Fig. 26).

Ecology and geographical distribution

Rheocricotopus costai sp. n. and *R. pyrenaeus* sp. n. are both rheophilic species exclusively encountered in lotic habitats (peat bogs, springs, upper streams) with siliceous water and low water conductivity. Localities where larvae and pharate adults were collected consist of moderately to weakly shaded ruisselets and cold mountain streams. Bryocolous and hygropetric habitats including waterfalls probably represent the most common aquatic areas for larval populations. Environmental data of habitat recorded along the crenal and upper rhithral of the Rivers Asco (Corsica) and Mantet (Pyrenees) are: siliceous water, low value of conductivity (20-40) µS/cm; pH 5.5-5.7; temperature 6-12°C. Such pristine habitats, which are endangered by pastoralism and both natural and accidental flooding, deserve much greater consideration, protection and preservation. Material was collected in some glacial helocrenes and streams delimited by well preserved and protected areas covered by local Nature Reserves located in both Corsica and the Eastern Pyrenees.

The two new species are regarded as typical relict representatives of glacial helocrenes and cold stenothermic streams. They belong to the crenobiontic and crenophilous community of species as documented by Lindegaard (1995). The discovery of *R. costai* sp. n. and *R. pyrenaeus* sp. n. in such preserved lotic habitats highlights the importance of glacial springs and streams, which are considered to be microrefugia and hotspots of diversity.

Rheocricotopus costai sp. n. is known from both western Corsica and the Eastern Pyrenees, while the geographical distribution of *R. pyrenaeus* sp. n. is currently restricted to springs and streams located in the Eastern Pyrenees. In particular, *R. costai* sp. n. can be expected to occur in other similar areas all around both the continental and insular Tyrrhenian Provinces (Italy, Spain). This indicates and reinforces the importance of headwaters and cold enclaves in the preservation and persistence of autochthonous glacial relict species, which can be considered as biological indicators of the global warming and climate change in the Mediterranean biogeographical region.

- Associated species encountered in the same localities with *R. costai* sp. n. include: *Boreoheptagyia cinctipes* (Edwards, 1928); *B. dasyops* Serra-Tosio, 1989; *B. legeri* (Goetghebuer, 1933); *Diamesa aberrata* Lundbeck, 1898; *D. cinerella* Meigen, 1835; *D. macronyx* (Kieffer, 1918); *D. veletensis* Serra-Tosio, 1971; *Pseudodiamesa branickii* (Nowicki, 1873); *Syndiamesa nigra* Rossaro, 1980; *Bryophaenocladius subvernalis* (Edwards, 1929); *Chaetocladius laminatus* Brundin, 1947; *C. suecicus* (Kieffer, 1916); *Corynoneura tyrrhena* Moubayed-Breil, 2015; *Eukiefferiella fittkaui* Lehmann, 1972; *Heleniella ornaticollis* (Edwards, 1929); *Krenosmittia boreoalpina* (Goetghebuer, 1944); *Parametriocnemus boreoalpinus* Gowin & Thienemann, 1942; *Paratrissocladius orsinii* Moubayed-Breil & Ashe, 2016; *Thienemannia corsicana* Moubayed-Breil, 2013; *T. gracilis* Kieffer, 1909.

- Associated species encountered in the same localities with *R. pyrenaeus* sp. n. include: *Boreoheptagyia cinctipes* (Edwards, 1928); *B. legeri* (Goetghebuer, 1933); *Diamesa aberrata* Lundbeck, 1898; *D. bertrami* Edwards, 1935; *D. bohemani* Goetghebuer, 1932; *D. cinerella* Meigen, 1835; *D. modesta* Serra-Tosio, 1968; *D. thomasi* Serra-Tosio,

1970; *D. veletensis* Serra-Tosio, 1971; *Pseudodiamesa branickii* (Nowicki, 1873); *P. nivosa* (Goetghebuer, 1928); *Syndiamesa edwardsi* Pagast, 1947; *S. hygropetrica* (Kieffer, 1909); *Bryophaenocladius subvernalis* (Edwards, 1929); *Chaetocladius guisseti* Moubayed-Breil, 2017; *C. laminatus* Brundin, 1947; *C. suecicus* (Kieffer, 1916); *Eukiefferiella fittkaui* Lehmann, 1972; *Heleniella ornaticollis* (Edwards, 1929); *Krenosmittia boreoalpina* (Goetghebuer, 1944); *Parametriocnemus boreoalpinus* Gowin & Thienemann, 1942; *Rheocricotopus effusus* (Walker, 1856); *Rheosmittia spinicornis* (Brundin, 1956); *Thienemannia gracilis* Kieffer, 1909 and *T. valespira* Moubayed-Breil & Ashe, 2013.

References

1. Albu, P. 1968. Chironomide din Carpaţii româneşti (III). *Studii şi Cercetări de Biologie, Série de Zoologie* 20: 455-465.
2. Ashe, P. & O'Connor, J.P. 2012. *A World Catalogue of Chironomidae (Diptera). Part 2. Orthocladiinae.* Irish Biogeographical Society & National Museum of Ireland, Dublin. 968 pp.
3. Bhattacharyay, S., Ali, A. & Chaudhuri, P.K. 1991. Orthoclads of tribe Orthocladiini (Diptera: Chironomidae) from India. *Beiträge zur Entomologie,* 41(2): 333-349.
4. Brundin, L. 1956. Zur Systematik der Orthocladiinae (Dipt., Chironomidae). *Report of the Institute of Freshwater Research, Drottningholm*, 37: 5-185.
5. Caspers, N. & Reiss, F. 1989. Die Chironomidae (Diptera, Nematocera) der Türkei. Teil I: Podonominae, Diamesinae, Prodiamesinae, Orthocladiinae. *Entomofauna*, 10(8): 105-160.
6. Chaudhuri, P.K. & Sinharay, D.C. 1983. A study on Orthocladiinae (Diptera, Chironomidae) of India. The genus *Rheocricotopus* Thienemann & Harnisch. *Entomologica Basiliensia*, 8: 398-407.
7. Coffman, W.P., Cranston, P.S., Oliver, D.R. & Sæther, O.A. 1986. The pupae of Orthocladiinae (Diptera, Chironomidae) of the Holarctic Region – Keys and diagnoses. In Wiederholm, T. (ed.): Chironomidae of the Holarctic Region. Keys and diagnoses. Part 2. Pupae. *Entomologica Scandinavica, Supplement* 28: 147-296.
8. Langton, P.H. 1991. *A key to pupal exuviae of the West Palaearctic Chironomidae*. Privately published. Huntingdon, England, 386 pp.
9. Langton, P.H. & Pinder, L.C.V. 2007. Keys to the adult males of Chironomidae of Britain and Ireland. Volume 1 (Pp: 1-239) and volume 2 (Pp: 1-168). *Freshwater Biological Association,* Scientific Publication, no: 64.
10. Lehmann, J. 1969. Die europäischen Arten der Gattung *Rheocricotopus* Thien. und Harn. und drei neue Artvertreter dieser Gattung aus der Orientalis (Diptera, Chironomidae). *Archiv für Hydrobiologie*, 66(3): 348-381.
11. Lindegaard, C. 1995. Chironomidae (Diptera) of European cold springs and factors influencing their distribution. *Journal of the Kansas Entomological Society, Supplement* 68(2): 108-131.
12. Liu, W., Lin, X. & Wang, X. 2014a. A review of *Rheocricotopus* (*Psilocricotopus*) *chalybeatus* species group from China, with the description of three new species (Diptera, Chironomidae). *ZooKeys*, 388: 17-34.
13. Liu, W., Song, C. & Wang, X. 2014b. Review of the subgenus *Rheocricotopus* (s. str.) Brundin, 1956 from China (Diptera: Chironomidae). *Pan-Pacific Entomologist*, 90(2): 100-106.
14. Makarchenko, E. & Makarchenko, M.A. 2005. Chironomids of the genus *Rheocricotopus* Thienemann and Harnisch, 1932 (Diptera, Chironomidae, Orthocladiinae) of the Russian Far East. *Eurasian Entomological Journal*, 4(2): 125-136. [In Russian, English Summary]
15. Moubayed-Breil, J. 2016. *Rheocricotopus* (*Psilocricotopus*) *meridionalis* sp. n. and *R.* (*Psc*.) *thomasi* sp. n., two crenophilous species inhabiting cold helocrenes and streams in the Mediterranean Region [Diptera, Chironomidae, Orthocladiinae]. *Ephemera*, 9(1): 17-32.
16. Moubayed-Breil, J. & Ashe, P. 2012. An updated checklist of the Chironomidae of Corsica with an outline of their altitudinal and geographical distribution (Diptera). *Ephemera*, 13(1): 13-39.
17. Moubayed-Breil, J. & Ashe, P. 2016. New records and additions to the database on the geographical distribution of some threatened chironomid species from continental France (Diptera, Chironomidae). *Ephemera*, 16(2): 93-108.
18. Ree, H.I. 2013. Description of twelve new species and eight new Korean records of Chironomidae (Diptera) in Korea. *Entomological Research Bulletin*, 29(2): 142-171.
19. Sasa, M. 1981. Studies on chironomid midges of the Tama River. Part 4. Chironomidae recorded at a winter survey. *Research report from the National Institute for Environmental studies*, 29: 79-148.
20. Sæther, O.A. 1980. Glossary of chironomid morphology terminology (Diptera, Chironomidae). *Entomologica Scandinavica, Supplement*, 14: 1-51.
21. Sæther, O.A. 1986. A review of the genus *Rheocricotopus* Thienemann & Harnish, 1932, with a description of three new species (Diptera, Chironomidae). *Spixiana Supplement*, 11: 59-108.
22. Sæther, O.A. & Schnell, O.A. 1988. Two new species of the *Rheocricotopus* (*R.*) *effusus*-group group (Diptera: Chironomidae). *Spixiana*, 14: 65-74.
23. Sæther, O.A. & Spies, M. 2013. Fauna Europaea: Chironomidae. In P. Beuk, P. & Pape, T. (eds): *Fauna Europaea: Diptera Nematocera. Fauna Europaea version* 2.6. Internet data base at http://www.faunaeur.org [accessed November 2018].
24. Wang, X. 1995. *Rheocricotopus* (*R.*) *orientalis*, a new species from China (Diptera, Chironomidae). *Aquatic Insects*, 17(1): 37-40.
25. Wang, X. & Sæther, O.A. 2001. Two new species of the *orientalis* group of *Rheocricotopus* (*Psilocricotopus*) from China (Diptera, Chironomidae). *Hydrobiologia*, 444: 237-240.
26. Wang, X. & Zheng, L. 1989. Two new species of the genus *Rheocricotopus* from China (Diptera, Chironomidae). *Entomotaxonomia*, 11(4): 311-313. [In Chinese, English Summary]

http://dergipark.gov.tr/trkjnat
Trakya University Journal of Natural Sciences, 20(1): 47-55, 2019
ISSN 2147-0294, e-ISSN 2528-9691
DOI: 10.23902/trkjnat.521256

Research Article

FUNGI DETERMINED IN ANKARA UNIVERSITY TANDOĞAN CAMPUS AREA (ANKARA-TURKEY)

Ilgaz AKATA[1*], Deniz ALTUNTAŞ[1], Şanlı KABAKTEPE[2]

[1]Ankara University, Faculty of Science, Department of Biology, Ankara, TURKEY
[2]Turgut Ozal University, Battalgazi Vocational School, Battalgazi, Malatya, TURKEY
*Corresponding author: ORCID ID: orcid.org/0000-0002-1731-1302, e-mail: akata@science.ankara.edu.tr

Cite this article as:

Akata I., Altuntaş D., Kabaktepe Ş. 2019. Fungi Determined in Ankara University Tandoğan Campus Area (Ankara-Turkey). *Trakya Univ J Nat Sci*, 20(1): 47-55, DOI: 10.23902/trkjnat.521256

Received: 02 February 2019, Accepted: 14 March 2019, Online First: 15 March 2019, Published: 15 April 2019

Abstract: The current study is based on fungi and infected host plant samples collected from Ankara University Tandoğan Campus (Ankara) between 2017 and 2019. As a result of the field and laboratory studies, 148 fungal species were identified. With the addition of formerly recorded 14 species in the study area, a total of 162 species belonging to 87 genera, 49 families, and 17 orders were listed.

Key words: *Ascomycota*, *Basidiomycota*, Ankara, Turkey.

Özet: Bu çalışma, Ankara Üniversitesi Tandoğan Kampüsü'nden (Ankara) 2017 ve 2019 yılları arasında toplanan mantar ve enfekte olmuş konukçu bitki örneklerine dayanmaktadır. Arazi ve laboratuvar çalışmaları sonucunda 148 mantar türü tespit edilmiştir. Daha önce bildirilen 14 tür dahil olmak üzere 17 ordo, 49 familya, 87 cinse mensup 162 tür listelenmiştir.

Introduction

Ankara, the capital city of Turkey, is situated in the center of Anatolia, surrounded by Çankırı in the north, Bolu in the northwest, Kırşehir, and Kırıkkale in the east, Eskisehir in the west, Konya and Aksaray in the south. Ankara University Tandoğan Campus is located in Tandoğan locality within the boundaries of Çankaya district and it is situated at an elevation between 850 and 870 meters above the sea level. The campus covers a total surface area of 195.000 m^2 and includes the faculty of science, the faculty of pharmacy, the biotechnology institute, the sports complex, the rectorate, and various administrative buildings (Fig. 1). Since its first establishment, local and exotic trees, shrubs and herbaceous plants have been planted in various areas of the campus, and the current flora comprises over 300 plant species, of which approximately 60 are in tree forms.

Fungi significant members of the ecosystem by playing important roles in not only in the ecosystem itself but also in various fields including, pharmacology, food industry, and biodegradation. More than 120.000 fungal species have been described and reported to currently exist throughout the world but global fungal biodiversity has been estimated to comprise approximately 1.5 million species (Servi *et al*. 2010).

Studies on Turkish fungal diversity is based on a study period of more than 100 years. Over the last decade, the number of studies has significantly increased and the compiled literature data were published as checklists in different times (Bahçecioğlu & Kabaktepe 2012, Doğan *et al.* 2005, Sesli & Denchev 2008, Kabaktepe *et al.* 2015). Recently, data of the new studies on the Turkish macrofungal diversity were also incorporated into these data that are not included in these checklists (Acar & Uzun 2017, Akata 2017, Akata & Uzun 2017, Akata *et al.* 2018, Akgül *et al.* 2015, Allı *et al.* 2017, Altuntaş *et al.* 2017, Demirel *et al.* 2017, Doğan *et al.* 2018, Ekici et al. 2012, Erdoğdu & Hüseyin 2008, Hüseyin & Selçuk 2016, Hüseyin *et al.* 2016, Işık & Türkekul 2018, Kabaktepe *et al*. 2016, 2017, Kabaktepe & Akata 2018, Öztürk *et al.* 2017; Selçuk & Ekici 2014, Sesli & Vizzini 2017, Sesli & Liimatainen 2018, Şen *et al.* 2018, Uzun *et al.* 2014). Previous mycological investigations in the research area were conducted by Akata (2010), Akata & Heluta (2015), Akata *et al.* (2009) and totally 35 fungal species reported. However, up until now, no detailed mycological research devoted to Ankara University Tandoğan Campus has been conducted.

Materials and Methods

The study was conducted between the years 2017 and 2019 in Ankara University Tandoğan Campus. Fungal specimens and the infected host plants in the campus area were collected and were brought to the laboratory for identifications. Macroscopic and some ecological features of the samples were noted in the field and the specimens

were photographed in their natural environment. Microfungal samples were isolated from the plant material either by scraping or by thin sectioning using a razor blade, spore prints were obtained from macrofungal samples and microstructureswere examined with light microscopy. The reagents such as distilled water, Melzer's reagent, Lactophenol, 5% KOH, H_2SO_4, Cotton blue, Congo red etc. were used. Identification of the samples was performed according to Breitenbach & Kränzlin (1984, 1986, 1991, 1995, 2000), Braun & Cook (2012), Ellis & Ellis (1987), Hansen & Knudsen (1992, 1997, 2000), Jordan (2004), Kränzlin (2005), Wilson & Henderson (1966) and Vánky (2012). The identified fungal samples are kept at Ankara University Herbarium (ANK).

Results

The taxa identified were listed in alphabetical order with notes on their habitats, host plants, collection dates, and accession numbers before which "ANK Akata & Altuntaş" was added. Their systematics were given in accordance with the Index Fungorum (www.indexfungorum.org; accessed 25 January 2019).

Division *ASCOMYCOTA*

Order *Capnodiales*

Family *Cladosporiaceae*

Cladosporium herbarum (Pers.) Link: On leaf and stem of *Triticum aestivum* L. (*Poaceae*), 27.05.2018, ANK Akata & Altuntaş 107.

Cladosporium macrocarpum Preuss: On leaf of *Triticum aestivum* L. (*Poaceae*), 17.05.2018, ANK Akata & Altuntaş 102.

Family *Mycosphaerellaceae*

Mycosphaerella populnea (Sacc.) House: On leaf of *Populus nigra* L. (*Salicaceae*), 08.07.2018, ANK Akata & Altuntaş 127; 18.08.2018, ANK Akata & Altuntaş 156.

Stigmina carpophila (Lév.) M.B. Ellis: On leaf and fruit of *Prunus domestica* L. (*Rosaceae*), 05.06.2018, ANK Akata & Altuntaş 118.

Order *Diaporthales*

Family *Gnomoniaceae*

Ophiognomonia leptostyla (Fr.) Sogonov: On leaf of *Juglans regia* L. (*Juglandaceae*), 05.07.2018, ANK Akata & Altuntaş 123; 17.08.2018, ANK Akata & Altuntaş 148.

Order *Erysiphales*

Family *Erysiphaceae*

Blumeria graminis (DC.) Speer: On leaf and stem of *Avena barbata* Pott ex Link (*Poaceae*), 28.09.2017, ANK Akata & Altuntaş 17; On leaf and stem of *T. aestivum* L. (*Poaceae*), 14.08.2018, ANK Akata & Altuntaş 138.

Erysiphe alphitoides (Griffon & Maubl.) U. Braun & S. Takam.: On leaf of *Quercus robur* L. (*Fagaceae*), 17.08.2018, ANK Akata & Altuntaş 142; 20.09.2018, ANK Akata & Altuntaş 173; 15.10.2018, ANK Akata & Altuntaş 262.

Erysiphe aquilegiae DC.: On leaf and stem of *Ranunculus neopolitanus* Ten. (*Ranunculaceae*), 13.10.2018, ANK Akata & Altuntaş 248.

Erysiphe berberidis DC.: On leaf of *Berberis aquifolium* Pursh (*Berberidaceae*), 17.08.2018, ANK Akata & Altuntaş 145.

Erysiphe convolvuli DC.: On leaf of *Convolvulus arvensis* L. (*Convolvulaceae*), 16.10.2017, ANK Akata & Altuntaş 28.

Erysiphe flexuosa (Peck) U. Braun & S. Takam.: On leaf of *Aesculus hippocastanum* L. *(Sapindaceae*), 09.10.2018 ANK Akata & Altuntaş 229.

Erysiphe heraclei DC.: On leaf, stem and fruit of *Torilis arvensis* (Huds.) Link (*Apiaceae*), 01.10.2018, ANK Akata & Altuntaş 207.

Erysiphe lycopsidis R.Y. Zheng & G.Q. Chen: On leaf and stem of *Anchusa leptophylla* Roem. & Schult. (*Boraginaceae*), 01.10.2017, ANK Akata & Altuntaş 24.

Erysiphe necator Schwein.: On leaf of *Vitis vinifera* L. (*Vitaceae*), 25.09.2018, ANK Akata & Altuntaş 196.

Erysiphe pisi DC.: On leaf and stem of *Medicago sativa* L. (*Fabaceae*), 23.10.2017, ANK Akata & Altuntaş 41; 02.10.2018, ANK Akata & Altuntaş 210.

Erysiphe polygoni DC.: On leaf and stem of *Polygonum aviculare* L. (*Polygonaceae*), 13.10.2018, ANK Akata & Altuntaş 249.

Erysiphe syringae-japonicae (U. Braun) U. Braun & S. Takam.: Akata & Heluta (2015).

Erysiphe urticae (Wallr.) S. Blumer: On leaf and stem of *Urtica dioica* L. (*Urticaceae*), 25.09.2018, ANK Akata & Altuntaş 197.

Golovinomyces cichoracearum (DC.) V.P. Heluta: On leaf and stem of *Taraxacum officinale* F.H. Wigg. (*Asteraceae*)17.08.2018, ANK Akata & Altuntaş 150.

Golovinomyces depressus (Wallr.) V.P. Heluta: On leaf of *Arctium minus* (Hill) Bernh. (*Asteraceae*), 21.09.2018, ANK Akata & Altuntaş 183.

Golovinomyces sordidus (L. Junell) V.P. Heluta: On leaf and stem of *Plantago major* L. (*Plantaginaceae*), 17.08.2018, ANK Akata & Altuntaş 143.

Leveillula lactucarum Durrieu & Rostam: On leaf of *Lactuca serriola* L. (*Asteraceae*), 09.10.2018 ANK Akata & Altuntaş 230.

Leveillula lappae (Castagne) U. Braun: On leaf and stem of *Cirsium arvense* (L.) Scop. (*Asteraceae*), 21.09.2018, ANK Akata & Altuntaş 182.

Leveillula papilionacearum (Kom.) U. Braun: On leaf and stem of *Medicago sativa* L. (*Fabaceae*), 23.10.2017, ANK Akata & Altuntaş 39; On leaf and stem of *Vicia sativa* L. ssp. *nigra* (L.) Ehrh. (*Fabaceae*), 06.10.2018, ANK Akata & Altuntaş 222.

Neoerysiphe galeopsidis (DC.) U. Braun: On leaf and stem of *Lamium purpureum* L. (*Lamiaceae*), 28.09.2018, ANK Akata & Altuntaş 201.

Podosphaera clandestina (Wallr.) Lév.: On leaf of *Cydonia oblonga* Mill. (*Rosaceae*), 21.09.2018, ANK Akata & Altuntaş 180.

Podosphaera dipsacacearum (Tul. & C. Tul.) U. Braun & S. Takam.: On leaf and stem of *Scabiosa rotata* M. Bieb. (*Dipsacaceae*), 02.10.2018, ANK Akata & Altuntaş 212.

Podosphaera ferruginea (Schltdl.) U. Braun & S. Takam.: On leaf and stem of *Sanguisorba minor* Scop. (Rosaceae), 25.09.2018, ANK Akata & Altuntaş 194.

*Podosphaera f*usca (Fr.) U. Braun & Shishkoff: On leaf and stem of *Xanthium spinosum* L. (*Asteraceae*), 17.08.2018, ANK Akata & Altuntaş 149.

Podosphaera pannosa (Wallr.) de Bary: On leaf of *Rosa canina* L. (*Rosaceae*), 19.08.2018, ANK Akata & Altuntaş 162.

Podosphaera plantaginis (Castagne) U. Braun & S. Takam.: On leaf and stem of *Plantago major* L. (*Plantaginaceae*), 13.09.2017, ANK Akata & Altuntaş 14.

Phyllactinia fraxini (DC.) Fuss: On leaf of *Fraxinus angustifolia* Vahl (*Oleaceae*), 02.10.2018, ANK Akata & Altuntaş 215.

Phyllactinia guttata (Wallr.) Lév. On leaf of *Corylus avellana* L. (*Betulaceae*), 17.08.2018, ANK Akata & Altuntaş 147.

Phyllactinia mali (Duby) U. Braun: On leaf and stem of *Crataegus monogyna* Jacq. (*Rosaceae*), 17.08.2018, ANK Akata & Altuntaş 144.

Sawadaea bicornis (Wallr.) Homma: On leaf of *Acer platanoides* L (*Aceraceae*), 06.10.2018 ANK Akata & Altuntaş 218.

Order *Glomerellales*

Family *Glomerellaceae*

Colletotrichum gloeosporioides (Penz.) Penz. & Sacc.: On leaf of *Pyrus communis* L. (*Rosaceae*), 14.05.2018, ANK Akata & Altuntaş 98; 27.05.2018, ANK Akata & Altuntaş 109.

Family *Plectosphaerellaceae*

Verticillium albo-atrum Reinke & Berthold: On leaf and stem of *Morus alba* L. (*Moraceae*), 27.05.2018, ANK Akata & Altuntaş 108; 17.08.2018, ANK Akata & Altuntaş 146; 25.09.2018, ANK Akata & Altuntaş 195.

Order *Hypocreales*

Family *Hypocreaceae*

Hypomyces chrysospermus Tul. & C. Tul.: On *Xerocomellus chrysenteron* (Bull.) Šutara (*Boletaceae*), 14.08.2018, ANK Akata & Altuntaş 141.

Order *Pezizales*

Family *Helvellaceae*

Helvella acetabulum (L.) Quél.; On path, 05.05.2018, ANK Akata & Altuntaş 79.

Helvella costifera Nannf.: Under *Picea pungens* Engelm. (*Pinaceae*), 17.10.2018, ANK Akata & Altuntaş 275.

Helvella leucomelaena (Pers.) Nannf.: Under *Pinus nigra* J.F Arnold (*Pinaceae*), 14.05.2018, ANK Akata & Altuntaş 96.

Family *Pyronemataceae*

Geopora arenicola (Lév.) Kers: Under *Pinus nigra* J.F Arnold (*Pinaceae*), 14.10.2018, ANK Akata & Altuntaş 254.

Geopora sumneriana (Cooke) M. Torre: Under *Cedrus libani* A. Rich. (*Pinaceae*), 10.05.2018, ANK Akata & Altuntaş 92.

Pulvinula convexella (P. Karst.) Pfister: Under *Crataegus monogyna* Jacq. (*Rosaceae*), 12.10.2018, ANK Akata & Altuntaş 236.

Order *Pleosporales*

Family *Venturiaceae*

Venturia pyrina Aderh.: On leaf and fruit of *Pyrus communis* L. (*Rosaceae*), 18.08.2018, ANK Akata & Altuntaş 158.

Order *Phyllachorales*

Family *Phyllachoraceae*

Polystigma rubrum (Pers.) DC.: On leaf of *Prunus domestica* L. (*Rosaceae*), 23.09.2018, ANK Akata & Altuntaş 188; 20.09.2018, ANK Akata & Altuntaş 171.

Order *Rhytismatales*

Family *Rhytismataceae*

Rhytisma acerinum (Pers.) Fr.: On leaf of *Acer platanoides* L. (*Aceraceae*), 27.09.2018, ANK Akata & Altuntaş 200.

Division *BASIDIOMYCOTA*

Order *Agaricales*

Family *Agaricaceae*

Agaricus campestris L.: In meadow, 16.10.2018, ANK Akata & Altuntaş 270; 29.10.2018, ANK Akata & Altuntaş 575; Akata *et al*. (2009).

Agaricus xanthodermus Genev. In meadow, 05.06.2018, ANK Akata & Altuntaş 112; 29.09.2018, ANK Akata & Altuntaş 205; 14.08.2018, ANK Akata & Altuntaş 139.

Coprinus comatus (O.F. Müll.) Pers.: In meadow, 20.09.2018, ANK Akata & Altuntaş 174; 16.10.2018, ANK Akata & Altuntaş 271; 26.10.2018, ANK Akata & Altuntaş 565; Akata *et al*. (2009).

Crucibulum laeve (Huds.) Kambly: On dead branch of *Quercus robur* L. (*Fagaceae*), 29.09.2017, ANK Akata & Altuntaş 19.

Lepiota brunneoincarnata Chodat & C. Martín: Under *Aesculus hippocastanum* L. (*Sapindaceae*), 13.10.2018, ANK Akata & Altuntaş 247.

Lepiota cristata (Bolton) P. Kumm.: In meadow, 15.10.2018, ANK Akata & Altuntaş 260; 17.10.2018, ANK Akata & Altuntaş 276; Akata *et al*. (2009).

Lepiota lilacea Bres.: In meadow, 08.09.2017, ANK Akata & Altuntaş 03.

Leucoagaricus leucothites (Vittad.) Wasser: In meadow, 16.10.2018, ANK Akata & Altuntaş 269; Akata *et al*. (2009).

Family *Bolbitiaceae*

Conocybe apala (Fr.) Arnolds: Akata *et al.* (2009).

Conocybe tenera (Schaeff.) Fayod: In meadow, 07.10.2018 ANK Akata & Altuntaş 223; Akata *et al.* (2009).

Family *Clavariaceae*

Clavaria fragilis Holmsk.: In meadow, 14.10.2018, ANK Akata & Altuntaş 252.

Family *Cortinariaceae*

Cortinarius decipiens (Pers.) Fr.: Under *Betula pendula* Roth (*Betulaceae*), 15.09.2017, ANK Akata & Altuntaş 16.

Family *Cyphellaceae*

Chondrostereum purpureum (Pers.) Pouzar: On dead branch of *Quercus robur* L. (*Fagaceae*), 13.01.2019, ANK Akata & Altuntaş 605; Akata *et al*. (2009).

Family *Entolomataceae*

Entoloma sericeoides (J.E. Lange) Noordel.: In meadow, 28.04. 2018, ANK Akata & Altuntaş 60.

Family *Hymenogastraceae*

Hebeloma crustuliniforme (Bull.) Quél.: Under *Betula pendula* Roth (*Betulaceae*), 18.10.2018, ANK Akata & Altuntaş 279.

Hebeloma hiemale Bres.: Under *Quercus robur* L. (*Fagaceae*), 14.10.2018, ANK Akata & Altuntaş 255.

Hebeloma mesophaeum (Pers.) Quél.: Under *Picea pungens* Engelm. (*Pinaceae*), 17.10.2018, ANK Akata & Altuntaş 272; 10.12.2018, ANK Akata & Altuntaş 602.

Hebeloma sinapizans (Paulet) Gillet: Under *Quercus robur* L. (*Fagaceae*), 12.10.2018, ANK Akata & Altuntaş 237.

Family *Inocybaceae*

Crepidotus caspari Velen.: On stump of *Cercis siliquastrum* L. (*Fabaceae*), 13.10.2018, ANK Akata & Altuntaş 246.

Inocybe geophylla (Bull.) P. Kumm.: Akata *et al.* (2009).

Inocybe grammata Quél.: Under *Picea pungens* Engelm. (*Pinaceae*), 14.10.2018, ANK Akata & Altuntaş 251.

Inocybe griseolilacina J.E. Lange: Under *Pinus nigra* J.F Arnold (*Pinaceae*), 14.10.2018, ANK Akata & Altuntaş 257.

Inocybe queletii Konrad: Akata *et al*. (2009).

Inocybe pseudohiulca Kühner: Under *Picea pungens* Engelm. (*Pinaceae*), 17.10.2018, ANK Akata & Altuntaş 273.

Inocybe rimosa (Bull.) P. Kumm.: Under *Pinus nigra* J.F Arnold *(Pinaceae*), 05.06.2018, ANK Akata & Altuntaş 121.

Inocybe squamata J.E. Lange: Under *Populus nigra* L. (*Salicaceae*), 14.10.2018, ANK Akata & Altuntaş 253.

Inocybe splendens R. Heim: Under *Quercus robur* L. (*Fagaceae*), 12.10.2018, ANK Akata & Altuntaş 235.

Family *Lyophyllaceae*

Calocybe ionides (Bull.) Donk: Under *Pyrus communis* L. (*Rosaceae*), 15.10.2018, ANK Akata & Altuntaş 261.

Lyophyllum decastes (Fr.) Singer: In meadow, 02.11.2018, ANK Akata & Altuntaş 586.

Family *Omphalotaceae*

Gymnopus hariolorum (Bull.) Antonín, Halling & Noordel.: Under *Pyrus communis* L. (*Rosaceae*), 25.10.2018, ANK Akata & Altuntaş 553.

Family *Physalacriaceae*

Armillaria mellea (Vahl) P. Kumm.: On stump of *Quercus robur* L. (*Fagaceae*), 28.09.2018, ANK Akata & Altuntaş 202; Akata *et al*. (2009).

Flammulina velutipes (Curtis) Singer: On stump of *Populus nigra* L. (*Salicaceae*), 26.11.2017, ANK Akata & Altuntaş 49; 15.01.2019, ANK Akata & Altuntaş 610; Akata *et al*. (2009).

Strobilurus tenacellus (Pers.) Singer: On cone of *Pinus nigra* J.F Arnold (*Pinaceae*), 15.04.2018, ANK Akata & Altuntaş 58; Akata *et al.* (2009).

Family *Pleurotaceae*

Pleurotus ostreatus (Jacq.) P. Kumm.: On *Populus nigra* L. (*Salicaceae*), 21.09.2018, ANK Akata & Altuntaş 184; Akata *et al*. (2009).

Family *Pluteaceae*

Pluteus podospileus Sacc. & Cub.: On stump of *Pyrus communis* L. (*Rosaceae*), 27.10.2018, ANK Akata & Altuntaş 568.

Family *Psathyrellaceae*

Coprinellus disseminatus (Pers.) J.E. Lange: On stump of *Populus nigra* L. (*Salicaceae*), 07.10.2017, on stump of *Quercus robur* L. (*Fagaceae*), 17.10.2018, ANK Akata & Altuntaş 279; Akata *et al*. (2009).

Coprinellus micaceus (Bull.) Vilgalys, Hopple & Jacq. Johnson: On stump of *Quercus robur* L.

(*Fagaceae*), 07.10.2018 ANK Akata & Altuntaş 224; Akata *et al*. (2009).

Coprinopsis atramentaria (Bull.) Redhead, Vilgalys & Moncalvo: In meadow, 06.10.2018 ANK Akata & Altuntaş 217; 17.10.2018, ANK Akata & Altuntaş 278; Akata *et al*. (2009).

Lacrymaria lacrymabunda (Bull.) Pat.: In meadow, 25.09.2018, ANK Akata & Altuntaş 193.

Panaeolina foenisecii (Pers.) Maire: Akata *et al*. (2009).

Panaeolus fimicola (Pers.) Gillet: In meadow, 26.10.2018, ANK Akata & Altuntaş 561.

Panaeolus olivaceus F.H. Møller: In meadow, 25.10.2018, ANK Akata & Altuntaş 559.

Panaeolus papilionaceus (Bull.) Quél.: In meadow, on manure, 27.10.2018, ANK Akata & Altuntaş 567.

Parasola conopilea (Fr.) Örstadius & E. Larss.: In meadow, 02.10.2018, ANK Akata & Altuntaş 214.

Parasola plicatilis (Curtis) Redhead, Vilgalys & Hopple: In meadow, 12.10.2018, ANK Akata & Altuntaş 240.

Psathyrella candolleana (Fr.) Maire: In meadow, 20.09.2018, ANK Akata & Altuntaş 170; 14.10.2018, ANK Akata & Altuntaş 250.

Family *Schizophyllaceae*

Schizophyllum amplum (Lév.) Nakasone: Akata (2010).

Schizophyllum commune Fr.: On dead branch of *Quercus robur* L. (*Fagaceae*), 19.10.2017, ANK Akata & Altuntaş 30; 15.10.2018, ANK Akata & Altuntaş 265; Akata *et al*. (2009).

Family *Strophariaceae*

Cyclocybe cylindracea (DC.) Vizzini & Angelini: On stump of *Populus nigra* L. (*Salicaceae*), 21.09.2018, ANK Akata & Altuntaş 185; Akata *et al*. (2009).

Pholiota aurivella (Batsch) P. Kumm.: Akata *et al*. (2009).

Pholiota lubrica (Pers.) Singer: Under *Pyrus communis* L. (*Rosaceae*), 15.10.2018, ANK Akata & Altuntaş 263.

Pholiota populnea (Pers.) Kuyper & Tjall.-Beuk.: Akata *et al*. (2009).

Family *Tricholomataceae*

Lepista nuda (Bull.) Cooke: In meadow, 03.10.2017, ANK Akata & Altuntaş 25; Akata et al. (2009).

Leucocybe candicans (Pers.) Vizzini, P. Alvarado, G. Moreno & Consiglio: Under *Syringa vulgaris* L. (*Oleaceae*), 15.10.2018, ANK Akata & Altuntaş 259.

Melanoleuca exscissa (Fr.) Singer: In meadow, 15.10.2018, ANK Akata & Altuntaş 260.

Tricholoma scalpturatum (Fr.) Quél.: Under *Pinus nigra* J.F Arnold (*Pinaceae*), 25.10.2018, ANK Akata & Altuntaş 552; 10.12.2018, ANK Akata & Altuntaş 601; 15.01.2019, ANK Akata & Altuntaş 609.

Tricholoma terreum (Schaeff.) P. Kumm.: Akata *et al*. (2009).

Family *Tubariaceae*

Tubaria conspersa (Pers.) Fayod: In meadow, among grasses, 16.10.2018, ANK Akata & Altuntaş 268.

Order *Boletales*

Family *Boletaceae*

Rheubarbariboletus armeniacus (Quél.) Vizzini, Simonini & Gelardi: Akata *et al*. (2009).

Xerocomellus chrysenteron (Bull.) Šutara: Under *Pinus nigra* J.F Arnold (*Pinaceae*), 14.08.2018, ANK Akata & Altuntaş 140.

Family *Paxillaceae*

Paxillus involutus (Batsch) Fr.: Under *Picea pungens* Engelm. (*Pinaceae*), 28.09.2017, ANK Akata & Altuntaş 18.

Family *Sclerodermataceae*

Pisolithus arhizus (Scop.) Rauschert: Under *Pinus nigra* J.F Arnold (*Pinaceae*), 14.08.2018, ANK Akata & Altuntaş 137.

Scleroderma citrinum Pers.: On path, 14.10.2018, ANK Akata & Altuntaş 256; Akata *et al*. (2009).

Scleroderma verrucosum (Bull.) Pers.: Under *Tilia tomentosa* Moench (*Malvaceae*), 08.09.2017, ANK Akata & Altuntaş 10; 23.09.2018, ANK Akata & Altuntaş 189; 09.10.2018 ANK Akata & Altuntaş 231; 15.10.2018, ANK Akata & Altuntaş 264.

Family *Suillaceae*

Suillus collinitus (Fr.) Kuntze: Under *Pinus nigra* J.F Arnold *(Pinaceae*), 01.10.2018, ANK Akata & Altuntaş 206; 06.10.2018, ANK Akata & Altuntaş 274.

Order *Hymenochaetales*

Family *Hymenochaetaceae*

Fomitiporia punctata (P. Karst.) Murrill: On *Pyracantha coccinea* M.Roem. (*Rosaceae*) 15.10.2018, ANK Akata & Altuntaş 258.

Fuscoporia torulosa (Pers.) T. Wagner & M. Fisch.: On *Crataegus monogyna* Jacq. (*Rosaceae*), 12.10.2018, ANK Akata & Altuntaş 239.

Inonotus hispidus (Bull.) P. Karst.: On hardwood, 01.10.2017, ANK Akata & Altuntaş 21.

Phellinus igniarius (L.) Quél: On *Salix babylonica* L. (*Salicaceae*), 19.10.2017, ANK Akata & Altuntaş 33.

Order *Phallales*

Family *Phallaceae*

Phallus hadriani Vent.: On path, 21.09.2018, ANK Akata & Altuntaş 179.

Order *Polyporales*

Family *Ganodermataceae*

Ganoderma adspersum (Schulzer) Donk: On stump of *Acer platanoides* L. (*Aceraceae*), 27.10.2018, ANK Akata & Altuntaş 569.

Ganoderma applanatum (Pers.) Pat.: Akata *et al*. (2009).

Ganoderma lucidum (Curtis) P. Karst.: On *Euonymus japonicus* Thunb. (*Celastraceae*), 05.06.2018, ANK Akata & Altuntaş 116.

Family *Meruliaceae*

Bjerkandera adusta (Willd.) P. Kars.: On stump of *Quercus robur* L. (*Fagaceae*), 15.01.2019, ANK Akata & Altuntaş 611; Akata *et al*. (2009).

Family *Polyporaceae*

Cerioporus squamosus (Huds.) Quél.: On *Robinia pseudoacacia* L. (*Fabaceae*), 26.10.2018, ANK Akata & Altuntaş 566; Akata *et al*. (2009).

Fomes fomentarius (L.) Fr.: On *Salix babylonica* L. (*Salicaceae*), 02.10.2018, ANK Akata & Altuntaş 208; Akata *et al*. (2009).

Polyporus tuberaster (Jacq. ex Pers.) Fr.: On *Prunus avium* (L.) L. (*Rosaceae*), 08.09.2017, ANK Akata & Altuntaş 05.

Trametes trogii Berk.: Akata *et al*. (2009).

Trametes versicolor (L.) Lloyd: Akata *et al*. (2009).

Order *Pucciniales*

Family *Melampsoraceae*

Melampsora allii-populina Kleb.: On leaf of *Populus nigra* L. (*Salicaceae*), 05.06.2018, ANK Akata & Altuntaş 113.

Melampsora euphorbiae (Ficinus & C. Schub.) Castagne: leaf and stem of *Euphorbia peplus* L. (*Euphorbiaceae*), 21.08.2018, ANK Akata & Altuntaş 165.

Melampsora salicis-albae Kleb.: On leaf of *Salix babylonica* L. (*Salicaceae*), 08.09.2017, ANK Akata & Altuntaş 08.

Family *Phakopsoraceae*

Cerotelium fici (Castagne) Arthur: On leaf of *Ficus carica* L. (*Moraceae*), 20.09.2018, ANK Akata & Altuntaş 175.

Family *Phragmidiaceae*

Phragmidium mucronatum (Pers.) Schltdl.: Leaf of *Rosa canina* L. (*Rosaceae*), 09.07.2018, ANK Akata & Altuntaş 132; 18.08.2018, ANK Akata & Altuntaş 153; 02.10.2018, ANK Akata & Altuntaş 216.

Phragmidium potentillae (Pers.) P. Karst.: On leaf and stem of *Potentilla reptans* L. (*Rosaceae*), 29.09.2018, ANK Akata & Altuntaş 204.

Phragmidium sanguisorbae (DC.) J. Schröt.: On leaf and stem of *Sanguisorba minor* L. (*Rosaceae*), 08.10.2018 ANK Akata & Altuntaş 226.

Phragmidium tuberculatum Jul. Müll.: On leaf of *Rosa canina* L. (*Rosacea*e), 29.09.2017, ANK Akata & Altuntaş 20.

Family *Pucciniaceae*

Cumminsiella mirabilissima (Peck) Nannf.: On leaf of *Berberis aquifolium* Pursh (*Berberidaceae*), 08.07.2018, ANK Akata & Altuntaş 129.

Gymnosporangium clavariiforme (Wulfen) DC.: On leaf of *Crataegus monogyna* Jacq. (*Rosaceae*), 02.10.2018, ANK Akata & Altuntaş 211.

Gymnosporangium confusum Plowr.: On leaf of *Cotoneaster nummularius* Fisch.& C.A. Mey. (*Rosaceae*), 23.07. 2018, ANK Akata & Altuntaş 135.

Puccinia acetosae (Schumach.) Körn.: On leaf and stem of *Rumex crispus* L. (*Polygonaceae*), 05.07.2018, ANK Akata & Altuntaş 125.

Puccinia calcitrapae DC.: On leaf and stem of *Taraxacum officinale* F.H.Wigg. (*Asteraceae*), 05.06.2018, ANK Akata & Altuntaş 119.

Puccinia crepidicola Syd. & P. Syd.: On leaf and stem of *Crepis foetida* L. ssp. *rhoeadifolia* (M.Bieb.) Celak. (*Asteraceae*), 17.08.2018, ANK Akata & Altuntaş 152.

Puccinia chondrillina Bubák & Syd.: leaf and stem of *Chondrilla juncea* L. (*Asteraceae*), 05.06.2018, ANK Akata & Altuntaş 114.

Puccinia cnici H. Mart.: On leaf and stem of *Cirsium vulgare* (Savi) Ten (*Asteraceae*), 02.08.2018, ANK Akata & Altuntaş 136.

Puccinia graminis Pers.: On leaf and stem of *Avena barbata* Pott ex Link (*Poaceae*), 05.06.2018, ANK Akata & Altuntaş 117; On leaf and stem of *Triticum aestivum* L. (*Poaceae*), 18.08.2018, ANK Akata & Altuntaş 157.

Puccinia jasmini DC.: On leaf of *Jasminum fruticans* L. (*Oleaceae*), 05.07.2018, ANK Akata & Altuntaş 124.

*Puccinia malv*acearum Bertero ex Mont.: On leaf and stem of *Malva neglecta* Wallr. (*Malvaceae*), 08.07.2018, ANK Akata & Altuntaş 128; On leaf and stem of *Alcea rosea* L. (*Malvaceae*), 18.08.2018, ANK Akata & Altuntaş 160.

Puccinia polygoni-amphibii Pers.: On leaf and stem of *Polygonum aviculare* L. (*Polygonaceae*), 17.08.2018, ANK Akata & Altuntaş 151.

Puccinia recondita Roberge ex Desm.: On leaf and stem of *Hordeum bulbosum* L. (*Poaceae*), 18.08.2018, ANK Akata & Altuntaş 155.

Puccinia striiformis Westend.: On leaf and stem of *Hordeum bulbosum* L. (*Poaceae*), 05.06.2018, ANK Akata & Altuntaş 122.

Uromyces fischeri–eduardii Magn.: On leaf and stem of *Vicia sativa* L. (*Fabaceae*), 19.08.2018, ANK Akata & Altuntaş 163.

Uromyces geranii (DC.) G.H. Otth & Wartm.: On leaf and stem of *Geranium rotundifolium* L. (*Geraniaceae*), 05.06.2018, ANK Akata & Altuntaş 110.

Uromyces pisi-sativi (Pers.) Liro: On leaf and stem of *Medicago sativa* L. (*Fabaceae*), 18.08.2018, ANK Akata & Altuntaş 159.

Uromyces polygoni-avicularis (Pers.) G.H. Otth: On leaf and stem of *Polygonum aviculare* L. (*Polygonaceae*), 05.06.2018, ANK Akata & Altuntaş 115.

Uromyces rumicis (Schum.) Wint: On leaf and stem of *Rumex crispus* L. (*Polygonaceae*), 18.08.2018, ANK Akata & Altuntaş 154.

Uromyces tinctoriicola Magnus: On leaf and stem of *Euphorbia peplus* L. (*Euphorbiaceae*), 08.07.2018, ANK Akata & Altuntaş 131.

Uromyces trifolii (R. Hedw.) Lév.: On leaf and stem of *Trifolium pratense* L. (*Fabaceae*), 05.06.2018, ANK Akata & Altuntaş 120.

Family *Uropyxidaceae*

Tranzschelia discolor (Fuckel) Tranzschel & M.A. Litv. On leaf of *Prunus domestica* L. (*Rosaceae*), 05.07.2018, ANK Akata & Altuntaş 126.

Tranzschelia pruni-spinosae (Pers.) Dietel: On leaf of *Prunus armeniaca* L. (*Rosaceae*), 23.07. 2018, ANK Akata & Altuntaş 134; On *Prunus domestica* L. (*Rosaceae*), 19.08.2018, ANK Akata & Altuntaş 161.

Order *Russulales*

Family *Amylostereaceae*

Amylostereum areolatum (Chaillet ex Fr.) Boidin: Akata *et al*. (2009).

Family *Peniophoraceae*

Gloiothele lactescens (Berk.) Hjortstam: On stump of *Quercus robur* L. (*Fagaceae*), 27.10.2018, ANK Akata & Altuntaş 570.

Family *Russulaceae*

Russula pallidospora J. Blum ex Romagn.: Under *Quercus robur* L. (*Fagaceae*), 20.09.2018, ANK Akata & Altuntaş 169.

Family *Stereaceae*

Stereum hirsutum (Willd.) Pers.: On stump of *Quercus robur* L. (*Fagaceae*), 23.10.2017, ANK Akata & Altuntaş 35; 09.10.2018 ANK Akata & Altuntaş 232; Akata *et al*. (2009).

Order *Ustilaginales*

Family *Ustilaginaceae*

Ustilago avenae (Pers.) Rostr.: On fruit of *Avena barbata* Pott ex Link (*Poaceae*) 12.09.2017, ANK Akata & Altuntaş 12.

Discussion

A total of 162 fungal species belonging to 87 genera within 49 families were determined in the study area. The determined fungi included 47 *Ascomycota (Erysiphaceae* 30, *Helvellaceae* and *Pyronemataceae* 3, *Cladosporiaceae* and *Mycosphaerellaceae* 2, *Gnomoniaceae, Glomerellaceae, Plectosphaerellaceae, Hypocreaceae, Venturiaceae, Phyllachoraceae* and *Rhytismataceae* 1) and 115 *Basidiomycota (Pucciniaceae* 23, *Psathyrellaceae* 11, *Inocybaceae* 9, *Agaricaceae* 8, *Polyporaceae* and *Tricholomataceae* 5, *Hymenochaetaceae, Hymenogastraceae, Phragmidiaceae* and *Strophariaceae* 4, *Ganodermataceae, Melampsoraceae, Physalacriaceae* and *Sclerodermataceae* 3, *Bolbitiaceae, Boletaceae, Lyophyllaceae* and *Schizophyllaceae* 2, *Clavariaceae, Cortinariaceae, Cyphellaceae, Entolomataceae, Meruliaceae, Omphalotaceae, Pleurotaceae, Pluteaceae, Tubariaceae, Paxillaceae, Suillaceae, Phallaceae, Phakopsoraceae, Amylostereaceae, Peniophoraceae, Russulaceae, Stereaceae* and *Ustilaginaceae* 1) species.

Eighty-five of one hundred and sixty-two species determined in the campus area were parasite infecting plant tissues except for the fungicolous species (*Hypomyces chrysospermus*). Plant parasitic species belongs to Erysiphales or powdery mildews (30 species), *Pucciniales* or rusts (31 species), *Ustilaginales* or smuts (1), larger basidiomycete fungi (11) and other microscopic ascomycete fungi (11). Seventy-seven species reported from the research area are saprobes, among which 63 are terricolous and the number of lignicolous species is 14.

Although 15 species (*Helvella leucomelaena, Agaricus campestris, Coprinus comatus, Leucoagaricus leucothites, Lyophyllum decastes, Armillaria mellea, Flammulina velutipes, Pleurotus ostreatus, Cyclocybe cylindracea, Lepista nuda, Melanoleuca exscissa, Tricholoma terreum, Xerocomellus chrysenteron, Suillus collinitus,* and *Cerioporus squamosus*) are suitable for human consumption, 17 species (*Agaricus xanthodermus, Inocybe geophylla, I. grammata, I. griseolilacina, I. queletii, I. pseudohiulca, I. squamata, I. rimosa, Lepiota brunneoincarnata, L. cristata, Leucocybe candicans, Paxillus involutus, Hebeloma crustuliniforme, H. mesophaeum, H. sinapizans, Sleroderma citrinum* and *S. verrucosum*) are determined as poisonous fungi in the campus area. Among them, *L.brunneoincarnata* is a deadly poisonous fungus containing alpha-amanitin which is responsible for the most deadly mushroom poisoning cases in Turkey (Akata *et al.* 2015). No poisoning case has been reported from the campus area so

far because no one in the campus has been interested in collecting and consuming the mushrooms found inside the campus.

One hundred and twenty-seven species were determined as new species for campus area and 5 of them (*Hypomyces chrysospermus, Calocybe ionides, Gloiothele lactescens, Inocybe griseolilacina* and *Pulvinula convexella*) were recorded for the second time in Turkey.

Acknowledgement

We thank Ankara University Research Fund (Project No: 18B0430001) for their financial support. Dr. İsa Başköse and Dr. Ergin Şahin are also thanked for their valuable contributions in the field.

Editor-in-Chief note: Author Ilgaz Akata is a member of Editorial Board of Trakya University Journal of Natural Sciences. However, he wasn't involved in the decision process during manuscript evaluation.

References

1. Acar, İ. & Uzun Y. 2017. Türkiye Mikobiyotası İçin İlginç Bir Yarı-Serbest Morel Kaydı (*Morchella populiphila* M. Kuo, M.C. Carter & J.D. Moore). *Mantar Dergisi*, 8(2): 125-128.
2. Akata, I. 2010. Türkiye mikobiyotası için yeni bir kayıt, *Schizophyllum amplum* (Lev.) Nakasone. *Ot Sistematik Botanik Dergisi*, 17(2): 155-163.
3. Akata, I. 2017. Macrofungal Diversity of Belgrad Forest (İstanbul). *Kastamonu Üniversitesi Orman Fakültesi Dergisi*, 17(1): 150-164.
4. Akata, I. & Heluta, V.P. 2015. First record of *Erysiphe syringae-japonicae* in Turkey. *Mycotaxon*, 130: 259-264.
5. Akata, I. & Uzun, Y. 2017. Macrofungi determined in Uzungöl Nature Park (Trabzon). *Trakya Unıversity Journal of Natural Sciences*, 18(1): 15-24.
6. Akata, I., Doğan, H.H., Körüklü, T. & İslek, C. 2009. Ankara Üniversitesi Tandoğan Kampüsü Makrofungusları. *Kafkas Üniversitesi Fen Bilimleri Enstitüsü Dergisi*, 2(1): 15-19.
7. Akata I., Kaya E., Yılmaz İ., Bakırcı S. & Bayram R. 2015. Türkiye'de Yetişen Alfa Amanitin İçeren Mantarlar. *Düzce Tıp Fakültesi Dergisi*, 17(1): 39-44.
8. Akata, I., Kabaktepe, Ş., Sevindik, M. & Akgül, H. 2018. Macrofungi determined in Yuvacık Basin (Kocaeli) and its close environs. *Kastamonu Üniversitesi Orman Fakültesi Dergisi*, 18(2): 152-163.
9. Akgül, H., Ergül, C.C., Yılmazkaya, D., Akata, I., Selçuk, F. & Hüseyin, E. 2015. Diversity of Microfungi on *Fagaceae* in Uludağ Forests. *Oxidation Communications*, 38(3): 1529-1538.
10. Allı, H., Candar, S.S. & Akata, I. 2017. Macrofungal Diversity of Yalova Province. *Mantar Dergisi*, 8(2): 76-84.
11. Altuntaş, D., Allı, H. & Akata, I. 2017. Macrofungi of Kazdağı National Park (Turkey) and its close environs. *Biological Diversity and Conservation*, 10(2): 17-25.
12. Bahçecioğlu, Z. & Kabaktepe, Ş. 2012. Checklist of rust fungi in Turkey. *Mycotaxon*, 119: 494.
13. Braun, U. & Cook, R.T.A. 2012. *Taxonomic manual of the Erysiphales (powdery mildews).* CBS Biodiversity Series II, CBS-KHAW Fungal Biodiversity Centre, Utrecht, The Netherlands, 707 pp.
14. Breitenbach, J. & Kränzlin, F. 1984. *Fungi of Switzerland, Vol: 1, Ascomycetes.* Verlag Mykologia CH-6000 Luzern 9, Switzerland, 310 pp.
15. Breitenbach, J. & Kränzlin, F. 1986. *Fungi of Switzerland, Vol: 2, Nongilled Fungi.* Verlag Mykologia CH-6000 Luzern 9, Switzerland, 412 pp.
16. Breitenbach, J. & Kränzlin, F. 1991. *Fungi of Switzerland, Vol: 3, Boletes and Agarics 1. Part.* Verlag Mykologia CH6000 Luzern 9, Switzerland, 361 pp.
17. Breitenbach, J. & Kränzlin, F. 1995. *Fungi of Switzerland, Vol: 4, Agarics 2. Part.* Verlag Mykologia CH-6000 Luzern 9, Switzerland, 368 pp.
18. Breitenbach, J. & Kränzlin, F. 2000. *Fungi of Switzerland, Vol: 5, Agarics 3. Part.* Verlag Mykologia CH-6000 Luzern 9, Switzerland, 338 pp.
19. Demirel, K., Uzun, Y., Keleş, A., Akçay, M.E. & Acar, İ. 2017. Macrofungi of Karagöl–Sahara National Park (Şavşat-Artvin/Turkey). *Biological Diversity and Conservation*, 10(2): 32-40.
20. Doğan, H.H., Öztürk, C., Kaşık, G. & Aktaş, S. 2005. A Checklist of *Aphyllophorales* of Turkey. *Pakistan Journal of Botany*. 37(2): 459-485.
21. Doğan, H.H., Bozok, F. & Taşkın, H. 2018. A new species of *Barssia* (*Ascomycota*, *Helvellaceae*) from Turkey. *Turkish Journal of Botany*, 42: 636-643.
22. Ekici, T., Erdogdu, M., Aytaç, Z. & Suludere, Z. 2012. *Septoria* species in Kıbrıs Village Valley (Ankara, Turkey). *Nova Hedwigia Band*, 95(3-4): 483-491.
23. Ellis, B.M. & Ellis, J.P. 1987. *Microfungi on Land Plants*. Croom Helm, London & Sydney, 818 pp.
24. Erdoğdu, M. & Hüseyin, E. 2008. Microfungi of Kurtboğazı Dam (Ankara) and its environment. *Ot Sistematik Botanik Dergisi*, 14(1): 131-150.
25. Hansen, L. & Knudsen, H. 1992. *Nordic Macromycetes, Volume 2, Polyporales, Boletales, Agaricales, Russulales.* Nordsvamp, Copenhagen, Denmark, 474 pp.
26. Hansen, L. & Knudsen, H. 1997. *Nordic Macromycetes, Volume 3, Heterobasidoid, Aphyllophoroid, and Gastromycetoid Basidiomycetes*. Nordsvamp, Copenhagen, Denmark, 444 pp.
27. Hansen, L. & Knudsen, H. 2000. *Nordic Macromycetes, Volume 1, Ascomycetes*. Nordsvamp, Copenhagen, Denmark, 209 pp.
28. Hüseyin E. & Selçuk, F. 2016. *Pileolaria azerii* (*Uredinales*), a new rust species from Turkey. *Sydowia*, 68: 1-6.

29. Hüseyin, E., Selçuk, F. & Ekici K. 2016. *Acrodictys*, *Corynespora*, *Karstenula*, *Oncopodium*, and *Sporocadus*: new genera for Turkey. *Mycotaxon*, 131: 331-335.

30. Index fungorum: www.indexfungorum.org; accessed 25 January 2019.

31. Işık, H. & Türkekul, İ. 2018. A New Record for Turkish Mycota from Tokat Province: *Arachnopeziza aurelia* (Pers.) Fuckel. *Mantar Dergisi*, 9(1): 54-57.

32. Jordan, M. 2004. *The Encyclopedia of Fungi of Britain and Europe*. Frances Lincoln, London, 384 pp.

33. Kabaktepe, Ş., Heluta, V.P. & Akata, I. 2015. Checklist of Powdery mildews (*Erysiphales*) in Turkey. *Biological Diversity and Conservation*, 8(3): 128-146.

34. Kabaktepe, Ş., Mutlu, B., Karakuş, Ş. & Akata, I. 2016. *Puccinia marrubii* (*Pucciniaceae*), a new rust species on *Marrubium globosum* subsp. *globosum* from Niğde and Malatya in Turkey. *Phytotaxa*, 272(4): 277-286.

35. Kabaktepe, Ş., Akata, I., Siahaan, S.A.S., Takamatsu, S. & Braun, U. 2017. Powdery mildew (*Ascomycota*, *Erysiphales*) on *Fontanesia phillyreoides* and *Jasminum fruticans* in Turkey. *Mycoscience*, 58: 30-34.

36. Kabaktepe, Ş. & Akata, I. 2018. *Septoria* Sacc. (*Mycosphaerellales*) Species Determined in Aladağlar and Bolkar Mountains (Turkey). *Mantar Dergisi*, 9(2): 142-147.

37. Kränzlin, F. 2005. Fungi of Switzerland, Volume 6, Russulaceae 2. Verlag Mykologia, Switzerland, 319 pp.

38. Öztürk, C., Pamukçu, D. & Aktaş, S. 2017. Macrofungi of Nallıhan (Ankara) District. *Mantar Dergisi*, 8(1): 60-67.

39. Selçuk, F. & Ekici, K. 2014. A new species of *Manoharachariella* (*Hyphomycetes*) from Central Anatolia, Turkey. *Mycosphere*, 5 (3): 419-423.

40. Servi, H., Akata, I. & Çetin, B. 2010. Macrofungal diversity of Bolu Abant Nature Park (Turkey). *African Journal of Biotechnology*, 9(24): 3622-3628.

41. Sesli, E. & Denchev, C.M. 2008. Checklists of the myxomycetes, larger ascomycetes, and larger basidiomycetes in Turkey. *Mycotaxon*, 106: 65-67.

42. Sesli, E. & Vizzini, A. 2017. Two new *Rhodocybe* species (sect. Rufobrunnea, *Entolomataceae*) from the East Black Sea coast of Turkey. *Turkish Journal of Botany*, 41: 200-210.

43. Sesli, E. & Liimatainen, K. 2018. *Cortinarius conicoumbonatus* (*Cortinarius* subgen. Telamonia sect. Hinnulei): a new species from spruce-beech forests of the East Black Sea Region of Turkey. *Turkish Journal of Botany*, 42: 327-334.

44. Şen, İ., Allı, H. & Çöl, B. 2018. *Tricholoma bonii*, A New Record for Turkish Mycota and Notes on its Taxonomic Status Based on Morphological and Molecular Evidence. *Turkish Journal of Life Sciences*, 3(1): 200-204.

45. Uzun, Y., Acar, İ., Akçay, M.E. & Akata, I. 2014. Additions to the Turkish *Discomycetes*. *Turkish Journal of Botany*, 38: 617-622.

46. Vánky, K. 2012. *Smut Fungi of the World*. APS press, St. Paul. Minnesota, 1480 pp.

47. Wilson, L.M. & Henderson, D.M. 1966. *British Rust Fungi*. Cambridge University Press, 384 pp.

http://dergipark.gov.tr/trkjnat
Trakya University Journal of Natural Sciences, 20(1): 57-62, 2019
ISSN 2147-0294, e-ISSN 2528-9691
DOI: 10.23902/trkjnat.471236

Research Article

DETERMINATION OF *in vitro* BIOFILM FORMATION ABILITIES OF FOOD BORNE *Salmonella enterica* ISOLATES

Deniz AKSOY

Trakya University, Faculty of Science, Department of Biology, Edirne TURKEY
ORCID ID: orcid.org/0000-0001-8696-9725, e-mail: denizyuksel@trakya.edu.tr

Cite this article as:

Aksoy D. 2019. Determination of *in vitro* Biofilm Formation Abilities of Food Borne *Salmonella enterica* Isolates. *Trakya Univ J Nat Sci*, 20(1); 57-62, DOI: 10.23902/trkjnat.471236

Received: 16 October 2018, Accepted: 18 March 2019, Online First: 19 March 2019, Published: 15 April 2019

Abstract: Salmonellosis caused by non-typhodial *Salmonella enterica* serotypes is one of the most important food-borne diseases worldwide and biofilm structure formed by these pathogens provide a reservoir for food contamination and a source for infections. This study was performed in order to determine biofilm formation abilities of food borne *Salmonella* isolates on polystyrene and on air liquid interphase and their colony morphologies when grown on Congo Red Agar plates. 32 food-borne *Salmonella* strains isolated from retail chicken carcasses in Edirne province of Turkey and belonging to the Infantis, Enteritidis, Kentucky and Telaviv serotypes were used. The microtiter plate technique was used to determine biofilm formation abilities of the isolates on polystyrene surfaces by measuring the optical density (OD) values of the stained bacterial biofilms. The results showed that the strongest biofilm formation capacities of the isolates were observed at 22°C for 3 days of incubation. Although all isolates formed pellicle on the liquid-air interface at 22°C, only 13% of the isolates belonging to the Infantis, Kentucky and Enteritidis serovars formed pellicle at liquid-air interface at 37°C. Three different colony morphotypes (saw; smooth and white, bdar; brown, dry and rough, rdar; red, dry and rough) were determined on Congo Red Agar among the isolates. High biofilm formation abilities of the tested *Salmonella* isolates can lead to widespread of virulence and resistance properties, especially to medically important antibiotics such as ciprofloxacin, via food chain. This situation constitutes an important concern for public health.

Key words: *Salmonella*, biofilm, food-borne pathogen, microbial food safety.

Özet: *Salmonella enterica* serotiplerinin neden olduğu salmonelloz vakaları dünya çapında en önemli gıda kökenli hastalıkların başında gelmektedir. Bu patojenlerin oluşturduğu biyofilm yapısı hem gıda kontaminasyonlarına neden olmakta hem de enfeksiyonlar için kaynak oluşturmaktadır. Bu çalışmada gıda kökenli *Salmonella enterica* izolatlarının polistirende ve hava-sıvı ara fazında biyofilm oluşturma yetenekleri ve ayrıca Kongo kırmızısı agar plakalarında koloni morfolojilerinin belirlenmesi amaçlanmıştır. Çalışmada Edirne ilinde satışa sunulan tavuk karkaslarından izole edilmiş 32 adet *Salmonella* izolatı kullanılmıştır. İzolatların plastik yüzeylerdeki biyofilm oluşturma yeteneklerinin belirlenmesinde boyanmış bakteriyel biyofilmlerin optik yoğunluklarının ölçülmesi esasına dayanan mikroplaka tekniği kullanılmıştır. Polistren plakalardaki biyofilm oluşturma sonuçlarına göre, izolatların en güçlü biyofilm oluşturma kapasitesi 22°C'de 3 günde gözlemlenmiştir. Bütün izolatlar 22°C'de sıvı-hava ara fazında pelikül oluştururken izolatların sadece % 13'ü (Infantis, Kentucky ve Enteritidis serovarlarını içeren) 37°C'de sıvı-hava ara fazında pelikül oluşturmaktadır. Kongo kırmızısı agarda üç farklı koloni morfolojisi (saw; pürüzsüz ve beyaz, bdar; kahverengi, kuru ve pürüzlü, rdar; kırmızı, kuru ve pürüzlü) belirlenmiştir. *Salmonella* izolatlarının yüksek biyofilm oluşturma kapasiteleri, virülens ve özellikle tıbbi olarak önemli antibiyotikleri içeren direnç faktörlerinin gıda zinciri yolu ile geniş çaplı yayılımına neden olabilir. Bu durum halk sağlığı açısından büyük bir endişe kaynağı oluşturmaktadır.

Introduction

Salmonellosis caused by non-typhodial *Salmonella enterica* serotypes is one of the most important food-borne diseases worldwide and an increasing number of human Salmonellosis cases have been linked to consumption of contaminated food (Panisello *et al.* 2000). Poultry and poultry associated products in particular are essential reservoirs for food-borne pathogens and these products have been identified as significant transmission vehicle for Salmonellosis by allowing *Salmonella* to be easily transmitted to humans from these products (Hoelzer *et al.* 2011, Antunes *et al.* 2016). It is also known that many pathogenic bacteria including *Salmonella* can attach to and grow on food and food contact surfaces to form biofilms in food processing industry which cause major economic and public health concerns and this biofilm formation ability can be the main reason of wide distribution of *Salmonella* isolates (Vestby 2009b). Biofilm formation depends on some characteristics of the bacteria and environmental factors such as pH, temperature and nutrient components (Shia & Zhu 2009).

Bacterial biofilms are highly resistant to environmental stress, antibiotics, and disinfectants and thus are difficult to sanitate (Hoiby *et al.* 2010, Steenackers *et al.* 2012). Biofilms constitute a source for clinical infections and pathogenic microorganisms in biofilms provide a reservoir for food contaminations (Costerton *et al.* 1999, Srey *et al.* 2013).

In the present study, biofilm formation abilities of food borne *Salmonella* isolates on an abiotic surface (polystyrene plate) were investigated. The tests were performed at three different incubation temperatures and times to determine how these variables affected biofilm formation by the isolates. The pellicle formation on air liquid interphase was also tested as an indication of biofilm formation. In addition, colony morphologies of the isolates on Congo Red Agar plates were evaluated to reveal the components of biofilm produced considering morphotypes on the agar plates.

Materials and Methods

Bacterial strains

Salmonella strains formerly isolated from retail chicken carcasses in Edirne province of Turkey were used (see Aksoy and Şen 2015). The strains were determined to belong to the Infantis (n=26), Enteritidis (n=4), Kentucky (n=1) and Telaviv (n=1) serotypes. The original codes assigned to the serotypes (from A1 to A32) were used throughout the text when it was necessary to refer to the serotypes individually.

Biofilm formation on polystyrene

96-well polystyrene microplates (Grenier Bio-One) were used for quantification of biofilm production based on the previously described method with some modifications (Stepanović *et al.* 2004). The wells were filled with 230 µL of LB^{wo}/NaCl broth. Liquid bacterial cultures (18 h old) were diluted in LB^{wo}/NaCl broth to OD570 = 0.2 and 20 µL of these cultures were transferred to each well (three parallels of each strain). The negative control wells contained broth only. Microplates were incubated statically for one (24 h), two (48 h) and three days (72 h) at 5°C, 22°C and 37°C. The incubation temperatures were selected to represent routine storage condition of foods, room temperature and optimum growth condition of *Salmonella*, respectively. After incubation, the contents of the wells were emptied, wells were washed three times with 300 µL sterile distilled water and then 250 µL of methanol (≥ 99.9 %) was added per well. After incubation for 15 min in room temperature, microplates were emptied and air dried. Then wells were stained with Cyristal violet (0.1%) used for Gram staining (Merck) for 5 min. Excess stain was rinsed off by washing the microplates with running tap water and the microplates were air dried. The dye bound to adherent cells was dissolved using 250 µL of 33 % (v/v) glacial acetic acid in each well. The optical density was measured at 570 nm using a Multiskan EX reader (Bio-Rad). Based on the OD results, strains were classified into four categories as no biofilm producers, weak, moderate or strong biofilm producers as previously described (Stepanović *et al.* 2000). The cut-off optical density (ODc) is defined as three standard deviations above the mean OD of the negative control. Strains were classified as follows: OD ≤ ODc = no biofilm producer, ODc < O.D. ≤ (2 x ODc) = weak biofilm producer, (2 x ODc) < OD ≤ (4 x ODc) = moderate biofilm producer and (4 x ODc) < OD = strong biofilm producer.

Pellicle formation at liquid-air interface

The pellicle formation at the liquid-air interface was tested by inoculation of 0.5 mL of bacterial cultures (18h) in 4.5 mL LB ^{wo}/NaCl for incubation at 5°C, 22°C and 37°C for eight days in static conditions. The strains were visually controlled every day for presence of pellicle formation (Solano *et al.* 2002). *S.* Typhimurium ATCC 14028 was used as the positive control.

Colony morphology on Congo Red (CR) Agar plates

The method described by Turki *et al.* (2012) was used with some modifications for determination of colony morphology. Bacterial cultures (18 h old) were plated on LB ^{wo}/NaCl agar supplemented with Congo Red (8 µg/mL). After incubation at 5°C, 22°C and 37°C for eight days, the colony morphology was determined based on the classification as saw (smooth and white), bdar (brown, dry and rough), and rdar (red, dry and rough). *S.* Typhimurium ATCC 14028 was used as the positive control for rdar morphology.

Statistical Analyses

Kruskal-Wallis test was used to calculate the significance of the differences between the biofilm formation abilities of the isolates on microtiter plates at different incubation times and temperatures ($p<0.05$). The differences between average biofilm formations on polystyrene by the bdar and rdar morphotypes were analyzed by the Student's t-test ($p<0.05$). Spearman's correlation test was used to determine the association between biofilm formation of the isolates on microtiter plates and their pellicle formation abilities. Analyses were performed with Graphpad PRISM software (Intuitive Software for Science, San Diego, CA).

Results and Discussion

In the present study, biofilm formation abilities of food borne *Salmonella* isolates belonging to four different serovars (Infantis, Enteritidis, Kentucky and Telaviv) were determined on polystyrene microtiter plates at different temperatures representing routine food storage conditions, room temperature and optimum growth condition of *Salmonella*, respectively. The effect of incubation temperature and times on biofilm formation ability of the isolates on microtiter plates is shown in Fig. 1.

The hygienic status of food contact and processing surfaces is very important and determined by the ability of cells to adhere to surfaces (van Houdt & Michiels, 2010). Polystyrene is a hydrophobic material and widely used in production of food contact, food packing and food service materials (Genualdi *et al.* 2014).

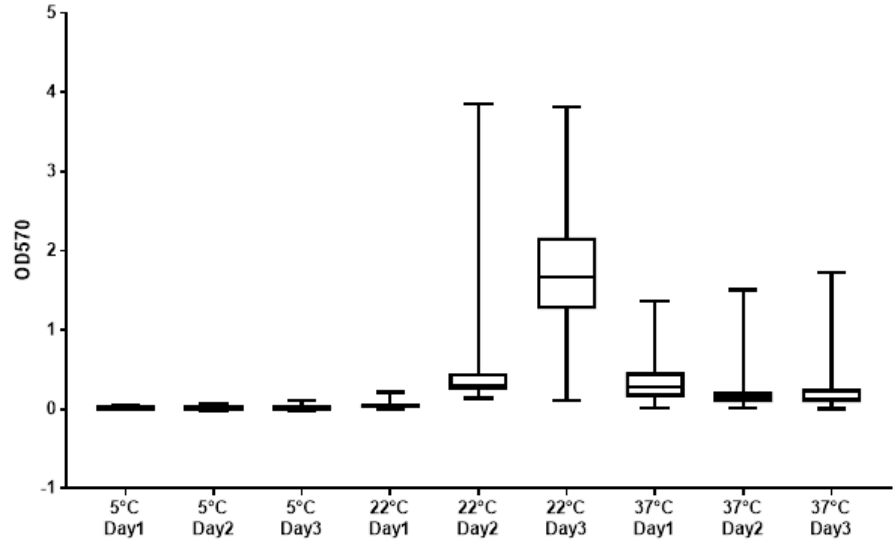

Fig. 1. The OD570 values of *Salmonella* isolates on microtiter plates at different incubation temperatures (5°C, 22°C and 37°C) and incubation times (1, 2 and 3 days). The OD value at 570 nm was used as the indication of level of biofilm formation.

Researchears commonly use microtiter plates as an *in vitro* mimic of the plastic surfaces in poultry production and daily use in houses (Díez-García *et al.* 2012, Piras *et al.* 2015, Borges *et al.* 2018). It has been previously showed that *Salmonella* spp. are capable of producing more biofilm on hydrophobic surfaces than hydrophilic surfaces (suchs as stainless steel, glass) (Sinde & Carballo 2000, Donlan 2002, Cunliffe *et al.* 1999). In a similar manner, biofilm formation was determined for all of the *Salmonella* isolates at 22°C (day1 and day2). When the average biofilm formation of the isolates on microtiter plates were compared, the results showed that there was no significant difference between different incubation days at 5°C while the differences at 22°C were significant ($p<0.05$). When the incubation temperature was 37°C, the difference between day1 and day2 was significant ($p<0.05$) but between day2 and day3 was not.

When the different incubation temperatures were compared based on a daily manner, the results revealed significant differences for all pairs for all days except 5°C and 22°C for day1. Biofilm forming abilities of bacteria depend on multiple factors one of which is the bacterial cell surface. For instance, in *S.* Typhimurium, expression of thin aggregative fimbriae was reported to increase at lower temperatures (20 and 28°C) (Römling *et al.* 1998). Increase in adherence to a surface at a low temperature may lead to persistence and survival in food-processing environments (Van Houdt and Michiels, 2010). It has been previously demonstrated that lower incubation temperature induced the biofim formation capacities of *Salmonella* serovars (Stepanović *et al.* 2003, Karaca *et al.* 2013, Milanov *et al.* 2017).

Accordingly, our results showed that the strongest biofilm formation capacities of the isolates were observed at 22°C for 3 days (Fig. 1.). At 37°C for 3 days, 22% of the isolates (Enteritidis and Infantis serovars) were determined as strong biofilm producers, 22% (Infantis and Kentucky serovars) were determined as moderate biofilm producers and 56% (Infantis and Telaviv serovars) were determined as weak biofilm producers. At 22°C (room temperature), 98% of the isolates (Enteridis, Infantis, Kentucky and Telaviv serovars) were determined as strong biofilm producers whereas only 2% (Enteritidis serovar) was determined as weak biofilm producers. At 5°C, 44% of the isolates (Enteritidis and Infantis serovars) were determined as weak biofilm producers and 56% (Infantis, Kentuck and Telaviv serovars) produced no biofilm. The lowest OD570 value (0.001) was obtained in one of the Infantis isolates (A27) with the incubation at 5°C for 1 day and the highest OD570 value (3,820) was obtained in the Telaviv isolate (A22) with the incubation at 22°C for 3 days. There are a few studies regarding the effects of incubation period and temperature on biofilm formation of *Salmonella* spp. strains. In a former study, Stepanović *et al*. (2003) studied with the serovars Enteritidis and Typhimurium, and showed that, although there was a significant difference in biofilm formed at 22°C incubation temperature after 24 and 48 h incubations, there was no significant difference when the temperature was set at 30°C/37°C for the same incubation periods. More recently, Vestby *et al*. (2009b) tested the effect of incubation period on biofilm formation in microtiter plates using the serovar Typhimurium, Agona, Montevideo, Senftenberg strains and found that only the serovar Sefteenberg strains exhibited increased biofilm forming capacities for 2 and 4 days of incubation. In the present study, the effects of prolonged incubation period and different incubation temperatures were tested on biofilm formation in microtiter plates based on a serovar manner. Serovar Infantis, Enteritidis, Kentucky and Telaviv isolates were used, of which Infantis, Enteritidis and Kentucky serovars are among the most common isolated serovars in Turkey. Interestingly, Telaviv has also been commonly isolated from food samples in Turkey although it is among the rare serovars throughout

the world (Ozdemir & Acar 2014, Erol 1999, Durul *et al.* 2015). The results showed that both the prolonged incubation period and the temperature effected the biofilm formation capacities depending on the serovars. Serovar Infantis strains were the only serovars which showed significant increase in OD570 values from day one to day three for all incubation temperature conditions (5°C, 22°C and 37°C). Serovar Telaviv and Kentucky strains showed significant increase only at 22°C and serovar Enteritidis strains showed significant increase only at 5°C. It was suggested that at 22°C, in the starionary phase of growth, utilization of nitrogen and phosphate induced the agfD promotor and contributed the multi-cellular state, but optimum growth condition (37°C) caused faster changes in oxygen tension and pH and this situation had a negative effect on multicellular status of *S.* Typhimurium (Gerstel and Romling, 2001, Stepanović *et al.* 2003). The results obtained in the present study revealed the importance of evaluation of all these factors on a serovar basis. These results reveal the necessity of further and more detailed studies on biofilm formation capacities of different serovars and isolates.

Three different colony morphotypes (saw, bdar, and rdar) of the isolates were determined on CR Agar. rdar which is caused by the coexpression of curli fimbriae and cellulose is a typical colony morphology that was observed between biofilm producer isolates. bdar and saw morphotypes were determined with deletion mutation in csg genes required for curli fimbriae synthesis or in both csg and bcs genes coding for cellulose synthesis, respectively. The production of cellulose and curli fimbriae is important in biofilm formation and its persistence on various surfaces (Römling, 2000, Cookson *et al.* 2002, Solano *et al.* 2002). When incubated at 37°C, 94% of the isolates exhibited bdar, 3% exhibited saw morphotype and one isolate belonging to the Infantis serovar presented a morphotype that has not been described previously. When the incubation temperature was 22°C, 81% and 19% of the isolates presented bdar and rdar morphotypes, respectively. On the other hand, isolates did not form biofilm on CR agar at low temperature (5°C). bdar and rdar morphotypes were good biofilm producers and both morphotype were commonly detected in *Salmonella* strains but studies showed that rdar strain was more tolerant to long-term desiccation and nutrient depletion in biofilm when compared to the bdar strain. (Vestby *et al.* 2009a). Average biofilm formations on polystyrene by the bdar and rdar morphotypes at 22°C were determined as 1.483±0.098 and 2.438±0.246, respectively and the difference between the two OD values was statistically significant ($p<0.05$) (Fig. 2).

When the different morphotypes were evaluated in terms of the serovars, the bdar morphotype was found to be exhibited by 96% of the Infantis serovars while the Enteritidis, Kentucky and Telaviv serovars isolates exhibited the rdar morphotype. Also, a similar serovar-morphotype relation was determined in a former study (Karaca *et al.* 2013).

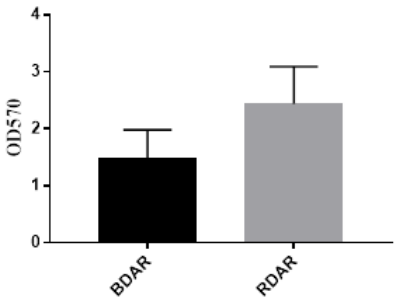

Fig. 2. Average biofilm formation on polystyrene of bdar and rdar strains.

Although all isolates formed pellicle at liquid-air interface at 22°C, only 13% of the isolates belonging to the Infantis (A3, A16), Kentucky (A10) and Enteritidis (A13) serovars formed pellicle at liquid-air interface at 37°C. No pellicle formation was detected at 5°C. No correlation was determined between biofilm formation of the isolates on microtiter plates and their pellicle formation abilities ($r=0.1545$, $p>0.05$). rdar and bdar morphotyped isolates formed pellicle with rigid and fragile structures, respectively.

In a recent study, antibiotic resistance profiles of the isolates used in the present study were determined (Aksoy & Şen 2015). 81.3% of the isolates exhibited multiple antibiotic resistance and *S.* Kentucky (A10) and *S.* Enteritidis (A32) isolates were resistant to ciprofloxacin. Ciprofloxacin resistance is important because it is a common antibiotic choice for invasive salmonellosis in humans (Velhner *et al.* 2014). 67.75% of the isolates were found to have high pathogenicity potential in *Caenorhabditis elegans* nematode model system (Aksoy & Şen 2015).

In a biofilm, avirulent and sensitive strains can become virulence and resistant via acquisition of virulence and resistance genes. It is also known that the rate of fluoroquinolone resistance of *Salmonella* strains was very low in Turkey (Albayrak *et al.* 2004, Ercis *et al.* 2006). However, fluoroquinolone resistance has recently become a common problem (Lin *et al.* 2015). High biofilm formation abilities of the present *Salmonella* strains can lead to widespread of virulence and resistance properties, especially to medically important antibiotics such as ciprofloxacin, via food chain. In addition, this situation constitutes an important public health concern. It is also known that biofilm formation abilities of *Salmonella* isolates are facilitated by long term persistence in food production environments (Vestby *et al.* 2009b). The present results suggested that almost all *Salmonella* isolates tested produced biofilm at room temperature. As a result, persistency of these isolates on abiotic surface increases which in turn increases cross contamination risk of the isolates. This can also be an explanation of widely distribution of *Salmonella* isolates in food. It is also an important public concern because poor sanitation of surfaces that comes in contact with food causes food borne outbreaks. This situation revealed the

importance of microbial food safety and sanitation in industrial processes. Further investigations are required to investigate sanitation methods and effects of disinfectants on biofilms. An efficient and environmentally friendly control strategy is desired to better meet food safety and processing necessities, keeping in mind the fact that the resistance of biofilms to conventional disinfection processes is increased. In addition, interrupting the quorum sensing abilities of biofilm forming bacteria by natural biological agents may also be an affective option to solve biofilm related problems.

Acknowledgement

This study was presented as an oral presentation at XIII. Congress of Ecology and Environment with International Participation held on September 12-15 2017 in Edirne, Turkey.

References

1. Aksoy, D. & Şen, E. 2015. Investigation of pathogenic phenotypes and virulence determinants of food-borne *Salmonella enterica* strains in *Caenorhabditis elegans* animal model. *Bulletin of Microbiology*, 49(4): 513-524.
2. Albayrak, F., Cokca, F., Erdem, B. & Aysev, A.D. 2004. Predictive value of nalidixic acid resistance for detecting salmonellae with decreased ciprofloxacin susceptibility. *International Journal of Antimicrobial Agents*, 23(4): 332-336.
3. Antunes, P., Mourão, J., Campos, J. & Peixe, L. 2016. Salmonellosis: the role of poultry meat. *Clinical Microbiology and Infection*, 22(2): 110-121.
4. Borges, K.A., Furian, T.Q., Souza, S.N., Menezes, R., Tondo, E.C., Salle, C.T., Moraes H.L.S. & Nascimento, V.P. 2018. Biofilm formation capacity of Salmonella serotypes at different temperature conditions. *Pesquisa Veterinária Brasileira*, 38(1): 71-76.
5. Cookson, A.L., Cooley, W.A. & Woodward, M.J. 2002. The role of type 1 and curli fimbriae of *Shiga* toxin-producing *Escherichia coli* in adherence in abiotic surfaces. *International Journal of Medical Microbiology*, 292(3/4): 195.
6. Costerton, J.W., Stewart, P.S. & Greenberg, E. P. 1999. Bacterial biofilms: a common cause of persistent infections. *Science*, 284(5418): 1318-1322.
7. Cunliffe, D., Smart, C.A., Alexander, C. & Vulfson, E.N. 1999. Bacterial adhesion at synthetic surfaces. *Applied and environmental microbiology*, 65(11): 4995-5002.
8. Díez-García, M., Capita, R. & Alonso-Calleja, C. 2012. Influence of serotype on the growth kinetics and the ability to form biofilms of *Salmonella* isolates from poultry. *Food Microbiology*, 31(2): 173-180.
9. Donlan, R.M. 2002. Biofilms: microbial life on surfaces. *Emerging Infectious Diseases*, 8(9): 881.
10. Durul, B., Acar, S., Bulut, E., Kyere, E. O. & Soyer, Y. 2015. Subtyping of *Salmonella* food isolates suggests the geographic clustering of serotype Telaviv. *Foodborne Pathogens and Disease*, 12(12): 958-965.
11. Ercis, S., Erdem, B., Hasçelik, G. & Gur, D. 2006. Nalidixic acid resistance in *Salmonella* strains with decreased susceptibility to ciprofloxacin isolated from humans in Turkey. *Japanese Journal of Infectious Diseases*, 59(2): 117.
12. Erol, İ. 1999. Ankara'da tüketime sunulan kıymalarda *Salmonella*'ların varlığı ve serotip dağılımı. *Turkish Journal of Veterinary and Animal Science*, 23(4): 321-5.
13. Gerstel, U. & Römling, U. 2001. Oxygen tension and nutrient starvation are major signals that regulate agfD promoter activity and expression of the multicellular morphotype in *Salmonella typhimurium*. *Environmental Microbiology*, 3(10): 638-648.
14. Genualdi, S., Nyman, P. & Begley, T. 2014. Updated evaluation of the migration of styrene monomer and oligomers from polystyrene food contact materials to foods and food simulants. *Food Additives & Contaminants: Part A*, 31(4): 723-733.
15. Hoelzer, K., Switt, A. I. M. & Wiedmann, M. 2011. Animal contact as a source of human non-typhoidal salmonellosis. *Veterinary Research*, 42(1): 34.
16. Hoiby, N., Bjarnsholt, T., Givskov, M., Molin, S. & Ciofu, O. 2010. Antibiotic resistance of bacterial biofilms. *International Journal of Antimicrobial Agents*, 35(4): 322-332.
17. Karaca, B., Akcelik, N. & Akcelik, M. 2013. Biofilm-producing abilities of *Salmonella* strains isolated from Turkey. *Biologia*, 68(1): 1-10.
18. Lin, D., Chen, K., Chan, E.W.C. & Chen, S. 2015. Increasing prevalence of ciprofloxacin-resistant food-borne S*almonella* strains harboring multiple PMQR elements but not target gene mutations. *Scientific Reports*, 5: 14754.
19. Milanov, D., Prunić, B., & Ljubojević, D. 2017. Biofilm forming ability of *Salmonella enterica* serovar Tennessee isolates originating from feed. *Veterinarski Arhiv*, 87(6): 691-702.
20. Ozdemir, K. & Acar, S. 2014. Plasmid profile and pulsed–field gel electrophoresis analysis of *Salmonella enterica* isolates from humans in Turkey. *PloS One*, 9(5): e95976.
21. Panisello, P.J., Rooney, R., Quantick, P.C. & Stanwell-Smith, R. 2000. Application of foodborne disease outbreak data in the development and maintenance of HACCP systems. *International Journal of Food Microbiology*, 59(3): 221-234.
22. Piras, F., Fois, F., Consolati, S.G., Mazza, R. & Mazzette, R. 2015. Influence of temperature, source, and serotype on biofilm formation of *Salmonella enterica* isolates from pig slaughterhouses. *Journal of Food Protection*, 78(10): 1875-1878.
23. Römling, U., Sierralta, W.D., Eriksson, K. & Normark, S. (1998). Multicellular and aggregative behaviour of *Salmonella typhimurium* strains is controlled by mutations in the agfD promoter. *Molecular Microbiology*, 28(2): 249-264.
24. Römling, U., Rohde, M., Olsén, A., Normark, S. & Reinköster, J. 2000. AgfD, the checkpoint of multicellular

and aggregative behaviour in *Salmonella typhimurium* regulates at least two independent pathways. *Molecular Microbiology*, 36(1): 10-23.

25. Shia, X. &, Zhu, X. 2009. Biofilm formation and food safety in food industries. *Trends in Food Science & Technology*, 20(9): 407-413.
26. Sinde, E. & Carballo, J. 2000. Attachment of *Salmonella* spp. and *Listeria monocytogenes* to stainless steel, rubber and polytetrafluorethylene: the influence of free energy and the effect of commercial sanitizers. *Food Microbiology*, 17(4): 439-447.
27. Solano, C., García, B., Valle, J., Berasain, C., Ghigo, J. M., Gamazo, C. & Lasa, I. 2002. Genetic analysis of *Salmonella enteritidis* biofilm formation: critical role of cellulose. *Molecular Microbiology*, 43(3): 793-808.
28. Srey, S., Jahid, I.K. & Ha, S.D. 2013. Biofilm formation in food industries: a food safety concern. *Food Control*, 31(2): 572-585.
29. Steenackers, H., Hermans, K., Vanderleyden, J. & De Keersmaecker, S.C. 2012. *Salmonella* biofilms: an overview on occurrence, structure, regulation and eradication. *Food Research International*, 45(2): 502-531.
30. Stepanović, S., Vuković, D., Dakić, I., Savić, B. & Švabić-Vlahović, M. 2000. A modified microtiter-plate test for quantification of staphylococcal biofilm formation. *Journal of Microbiological Methods*, 40(2): 175-179.
31. Stepanović, S., Ćirković, I., Mijač, V. & Švabić-Vlahović, M. 2003. Influence of the incubation temperature, atmosphere and dynamic conditions on biofilm formation by *Salmonella* spp. *Food Microbiology*, 20(3): 339-343.
32. Stepanović, S., Ćirković, I., Ranin, L. & Svabić-Vlahović, M. 2004. Biofilm formation by *Salmonella* spp. and *Listeria monocytogenes* on plastic surface. *Letters in Applied Microbiology*, 38(5): 428-432.
33. Turki, Y., Ouzari, H., Mehri, I., Aissa, R.B. & Hassen, A. 2012. Biofilm formation, virulence gene and multi-drug resistance in *Salmonella* Kentucky isolated in Tunisia. *Food Research International*, 45(2): 940-946.
34. Van Houdt, R. & Michiels, C. W. 2010. Biofilm formation and the food industry, a focus on the bacterial outer surface. *Journal of Applied Microbiology*, 109(4): 1117-1131.
35. Velhner, M., Kozoderović, G., Grego, E., Galić, N., Stojanov, I., Jelesić, Z., & Kehrenberg, C. 2014. Clonal spread of *Salmonella enterica* serovar Infantis in Serbia: Acquisition of mutations in the topoisomerase genes gyrA and parC leads to increased resistance to fsluoroquinolones. *Zoonoses and Public Health*, 61(5): 364-370.
36. Vestby, L.K., Møretrø, T., Ballance, S., Langsrud, S., & Nesse, L.L. 2009a. Survival potential of wild type cellulose deficient *Salmonella* from the feed industry. *BMC Veterinary Research*, 5(1): 43.
37. Vestby, L.K., Møretrø, T., Langsrud, S., Heir, E., & Nesse, L.L. 2009b. Biofilm forming abilities of *Salmonella* are correlated with persistence in fish meal-and feed factories. *BMC Veterinary Research*, 5(1): 20.

http://dergipark.gov.tr/trkjnat
Trakya University Journal of Natural Sciences, 20(1): 63-70, 2019
ISSN 2147-0294, e-ISSN 2528-9691
DOI: 10.23902/trkjnat.498426

Research Article

DETERMINATION OF GROWTH KINETICS AND BIOCHEMICAL COMPOSITION OF *Nitzschia palea* (Kützing) W. Smith ISOLATED FROM FRESHWATER SOURCES IN TURKEY

Dilek YALÇIN DUYGU

Gazi University, Faculty of Education, Department Secondary School Science and Mathematics Education, Division of Biology Education, Ankara, TURKEY
ORCID ID: orcid.org/0000-0003-2127-8186, e-mail: dilekduygu06@hotmail.com

Cite this article as:

Yalçın Duygu D. 2019. Determination of Growth Kinetics and Biochemical Composition of *Nitzschia palea* (Kützing) W.Smith Isolated from Freshwater Sources in Turkey. *Trakya Univ J Nat Sci*, 20(1): 63-70, DOI: 10.23902/trkjnat.498426

Received: 17 December 2018, Accepted: 22 March 2019, Online First: 27 March 2019, Published: 15 April 2019

Abstract: This study was performed in order to bring out a detailed information on growth dynamics and biochemical determination of the diatom species *Nitzschia palea* (Kützing) W. Smith under batch culture conditions in order to pave the way for further studies. The study material was isolated from a fresh water sample collected from Ankara, Turkey. The diatoms were cultured in Allen medium for 168 hours and the growth dynamics were determined by cell density and dry weight analyses. Specific growth rate, duplication time of the culture and biochemical compositions were also investigated. Molecular characterization of the *N. palea* strain was performed by applying Fourier Transform Infrared Spectroscopy. The cell density and the dry biomass of the culture at the end of the 168 hours incubation period was determined as $2.0x10^6 \pm 1.0x10^5$cells/mL and 0.212±0.041 g L^{-1}, respectively. The algal specific growth rate was found as 0.010 h^{-1} at 96-h and the doubling time was calculated as 68 h^{-1}. The protein content was measured as 41.21%, carbohydrate content as 21.74%, lipid content as 16.84% and ash content as 19.88%. These results indicated that *N. palea* may be used in different fields of industries, especially in biodiesel production.

Key words: *Nitzschia palea,* batch culture, lipid, carbohydrate, protein, ash, FTIR.

Özet: Bu çalışma, daha ileri çalışmaların önünü açmak amacıyla yığın kültür koşullarında, *Nitzschia palea* (Kützing) W. Smith diatom türünün biyokimyasal tayini ve büyüme dinamikleri hakkında ayrıntılı bilgi vermek amacıyla yapılmıştır. Çalışma materyali, Ankara, Türkiye'den toplanan tatlı su örneğinden izole edilmiştir. Diatom kültürü Allen besi ortamında 168 saat boyunca yetiştirilmiş ve büyüme dinamikleri hücre yoğunluğu ile kuru ağırlık analizleriyle belirlenmiştir. Spesifik büyüme hızı, kültürün ikilenme süresi ve biyokimyasal bileşimleri de incelenmiştir. *Nitzschia palea*'nın moleküler karakterizasyonu Fourier Transform Infrared Spektroskopisi kullanılarak gerçekleştirilmiştir. Ekimi takip eden 168. saatte, Allen besi kültür ortamında kültürlerin hücre yoğunluğu $2,0x10^6 \pm 1,0x10^5$ hücre/mL ve kuru biyokütlesi 0,212±0,041 (g L^{-1}) olarak tespit edilmiştir. *Nitzschia palea*'nın spesifik büyüme oranı 96. saatte (0,010 h^{-1}) ve ikilenme süresi 68 h^{-1} olarak hesaplanmıştır. *Nitzschia palea*'nın protein miktarı (%41,21), karbonhidrat miktarı (%21,74), lipit miktarı (%16,84) ve kül miktarı (%19,88) olarak belirlenmiştir. Bu sonuçlar, *N. palea*'nın farklı endüstri alanlarında özellikle biyodizel üretimi için kullanılabileceğini göstermiştir.

Introduction

Diatoms are single-celled, microscopic and photosynthetic algae. They are the most prominent oxygen synthesizers and play a key role by being one of the most important biomass sources in oceans (Bozarth *et al*. 2009). Every diatom is placed in a fine (nano-scale) micro shell, and thus is the most substantial organisms among microalgae (Belegratis *et al*. 2014). A distinctive feature of diatoms is that they have a frustule composed of hydrated silicon dioxide and organic materials. Although diatoms have mainly been the field of interest academic studies, they are currently been utilized in a wide range of other fields. Recently, diatoms have been used frequently in nanotechnology due to their nano-molecular biosilica shells. The applications of different materials and technologies inspired by diatoms are common and include multiple disciplines (Van den Hoek *et al*. 1995), including environmental indicators of aquatic systems, bioremediators of contaminated water, pharmaceuticals, molecular sieves, materials relevant to nanotechnology, sensors, filters, health foods, resins, biomolecules, isolators, electronics and optical coatings (Bozart *et al*. 2009, Lakshmi *et al*. 2014). Diatoms are also defined as an appropriate alternative for the biodiesel production because they can be easily converted into biodiesel by transesterification reaction of triacylglycerols (TAG), which make up 60% of their cells. *Nitzschia* is a freshwater diatom which is was determined to have high lipid production (Yu *et al*. 2009). Therefore,

in recent years, most of the studies on *Nitzschia* species focused on increasing the intracellular lipid content and related biodiesel production. Vitug & Baldia (2014) cultivated *Nitzschia palea* (Kützing) W. Smith under various culture conditions and reported that the diatoms increased their lipid contents with changing light intensity, pH and temperature conditions. *Nitzschia palea* was grown in different culture media with different nutrients and tested as a model diatom to reveal its suitability as biodiesel raw material. The results of these and similar studies revealed that more intensive and comprehensive studies are needed for production of biodiesel from *N. palea* (Abdel-Hamid *et al*. 2013). In recent years, researchers have investigated the ability of Bacillariophyceae members to produce biologically active compounds and they have reported that they might be appropriate for antibiotic production. For instance, Binea *et al*. (2009) tested the extracts obtained from *N. palea* on some pathogenic bacteria and reported that the extracts were effective on some gram-positive bacteria. However, some of the features of diatom metabolism and the production of natural compounds are still unknown.

Fourier Transform Infrared (FTIR) Spectroscopy has been a widely used method through its wavenumbers causing vibrations on the functional constituents in molecules. Concerning algae, infrared microscopy enables spatial resolution and allows the analysis of macromolecules (Murdock & Wetzel 2009). Algal infrared microscopy research has focused on several macromolecular pools, including proteins (amide I and II), lipids (methyl and methylene groups, esters), carbohydrates (starch, cellulose), nucleic acids and phosphorous groups, and silica (in diatoms). FTIR spectroscopy is also applied for taxonomic purposes for species differentiation and classification (Vardy & Uwins 2002, Dean *et al*. 2010).

Despite the potential role of diatoms in all these issues mention above, it is obvious that specific studies on the biomass, growth and biochemical composition of diatom species are needed in this field. The present study was carried as a pilot study of a project aiming to increase the intracellular lipid content in *N. palea*. More specifically, this study was performed to determine the effects of culture media and conditions on biomass and growth rates of *N. palea* and to determine biochemical composition and application of FTIR spectroscopy for molecular characterization of the species.

Materials and Methods

Isolation and culture conditions

The diatom species *N. palea* was isolated from a freshwater source (Bilkent University well) in Ankara, Turkey. The fresh water sample was brought to the laboratory and was transferred to the liquid nutrient medium prepared for pre-enrichment of cultures. The liquid nutrient medium consisted of $MgSO_4 \cdot 7H_2O$ (2.50 g), KNO_3 (5.0 g), KH_2PO_4 (1.25 g), $FeSO_4 \cdot 7H_2O$ (0.009 g), and distilled water (1000 mL). The micromanipulation technique was used for isolation of the diatoms. The examined cells were removed by means of a micropipette, dropped on a sterile agar plate and then transferred to culture tubes. The culture tubes were placed under appropriate low temperature conditions (19 - 20° C). Control of the growth was performed by microscopic investigations approximately 2-3 weeks after the transfer of cultures to the medium (Perumal *et al*. 2012). The isolated diatoms were inoculated into fresh medium, and were identified by using identification keys (Krammer & Lange-Bertalot 1999).

The Allen medium was used for growth of *N. palea* cultures. The medium contained $NaNO_3$ (1.5 g/L), P-IV Metal Solution (1 mL/L): [K_2HPO_4 (5 mL/L) (1.5 g/200 mL dH_2O)], [$MgSO_4 \cdot 7H_2O$ (5 mL/L) (1.5 g/200 mL dH_2O)], [Na_2CO_3 (5 mL/L) (0.8 g/200 mL dH_2O)], [$CaCl_2 \cdot 2H_2O$ (10 mL/L) (0.5 g/200 mL dH_2O)], [$Na_2SiO_3 \cdot 9H_2O$ (10 mL/L) (1.16 g/200 mL dH_2O), [Citric Acid$\cdot H_2O$ (1 mL/L) (1.2 g/200 mL dH_2O)] and distilled water was added to 1000 mL of final volume (UTEX 2018).

The ambient temperature of the laboratory where the experiments were conducted was kept at 23±3 °C. The illumination of the laboratory was provided by a cool daylight lamp (Philips, 50 μmol photons $m^{-2}s^{-1}$) at a horizontal distance of 22 cm from the cultures. Cultures were exposed to the light in a 16:8 light:dark regime. The pH of nutrient media was adjusted to 6.5–7. In the experiments, 250 mL nutrient media and 50 mL suspended culture were inoculated. Sterilized air was provided using a disposable syringe filter. Culture flasks were placed in a shaker (Stuart SSL1 Shakers) and the speed of the shaker was adjusted to 120 rpm. All tests were carried out in triplicate.

Fourier Transform Infrared (FTIR) Spectrometry

Morphology and surface structures of the diatoms were characterized by applying FTIR. Infrared analysis was carried out at Bilkent University Institute of Materials Science and Nanotechnology, Ankara, Turkey, using a Vertex 70 with a Hyperion microscope fitted with a Bruker Tensor 37 FTIR spectrometer. FTIR measurements were done in the range of 800 and 4000 cm^{-1}, with 4 cm^{-1} resolution and a 20×20 μm square aperture. 128 scans were taken for 1 spectrum (Duygu *et al*. 2012).

Analytical methods

Cell density (cells/mL) was determined by counting 16 medium squares in a Thoma counting slide. Cell counts were performed under a light microscope at 400X magnification. Diatom frustules devoid of chloroplasts were not included in the counts. After the diatom sample was homogenized, it was applied into the counting chamber using a Pasteur pipette. The cells were homogenously distributed to the entire chamber area and the counting process was started. The counting was repeated four times and the mean number of cells in mL was calculated (Cirik & Gökpınar 1993). The cell counts were carried out at the beginning of the showing

procedure at ranges of (0, 24, 48, 72, 96, 120, 144 and 168) hours. The formula N x 10,000 (cells/mL), where N=16 is the number of cells counted in the medium square, 10,000 is the invariant which is used to obtain a standard result and to convert the counting result from 0.1 mm^3 to 1 mL, was used for countings (Gürgün & Halkman 1990).

The specific growth rate (μ) was defined as the increase in cell density and formulated. Specific growth rate and duplication time were calculated using Eq. 1 and Eq. 2, respectively (Wong *et al*. 2017).

$$\mu = \frac{\ln(\frac{X1}{X0})}{t1-t0} \quad (1)$$ (μ: Specific growth rate; x0 and x1 = Biomass concentration at *t*0 and *t*1)

$$DT = \frac{ln2}{\mu} \quad (2)$$ (DT: Duplication time)

Determination of yields of *N. palea* cultures was carried out by measuring the weights at the 168th hour of cultivation of the cultures. During the exponential growth phase, approximately 10 mL aliquot of the culture was taken to determine the dry weight. Algal sample was centrifuged, the supernatant was discarded and washed with 20 mL of distilled water. The samples were filtered through vacuum filtration with glass-fiber filters (Whattman, GF/C), as pre-dried and weighed. The filters were dried at 105°C for 24 hours, the dry weight was determined and finally weighed with a digital balance. Biomass was determined by the difference in weights (Fimbres-Olivarría *et al*. 2015).

Biochemical analyses

Nitzschia palea samples (300 ml) were centrifuged with a high-speed centrifuge (Rotor R10A5) at 10,000 rpm and 4 °C. Approximately 5 ml samples were transferred to Falcon tubes and lyophilized for 48 hours at -85 °C and 0.002 mbar vacuum. Freeze-dried samples were used for nutrient analysis. Nutrients (crude protein, total lipid, and total carbohydrate), dry matter and ash of the samples were determined according to the AOAC (1990). Nutrient analysis was carried out at Ankara University Faculty of Veterinary Medicine, Ankara, Turkey.

Statistical Analysis

The minimum, maximum, mean and standard deviation values of quantitative measurements were obtained using the statistical analysis option of Microsoft Excel.

Results

The diatoms used in the study were isolated from the samples collected from the freshwater source described above, and they were identified as *N. palea*. The microscopic measurements revealed that the cell weight ranged from 2.5 to 3 µm and the cell length from 15 to 30 µm. In addition, the presence of 28-30 stria at 10 µm was determined. The taxonomic classification of *N. palea* and its appearance under the light microscope are shown in Fig. 1 (Krammer & Lange-Bertalot 1999; Guiry & Guiry 2018).

The first cell counts of the inoculations in the nutrient medium were in the range of $8.70x10^5$ - $8.71x10^5$ cells/mL. The total increase of cell density in the medium throughout the 168-h study period is given in Table 1. The cell density at the end of the culture period was determined as $2.0x10^6 \pm 1.0x10^5$ cells/mL (Fig. 2). Dry biomass of the cultures was measured at 168-h and found as 0.212±0.041 (g L^{-1}) (Table 1). The algal growth rate was found at 96-h (0.010 h^{-1}), and doubling time was calculated as 68 h^{-1} (Table 1 and Fig. 2).

The biochemical composition of *N. palea* was performed by applying standard methods and the results have been shown in Table 2.

The absorption spectra of the culture had 9 clear bands over the wavenumber range of 800 to 4000 cm^{-1} (Fig. 3). Each peak was assigned a functional group (Table 3). The bands were tentatively identified on the basis of published data for phytoplankton, bacteria, on other biological materials and reference standards (Kumar *et al*. 2018). The peak at 1072 cm^{-1} corresponds to Si-O bonding (Table 3). The other peaks have been considered as organic structural peaks.

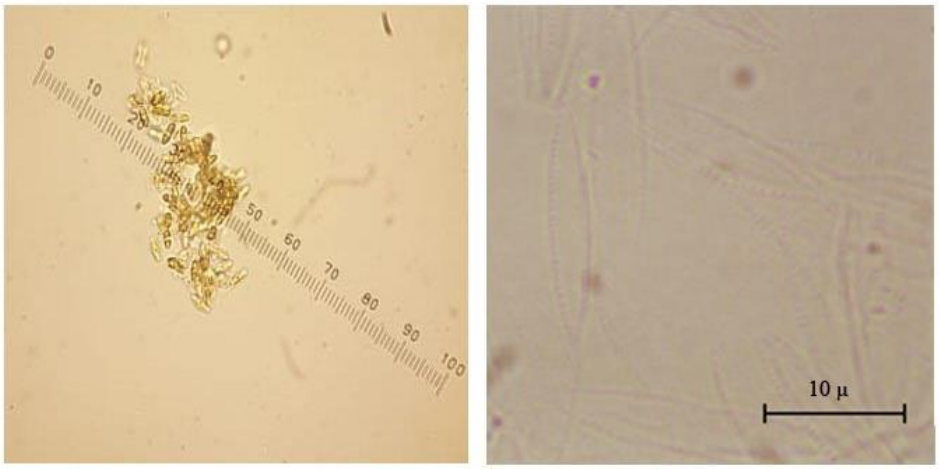

Fig. 1. Microscopic images of *N. palea* (400X right and 1000X left)

Table 1. Cell density, dry biomass weight, spesific growth rate (SGR μ) and duplication time (DT) of *N. palea*.

Cell Density (0h) (Cells/mL)		Cell Density (168h) (Cells/mL)		Dry Biomass (g L^{-1})		SGR (μ)	DT
Min.; Max.	Avr.±SD	Min.; Max.	Avr.±SD	Min.; Max.	Avr.±SD	(h^{-1})	(h^{-1})
$8.70x10^5$; $8.71x10^5$	$8.71x10^5$±$5.51x10^3$	$1.9x10^6$; $2.0x10^6$	$2.0x10^6$±$1.0x10^5$	0.171; 0.253	0.212±0.041	0.010	68

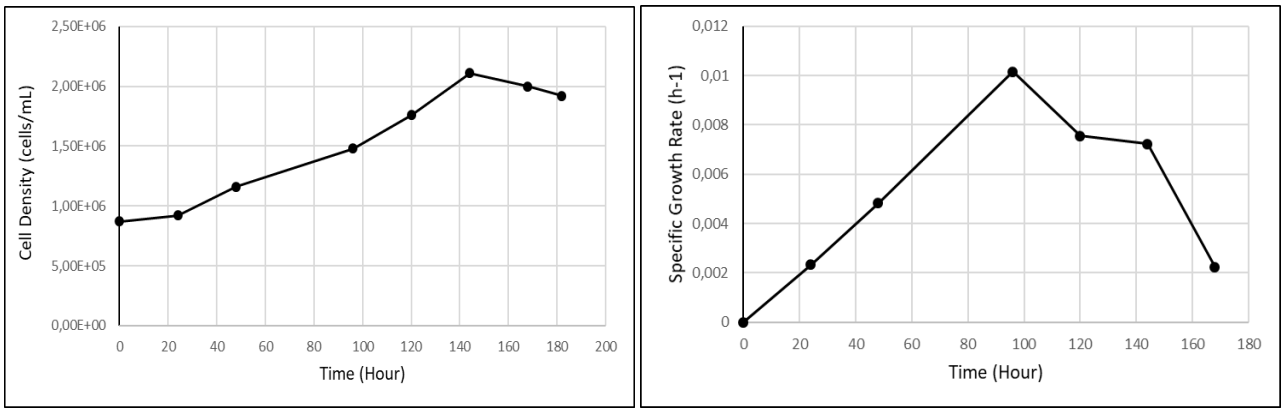

Fig. 2. Cell density and specific growth rate of *N. palea*.

Table 2. Total protein, carbohydrate, lipid and ash contents of *N. palea*.

Protein (%)	Carbohydrate (%)	Lipid (%)	Ash (%)
41.21±0.11	21.74±0.10	16.84±0.32	19.88±0.07

Data are given as mean ± standard deviation of triplicates. Mean values were given, n = 3.

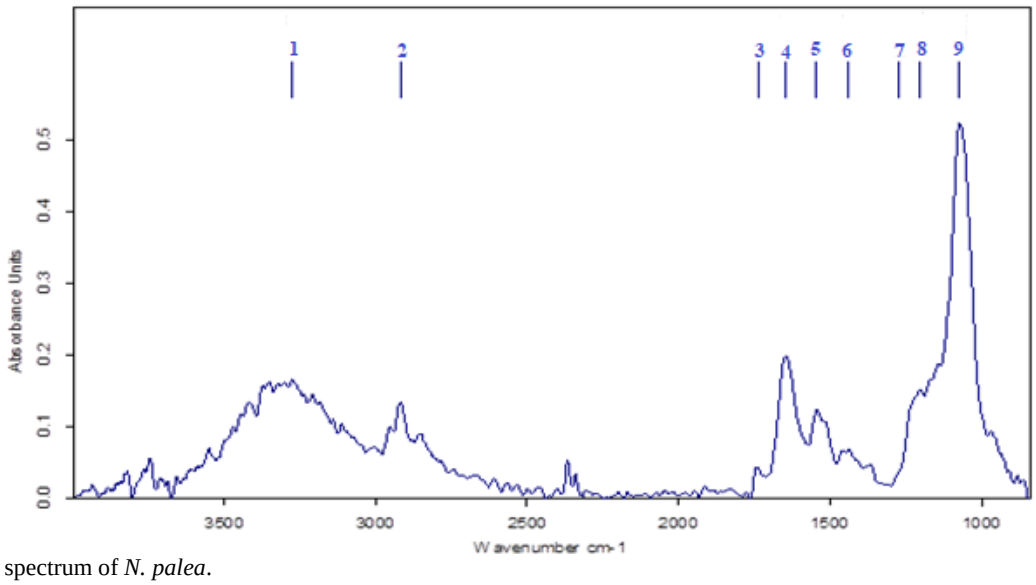

Fig. 3. FTIR spectrum of *N. palea*.

Discussion

Biomass and biochemical composition are critical parameters in selecting microalgal species for scale-up production. Adaptation and tolerance to environmental change is another significant factor to consider for cultivation and biomass production (Dębowski *et al.* 2012). In this study, *N. palea*, which was collected and isolated from its natural environment, was tried to be produced by providing optimum conditions in the laboratory. The culture conditions have sufficiently supported the growth of *N. palea* and this result is an important development in terms of biomass productivity.

The process of making microalgae cultures under laboratory conditions is based on the method in which a relatively small number of cells are inoculated and then exposed to appropriate light, temperature and ventilation conditions. The increase in the number of cells in such a culture follows a characteristic path in which different

Table 3. Tentative assignment of bands found in the FTIR spectra of *N. palea*[1]

Band No	Band Wavenumber (cm^{-1})	Region in (cm^{-1})	Tentative Assignment of Bands
1	3273	3029-3639	**Water** *v*(O-H) stretching **Protein** *v*(N-H) stretching (amide A)
2	2915	2809-3012	**Lipid – Carbohydrate** Mainly $\nu_{as}(CH_2)$ and $\nu_s(CH_2)$ stretching
3	1735	1763-1712	Cellulose–**Fatty Acids** *v*(C=O) stretching of esters
4	1643	1583-1709	**Protein** amide I band, mainly *v*(C=O) stretching
5	1516	1481-1585	**Protein** amide II band, mainly *δ*(N-H) bending and *v*(C-N) stretching
6	1432	1425-1477	**Protein** $\delta_{as}(CH_2)$ and $\delta_{as}(CH_3)$ bending of methyl **Lipid** $\delta_{as}(CH_2)$ bending of methyl
7	1381	1357-1423	**Protein** $\delta_s(CH_2)$ and $\delta_s(CH_3)$ bending of methyl **Carboxylic Acid** ν_s(C-O) of COO^- groups of carboxylates **Lipid** $\delta_s(N(CH_3)_3)$ bending of methyl
8	1202	1191-1356	**Nucleic Acid** (other phosphate-containing compounds) ν_{as}(>P=O); stretching of phosphodiesters
9	1072	1060, 1072, 1086	**For silica several bands Si-O-Si** stretching **Carbohydrate** *v*(C-O-C) of polysaccharides **Nucleic Acid** (and other phosphate-containing compounds) ν_s(>P=O) stretching of phosphodiesters

[1]Band assignment based on Kumar *et al*. (2018)

growth phases can be recognized (Chaumont 1993, Perumal *et al*. 2012). There are four growth phases for microalgae cultures. Cells, which are taken from stock cultures and inoculated into a new culture medium should be able to accommodate adaptation. Therefore, there is no cell division for a few hours and this stage is known as the lag or induction phase. Cells, which are adapted to the new medium, start to grow and the culture reach a maximum concentration in 12-18 hours. This phase is known as the exponential phase. At this phase, cells are logarithmically increased in successive equal intervals of time. When the cells reach their maximum concentration, cell growth and reproductions are gradually decreased. This phase is known as the declining phase. In stationary phase cultures, net reproduction is zero and cells undergo biochemical changes within certain hours. In the death phase (crash phase), metabolism of vegetative cell has not been in a good condition for a long time and this phase takes place very quickly. Reduction of nutrients, oxygen deficiency, overheating, and pH changes fall into factors causing deterioration of the cultures (Michelle *et al*. 2005, Ammar 2016).

In this study, four growth phases were observed during the growth of *N. palea* in Allen medium (Fig. 2). *Nitzschia palea* culture reached its maximum growth rate at 96-h. This phase can be defined as the exponential phase of *N. palea* under present culture conditions. After this phase, cell growth and reproduction began to decline gradually.

Nitzschia palea cell density increased in the following hours after inoculation and the cell density was determined as ($2.0x10^6 \pm 1.0x10^5$ cells/mL) at 168-h. Rodríguez-Núñez & Toledo-Agüero (2017) reported that the cell density of *Nitzschia* sp. was $1.3x10^7$ (cells/mL), which was higher than our results. Supriya *et al*. (2012) found the cell number as $5.31x10^4$ (cells/mL) when *Nitzschia* sp. was cultured in different media. This value is lower than the *N. palea* cell density value obtained in the present study. The maximum growth rate was reached at 96-h. The maximum growth rate calculated as 0.010 h^{-1} and the duplication time calculated as 68 h^{-1} are lower those found by (Rodríguez-Núñez & Toledo-Agüero 2017) (0.58 d^{-1}) and (Abdel-Hamid *et al.* 2013) (0.041 - 0.66 d^{-1}). In contrast, Supriya *et al*. (2012) determined the specific growth rate at 0.041 h^{-1}, which is higher than in this study.

Biomass amount and production are other evaluation features used in the selection of microalgae for cultivation. In other words, microalgae must have a short life cycle that can be reproduced under controlled conditions. The total biomass production (dry weight) of *N. palea* was recorded as 0.212 ± 0.041 g L^{-1} and reached its maximum value at 7th day. Lourduraj & Abraham (2016) found the dry weight of *N. palea* (0.524 ± 0.034 g L^{-1}) in the biomass and lipid increase study. A similar study by Abdel-Hamid *et al*. (2013) found the dry weight of *N. palea* as 0.16 - 0.27 g L^{-1}.

It has been considered that this change in the cell density and dry weight are observed due to the culture conditions, methods, different nutrient components in the media and the fact that the tested strains may be different.

In the production of biomass, the target microalgae should have appropriate nutritional contents. This content may depend on the microalgae culture and the phase in which the culture is harvested. In algal cultures, crude protein is produced as the primary organic component

during the logarithmic growth phase. Since the depletion of the components in the medium is in the stationary phase, the biochemical content in the cell decreases during this phase (Rodríguez-Núñeza & Toledo-Agüeroc 2017). Although this is more common in batch cultures, it can be removed by adding nutrients in continuous or semi-continuous cultures. In this study, biochemical analyses of *N. palea* was performed when the culture was in the exponential growth phase. In this study, the amount of protein was determined as 41.21%, carbohydrate content as 21.74%, lipid content as 16.84% and ash content as 19.88%. In a study carried out on the fatty acid profile and nutritional composition of diatoms by Rodríguez-Núñez & Toledo-Agüero (2017), the total lipid content was determined as 18.36%, crude protein content as 43.16%, carbohydrate content as18.88% and ash content as 19.60%, all in showing similaritiesto the findings of this study.

Recently, one of the areas where researchers had substantial interest was on obtaining lipid from microalgae. Microalgal lipids are used in two main fields: biofuels and food industry. Some microalgae produce large amounts of lipid in the form of triacylglycerides (TAGs). Microalgae synthesize very -long-chain polyunsaturated fatty acids (PUFA). Physical (pH, temperature, light) and chemical (nitrogen, carbon, phosphorus, iron, salt concentration) parameters affect the lipid composition of microalgae (Minhas *et al*. 2016). Many microalgae species show changes in their lipid contents in stress conditions. Examples of studies on the effect of stress factors on lipid and bioactive production include *Chlorella vulgaris* and *Pseudokirchneriella subcapitata* (Gonçalves *et al*. 2013), *Haematococcus pluvialis* (Imamoglu *et al*. 2009), *Scenedesmus* sp. (Rodolfi *et al*. 2009), *Nitzschia laevis* (Wen & Chen 2001) and *Arthrospira platensis* (Markou *et al*. 2013). Lipids are secondary metabolite products of diatoms and play a role in responding to changes in the environment and maintain specific membrane functions (Hu *et al*. 2008). In this study, total lipid amount was determined as 16.84%. However, Lourduraj & Abraham (2016) and Abdel-Hamid *et al*. (2013) determined total lipid amount as 40% and 20%, respectively, which were higher than the lipid obtained in this study. However, these studies have pointed out that the amount of intracellular lipid can be increased in diatoms.

Diatoms can rapidly adapt to changing nutrient conditions in aquatic environments. Where the water rises and the nutrients are deposited on the surface, the diatoms are highly effective for the intake of nutrients such as iron, nitrogen and silicon that limit growth. Diatoms can use a variety of nitrogen sources containing inorganic (NO_3^-, NH_4^+) and organic (urea, amino acids) nitrogen. The type of the nitrogen source can affect microalgae growth and microalgae adapt the nitrogen metabolism according to the nutrients available (Li *et al*. 2014). Sodium nitrate is an appropriate nitrogen source for cell growth and lipid production of diatoms. When the nitrogen sources were compared, it has been found that sodium nitrate was superior to urea. Li *et al*. (2008) observed that sodium nitrate is the best source of nitrogen for *Neochloris oleoabundane* for both cell growth and lipid accumulation. Similarly, sodium nitrate in the composition of Allen medium was found to be effective in the growth of *N. palea*. Silicon is an important nutrient that affects cellular metabolism for diatoms. The silicon source of Allen medium used in this study is $Na_2SiO_3 \cdot 9H_2O$. There are a wide range of freshwater nutrient media used for the cultivation of diatoms. The most commonly used media are Chu No.10 medium (Nichols 1973), WC medium (Guillard & Lorenzen 1972), DM (Diatom Medium) (CCAP 2018), f/2 Medium (Guillard & Ryther 1962). Although Allen nutrient medium is frequently applied in the production of blue green-algae, it was shown that this medium is also effective in the growth of diatom *N. palea*.

Diatom species have different types and concentrations of organic contents, and FTIR spectra can give very reliable information about this content. The FTIR study of a bioactive surface such as microorganisms and microalgae reveal the presence of many functional groups on their surfaces (Kumar *et al*. 2018). FTIR spectroscopy is applied in order to detect specific functional groups that help determine the presence of some components (Fig. 3). The peak area and intensity observed in the FTIR spectra reveal the abundance of a particular functional group. FTIR spectra of the diatom surface showed strong peaks around ~1049 and ~1070 cm^{-1}. This is characteristic of the Si-O bond, and the interaction of diatom surfaces with inorganic and organic materials leads to a change in the absorption band of Si-O, Si-OH and Si-O-Si (Losic *et al*. 2009). The FTIR spectra of *N. palea* given in Table 3 indicated the position and nature of absorption bands. *Nitzschia palea* has a strong extensive absorption band at 3273 cm^{-1} in the 3029–3639 cm^{-1} range. This absorption band is hydroxyl O–H stretching functional group. *Nitzschia palea* has a sharp band in the wavelength region of 2809–3012 cm^{-1}. The absorption band at 2915 cm^{-1} shows the aliphatic functional group with the asymmetric stretching CH_2 and the methyl C–H symmetric stretching/lipid (Swann & Patwardhan 2011). The absorption bands of 1643 cm^{-1} (amide I) and 1516 cm^{-1} (amide II) were due primarily to C=O stretching vibration and a combination of N-H and C-N stretching vibrations in amide complexes (Murdock & Wetzel 2009). Lipid spectra were characterized by two sets of strong vibrations: C-H at 2915 cm^{-1} and the C=O mode of the side chain from the ester carbonyl group at 1735 cm^{-1}. In the wave number range of 900-1300 cm^{-1}, *N. palea* showed strong and broader absorption band (1072 cm^{-1}). These bands showed the presence of polysaccharides (C–O str) and for silica several bands (Si-O-Si str).

Conclusion

In this study, *N. palea* isolated from fresh water resource was examined under culture conditions. The isolated and cultured *N. palea* strain showed rapid

reproduction and high biomass production during the study. The biochemical composition of the strain can be used for biodiesel production and nutritional purposes. Diatoms have been one of the most promising organisms in recent years, especially in nanotechnological applications, in addition to biomass for nutrition. Due to the remarkable characteristics of diatoms, it can be stated that it is possible to design and produce specific frustule morphologies for potential nanotechnology applications. FTIR spectra can provide data on the cellular content of macromolecular pools, using small amounts of cell material. By applying the information contained in the FTIR spectrum, the locations of specific biomolecules within the cell for algal species can be identified and analyzed. Due to this feature, FTIR has recently become a technique which have been applied by researchers to clarify the molecular structure of biological materials. As a result, researches on the use of diatoms' bioactive compounds in different areas of the industry especially biodiesel research need to be diversified.

References

1. Abdel-Hamid, M.I., El-Refaay, D.A., Abdel-Mogib, M. & Azab, Y.A. 2013. Studies on biomass and lipid production of seven diatom species with special emphasis on lipid composition of *Nitzschia palea* (Bacillariophyceae) as reliable biodiesel feedstock. *Algological Studies*, 143: 65-87.
2. Ammar, S.H. 2016. Cultivation of microalgae *Chlorella vulgaris* in airlift photobioreactor for biomass production using commercial NPK nutrients. *Al-Khwarizmi Engineering Journal*, 12(1): 90-99.
3. AOAC (Association of Official Analytical Chemists). 1990. *Official Methods of Analysis of the Association of Official Analytical Chemists.* Arlington, VA., 771 pp.
4. Belegratis, M.R., Schmidt, V., Nees, D., Stadlober, B. & Hartmann, P. 2014. Diatom-inspired templates for 3D replication: natural diatoms versus laser written artificial diatoms. *Bioinspiration & Biomimetics*, 9: 1-11.
5. Binea, H.K., Kassim, T.I. & Binea, A.K. 2009. Antibacterial activity of diatom *Nitzschia palea* (Kuetz.) W.SM. extract. *Iraqi Journal of Biotechnology*, 8(2): 562-566.
6. Bozarth, A., Maier, U.G. & Zauner, S. 2009. Diatoms in biotechnology: modern tools and applications. *Applied Microbiology and Biotechnology*, 82: 195-201.
7. CCAP, Culture Collection of Algae and Protozoa, Scottish Marine Institute, (https://www.ccap.ac.uk/), (Date accessed: 18 November 2018).
8. Cirik, S. & Gökpınar, Ş. 1993. *Plankton Bilgisi ve Kültürü*. Ege Üniversitesi Su Ürünleri Fakültesi Yayınları, İzmir, 269 s.
9. Chaumont D. 1993. Biotechnology of algal biomass production: a review of systems for outdoor mass culture. *Journal of Applied Phycology*, 5: 593-604.
10. Dean, A.P., Sigee, D.C., Estrada, B. & Pittman, J.K. 2010. Using FTIR spectroscopy for rapid determination of lipid accumulation in response to nitrogen limitation in freshwater microalgae. *Bioresource Technology*, 101: 4499-4507.
11. Dębowski, M., Zieliński, M., Krzemieniewski, M., Dudek, M. & Grala, A. 2012. Microalgae cultivation methods. *Polish Journal of Natural Sciences*, 27(2): 151-164.
12. Duygu, D., Udoh, A.U., Özer Baykal, T., Akbulut, A., Erkaya Açıkgöz, I., Yıldız, K. & Deniz, G. 2012. Fourier Transform Infrared (FTIR) spectroscopy for identification of *Chlorella vulgaris* Beijerinck 1890 and *Scenedesmus obliquus* (Turpin) Kützing 1833. *African Journal of Biotechnology*, 11(16): 3817-3824.
13. Fimbres-Olivarría, D., López-Elías, J.A., Martínez-Córdova, L.R., Carvajal-Millán, E., Enríquez-Ocaña, F., Valdéz-Holguín, E. & Miranda-Baeza, A. 2015. Growth and biochemical composition of *Navicula* sp. cultivated at two light intensities and three wavelengths. *The Israeli Journal of Aquaculture*, 1-7.
14. Gonçalves, A., Pires, J. & Simões, M. 2013. Lipid production of *Chlorella vulgaris* and *Pseudokirchneriella subcapitata*. *International Journal of Energy and Environmental Engineering*, 4: 1-6.
15. Gürgün, V. & Halkman K. 1990. *Mikrobiyolojide Sayım Yöntemleri.* Gıda Teknolojisi Derneği Yayınları, Ankara, 106 s.
16. Guillard, R.R. & Ryther, J.H. 1962. Studies on marine planktonic diatoms. I. *Cyclotella nana* Hustedt and *Detonula confervacaea* (Cleve) Gran. *Canadian Journal of Microbiology*, 8: 229-239.
17. Guillard, R.R.L. & Lorenzen, C.J. 1972. Yellow-green algae with chlorophyllide c. *Journal of Phycology*, 8: 10-14.
18. Guiry, M.D. & Guiry, G.M. 2018. *AlgaeBase*. (http://www.algaebase.org), (Date accessed: 26 November 2018).
19. Hu, Q., Sommerfeld, M., Jarvis, E., Ghirardi, M., Posewitz, M., Seibert, M. & Darzins, A. 2008. Microalgal triacylglycerols as feedstocks for biofuel production: perspectives and advances. *Plant Journal*, 54: 621-639.
20. Imamoglu, E., Dalay, M. C. & Sukan, F.V. 2009. Influence of different stress media and high light intensities on accumulation of astaxanthin in green alga *Haematococcus pluvialis*. *New Biotechnology*, 26: 199-204.
21. Krammer, K. & Lange–Bertalot, H. 1999. *Süßwasserflora von Mitteleuropa, Bacillariophyceae, Band 2/2, 2. Teil: Bacillariaceae, Epithemiaceae, Surirellaceae*. Gustav Fischer Verlag, Stuttgart, 584 pp.
22. Kumar, V., Kashyap, M., Gautam, S., Shukla, P., Joshi, K.B. & Vinayak, V. 2018. Fast Fourier Infrared spectroscopy to characterize the biochemical composition in diatoms. *Journal of Bioscience*, 43(4): 717-729.
23. Lakshmi, K.V., Jeyanthi, S., Santhanam, P., Devi, A.S. & Balamurugan, A. 2014. Study of self-assembled nanostructure and biomolecules of diatom *Nitzschia* sp. using electron microscopy and raman spectroscopy. *Bionano Frontier*, 2: 197-202.

24. Li, Q., Du, W. & Liu, D. 2008. Perspectives of microbial oils for biodiesel production. *Applied Microbiology and Biotechnology*, 80: 749-756.

25. Li, H.Y., Lu, Y., Zheng, J.W., Yang, W.D. & Liu, J.S. 2014. Biochemical and genetic engineering of diatoms for polyunsaturated fatty acid biosynthesis. *Marine Drugs*, 12: 153-166.

26. Lourduraj, J.J. & Abraham, D.R. 2016. Screening of microalgae based on biomass and lipid production at indoor and outdoor cultivation condition. *International Journal of Pure & Applied Bioscience*, 4(6): 107-113.

27. Losic, D., Mitchell, J.G. & Voelcker, N.H. 2009. Diatomaceous lessons in nanotechnology and advanced materials. *Advanced Materials*, 21: 2947-2958.

28. Markou, G. & Nerantzis, E. 2013. Microalgae for high-value compounds and biofuels production: a review with focus on cultivation under stress conditions. *Biotechnology Advances*, 8: 1532-1542.

29. Michelle, A., Everroad, R.C. & Wingard, L.M. 2005. Measuring Growth Rates in Algal Culturing Techniques. pp. 269-286 In: Andersen, R.A. (ed). *Algal Culturing Techniques*. Elsevier Academic Press, London, 589 pp.

30. Minhas, A.K., Hodgson, P., Barrow, C.J. & Adholeya, A. 2016. A review on the assessment of stress conditions for simultaneous production of microalgal lipids and carotenoids. *Frontiers of Microbiology*, 7: 1-19.

31. Murdock, J.N. & Wetzel, D.L. 2009. FT-IR microspectroscopy enhances biological and ecological analysis of algae. *Applied Spectroscopy Reviews*, 44: 335-361.

32. Nichols, H.W. 1973. Growth media-freshwater. Pp. 19-25. In: Stein, J.R. (ed). *Handbook of Phycological Methods: Culture Methods and Growth Measurements*. Cambridge University Press, New York, 472 pp.

33. Perumal, P., Prasath, B.B., Santhanam, P., Ananth, S., Shenbaga Devi, A. & Kumar, D. S. 2012. Isolation and culture of microalgae. *Workshop on Advances in Aquaculture Technology*, 166-181.

34. Rodolfi, L., Zittelli, C., Bassi, G., Padovani, N., Biondi, G. & Tredici, M.R. 2009. Microalgae for oil: strain selection, induction of lipid synthesis and outdoormass cultivation in a low-costphotobioreactor. *Biotechnology and Bioengineering*, 102: 100-112.

35. Rodríguez-Núñez, K. & Toledo-Agüero, P. 2017. Fatty acid profile and nutritional composition of two tropical diatoms from the Costa Rican Pacific Coast. *Grasas Aceites*, 68(3): 1-8.

36. Supriya, G., Asulabha, K.S. & Ramachandra, T.V. 2012. Use of Raman microspectroscopy to detect changes in lipid pools of microalgae, 1-8. LAKE 2012: National Conference on Conservation and Management of Wetland Ecosystems, 6-9 November, Kottayam-India.

37. Swann, G.E. & Patwardhan, S. 2011. Application of Fourier Transform Infrared Spectroscopy (FTIR) for assessing biogenic silica sample purity in geochemical analyses and palaeoenvironmental research. *Climate of the Past*, 7: 65-74.

38. UTEX, Culture Collection of Algae at the University of Texas at Austin. (http://web.biosci.utexas.edu/utex/Media%20PDF/allen%20medium.pdf), (Date accessed: 23 November 2018).

39. Van den Hoek, C., Mann, D. & Jahns, H.M. 1995. *Algae: an introduction to Phycology*. Cambridge University, Cambridge, 623 pp.

40. Vardy, S. & Uwins, P. 2002. Fourier transform infrared microspectroscopy as a tool to differentiate *Nitzschia closterium* and *Nitzschia longissima*. *Applied Spectroscopy*, 56: 1545-1548.

41. Vitug, L.V.D. & Baldia, S.F. 2014. Enhancement of some culture conditions for optimizing growth and lipid production in the diatom *Nitzschia palea*. *Acta Manilana*, 62: 25-34.

42. Wen, Z.Y., & Chen, F. 2001. A perfusion- cell bleeding culture strategy for enhancing the productivity of eicosapentaenoic acid by *Nitzschia laevis*. *Applied Microbiology and Biotechnology*, 57: 316-322.

43. Wong, Y.K., Ho, Y.H., Ho, K.C., Leung, H.M. & Yung, K.K.L. 2017. Maximization of cell growth and lipid production of freshwater microalga *Chlorella vulgaris* by enrichment technique for biodiesel production. *Environmental Science and Pollution Research*, 24: 9089-9101.

44. Yu, E.T., Zendejas, F.J., Lane, P.D., Gaucher, S., Simmons, B.A. & Lane, T.W. 2009. Triacylglycerol accumulation and profiling in the model diatoms *Thalassiosira pseudonana* and *Phaeodactylum tricornutum* (Bacillariophyceae) during starvation. *Journal of Applied Phycology*, 21: 669-681.

Trakya University Journal of Natural Sciences (TUJNS)

Copyright Release Form

Trakya University
Institute of Natural Sciences
Balkan Campus, Institutions Building
22030 EDİRNE, TURKEY

Telephone : 0 284 2358230
Fax : 0 284 2358237
e-mail : tujns@trakya.edu.tr

I, the undersigned, declare that I transfer the copyright and all related financial rights of the article with the title given below to Trakya University, granting Trakya University for rights of publishing and accepting University Publishing Regulations and Trakya University Publication Application Instructions for printing process.

Article Name:

Author(s):

Name, Surname :
Title :
Signature :
Date :

Name, Surname :
Title :
Signature :
Date :

Name, Surname :
Title :
Signature :
Date :

Name, Surname :
Title :
Signature :
Date :

Name, Surname :
Title :
Signature :
Date :

Additional page(s) can be used if the author number exceeds 5. All co-authors of the study are required to sign this form.

Yazım Kuralları

Trakya University Journal of Natural Sciences

(Trakya Univ J Nat Sci)

Trakya University Journal of Natural Sciences, her yıl Nisan ve Ekim aylarında olmak üzere yılda iki sayı olarak çıkar ve **Biyoloji, Biyoteknoloji, Çevre Bilimleri, Biyokimya, Biyofizik, Su Ürünleri, Ziraat, Veterinerlik, Ormancılık, Hayvancılık, Genetik, Gıda, Temel Tıp Bilimleri** alanlarındaki teorik ve deneysel yazıları yayınlar. Dergide yazılar İngilizce olarak yayınlanır. Ancak, yazıda Türkçe özet olmalıdır. Yabancı yazarlar için Türkçe özet desteği verilecektir. Özet kısmında kısaca giriş, materyal ve metot, sonuçlar ve tartışma başlıkları yer almalıdır. Dergide orijinal çalışma, araştırma notu, derleme, teknik not, editöre mektup, kitap tanıtımı yayınlanabilir. Değerlendirilmek üzere dergiye gönderilen yazıların yazımında ulusal ve uluslararası geçerli etik kurallara Committee on Publication Ethics (COPE) uyularak araştırma ve yayın etiğine dikkat edilmesi gerekmektedir. Yazılara konu olarak seçilen deney hayvanları için etik kurul onayı alınmış olmalı ve yazının sunumu esnasında dergi sistemine ek dosya olarak eklenerek belgelendirilmelidir. Basılacak yazıların daha önce hiçbir yerde yayınlanmamış ve yayın haklarının verilmemiş olması gerekir. Dergide yayınlanacak yazıların her türlü sorumluluğu yazar(lar)ına aittir.

Yazıların sunulması

Yazılar http://dergipark.gov.tr/trkjnat web adresi üzerinden gönderilmelidir. Dergiye yazı gönderimi mutlaka online olarak yapılmalıdır.

Yazı gönderiminde daha önce Dergi Park sistemine giriş yapmış olan kullanıcılar, üye girişinden kullanıcı adı ve şifreleri ile giriş yapabilirler.

Yazı gönderiminde sisteme ilk kez giriş yapacak ve yazı gönderecek yazarlar **"GİRİŞ"** bölümünden "**KAYDOL**" butonunu kullanacaklardır.

Yazarlar dergipark sistemine kaydolduktan sonra **"YAZAR"** bölümünden girecek ve yazıyı sisteme, yönergelere uygun olarak yükleyeceklerdir.

Yazı hazırlama ilkeleri

Yazılar, Yayın Komisyonu'na **MS Word** kelime işlemcisiyle **12 punto** büyüklüğündeki **Times New Roman** tipi yazı karakteriyle ve 1,5 aralıklı yazılmış olarak gönderilmelidir. İletişim bilgileri yazının ilk sayfasında tek başına yazılmalı, daha sonraki sayfada yazar isimleri ve iletişim bilgileri bulunmamalıdır. Tüm yazı her sayfası kendi arasında **satır numaraları** içerecek şekilde numaralandırılmalıdır. Yazar adları yazılırken herhangi bir akademik unvan belirtilmemelidir. Çalışma herhangi bir kurumun desteği ile yapılmış ise, teşekkür kısmında kurumun; kişilerin desteğini almış ise kişilerin bu çalışmayı desteklediği yazılmalıdır.

Yazı aşağıdaki sıraya göre düzenlenmelidir:

Yazarlar: Yazının ilk sayfasında sadece yazar isimleri ve adresleri bulunmalıdır. Adlar kısaltmasız, soyadlar büyük harfle ve ortalanarak yazılmalıdır. Adres(ler) tam yazılmalı, kısaltma kullanılmamalıdır. Birden fazla yazarlı çalışmalarda, yazışmaların hangi yazarla yapılacağı yazar ismi altı çizilerek belirtilmeli (sorumlu yazar) ve **yazışma yapılacak yazarın adres ve e-posta adresi yazar isimlerinin hemen altına yazılmalıdır. Bu sayfaya yazı ile ilgili başka bir bilgi yazılmamalıdır. Yazı, takip eden sayfada bulunmalı ve yazar-iletişim bilgisi içermemelidir.**

Başlık: İngilizce olarak Kısa ve açıklayıcı olmalı, büyük harfle ve ortalanarak yazılmalıdır.

Özet ve Anahtar kelimeler: Türkçe ve İngilizce özet 250 kelimeyi geçmemelidir. Özetin altına küçük harflerle anahtar kelimeler ibaresi yazılmalı ve yanına anahtar kelimeler virgül konularak sıralanmalıdır. Anahtar kelimeler, zorunlu olmadıkça başlıktakilerin tekrarı olmamalıdır. İngilizce özet koyu harflerle "Abstract" sözcüğü ile başlamalı ve başlık, İngilizce özetin üstüne büyük harflerle ortalanarak yazılmalıdır. Yazıdaki ana başlıklar ve varsa alt başlıklara **numara verilmemelidir.**

Giriş: Çalışmanın amacı ve geçmişte yapılan çalışmalar bu kısımda belirtilmelidir. Yazıda SI (Systeme International) birimleri ve kısaltmaları kullanılmalıdır. Diğer kısaltmalar kullanıldığında, metinde ilk geçtiği yerde 1 kez açıklanmalıdır. Kısaltma yapılmış birimlerin sonuna nokta konmamalıdır (45 m mesafe tespit edilmiştir). Kısaltma cümle sonunda ise nokta konmalıdır (… tespit edilen mesafe 45 m. Dolayısıyla…).

Materyal ve Metod: Eğer çalışma deneysel ise kullanılan deneysel yöntemler detaylı ve açıklayıcı bir biçimde verilmelidir. Yazıda kullanılan metod/metodlar, başkaları tarafından tekrarlanabilecek şekilde açıklayıcı olmalıdır. Fakat kullanılan deneysel yöntem herkes tarafından bilinen bir yöntem ise ayrıntılı

açıklamaya gerek olmayıp sadece yöntemin adı verilmeli veya yöntemin ilk kullanıldığı çalışmaya atıf yapılmalıdır.

Sonuçlar: Bu bölümde elde edilen sonuçlar verilmeli, yorum yapılmamalıdır**.** Sonuçlar gerekirse tablo, şekil ve grafiklerle de desteklenerek açıklanabilir.

Tartışma: Sonuçlar mutlaka tartışılmalı fakat gereksiz tekrarlardan kaçınılmalıdır. Bu kısımda, literatür bilgileri vermekten çok, çalışmanın sonuçlarına yoğunlaşmalı, sonuçların daha önce yapılmış araştırmalarla benzerlik ve farklılıkları verilmeli, bunların muhtemel nedenleri tartışılmalıdır. Bu bölümde, elde edilen sonuçların bilime katkısı ve önemine de mümkün olduğu kadar yer verilmelidir.

Teşekkür: Mümkün olduğunca kısa olmalıdır. Teşekkür, genellikle çalışmaya maddi destek sağlayan kurumlara, kişilere veya yazı yayına gönderilmeden önce inceleyip önerilerde bulunan uzmanlara yapılır. Teşekkür bölümü kaynaklardan önce ve ayrı bir başlık altında yapılır.

Kaynaklar: Yayınlanmamış bilgiler kaynak olarak verilmemelidir (*Yayınlanmamış kaynaklara örnekler: Hazırlanmakta olan veya yayına gönderilen yazılar, yayınlanmamış bilgiler veya gözlemler, kişilerle görüşülerek elde edilen bilgiler, raporlar, ders notları, seminerler gibi*). Ancak, tamamlanmış ve jüriden geçmiş tezler ve DOI numarası olan yazılar kaynak olarak verilebilir. Kaynaklar, yazı sonunda alfabetik sırada (yazarların soyadlarına göre) sıra numarası ile belirtilerek verilmelidir.

Yazıların ve kitapların referans olarak veriliş şekilleri aşağıdaki gibidir:

Makale: Yazarın soyadı, adının baş harfi, basıldığı yıl. Makalenin başlığı, *derginin adı*, cilt numarası, sayı, sayfa numarası. Dergi adı italik yazılır.

Örnek:

Tek yazarlı Makale için

Soyadı, A. Yıl. Makalenin adı. (Sözcüklerin ilk harfi küçük). *Yayınlandığı derginin açık ve tam adı*, Cilt(Sayı)**:** Sayfa aralığı.

Kıvan, M. 1998. *Eurygaster integriceps* Put. (Heteroptera: Scuteleridae)'nin yumurta parazitoiti *Trissolcus semistriatus* Nees (Hymenoptera: Scelionidae)'un biyolojisi üzerinde araştırmalar*. Türkiye Entomoloji Dergisi*, 22(4): 243-257.

İki ya da daha çok yazarlı makale için

Soyadı1, A1. & Soyadı2**,** A2. Yıl. Makalenin adı**.** (Sözcüklerin ilk harfi küçük). *Yayınlandığı derginin tam adı*, Cilt(Sayı): Sayfa aralığı.

Lodos, N. & Önder, F. 1979. Controbution to the study on the Turkish Pentatomoidea (Heteroptera) IV. Family: Acanthasomatidae Stal 1864. *Türkiye Bitki Koruma Dergisi*, 3(3): 139-160.

Soyadı1, A1., Soyadı2, A2. & Soyadı3, A3**.** Yıl. Makalenin adı**.** (Sözcüklerin ilk harfi küçük). *Yayınlandığı derginin tam adı*, Cilt (Sayı): Sayfa aralığı.

Önder, F., Ünal, A. & Ünal, E. 1981. Heteroptera fauna collected by light traps in some districts of Northwestern part of Anatolia. *Türkiye Bitki Koruma Dergisi***,** 5(3): 151-169.

Kitap: Yazarın soyadı, adının baş harfi, basıldığı yıl. Kitabın adı (varsa derleyen veya çeviren ya da editör), cilt numarası, baskı numarası, basımevi, basıldığı şehir,toplam sayfa sayısı.

Örnek:

Soyadı, A., Yıl. *Kitabın adı*. (Sözcüklerin ilk harfi büyük, italik). Basımevi, basıldığı şehir, toplam sayfa sayısı s./pp.

Önder F., Karsavuran, Y., Tezcan, S. & Fent, M. 2006. *Türkiye Heteroptera (Insecta) Kataloğu*. Meta Basım Matbaacılık, İzmir, 164 s.

Lodos, N., Önder, F., Pehlivan, E., Atalay, R., Erkin, E., Karsavuran, Y., Tezcan, S. & Aksoy, S. 1999. Faunistic *Studies on Lygaeidae (Heteroptera) of Western Black Sea, Central Anatolia and Mediterranean Regions of Turkey.* Ege University, İzmir, ix + 58 pp.

Kitapta Bölüm: Yazarın soyadı, adının baş harfi basıldığı yıl. Bölüm adı, sayfa numaraları. Parantez içinde: Kitabın editörü/editörleri, *kitabın adı*, yayınlayan şirket veya kurum, yayınlandığı yer, toplam sayfa sayısı.

Örnek:

Soyadı, A., Yıl. Bölüm adı, sayfa aralığı. In: (editör/editörler). *Kitabın adı*. (Sözcüklerin ilk harfi büyük, italik). Basımevi, basıldığı şehir, toplam sayfa sayısı s./pp.

Jansson, A. 1995. Family Corixidae Leach, 1815—The water boatmen. Pp. 26–56. In: Aukema, B. & Rieger, Ch. (eds) Catalogue of the Heteroptera of the Palaearctic Region. Vol. 1. Enicocephalomorpha, Dipsocoromorpha, Nepomorpha, Gerromorpha and Leptopodomorpha. The Netherlands Entomological Society, Amsterdam, xxvi + 222 pp.

Kongre, Sempozyum: Yazarlar, Yıl. "Bildirinin adı (Sözcüklerin ilk harfi küçük), sayfa aralığı". Kongre/Sempozyum Adı, Tarihi (gün aralığı ve ay), Yayınlayan Kurum, Yayınlanma Yeri.

Örnek:

Bracko, G., Kiran, K., & Karaman, C. 2015. The ant fauna of Greek Thrace, 33-34. Paper presented at the 6th Central European Workshop of Myrmecology, 24-27 July, Debrecen-Hungary.

Internet: Eğer bir bilgi herhangi bir internet sayfasından alınmış ise (*internetten alınan ve dergilerde yayınlanan yazılar hariç*), kaynaklar bölümüne internet sitesinin ismi tam olarak yazılmalı, siteye erişim tarihi verilmelidir.

Soyadı**,** A. Yıl. Çalışmanın adı. (Sözcüklerin ilk harfi küçük) (web sayfası) http://www.....) (Date accessed: 12.08.2009).

Hatch, S., 2001. Studentsperception of online education. Multimedia CBT Systems. (Web page: http://www.scu.edu.au/schools/sawd/moconf/papers2001/hatch.pdf) (Date accessed: 12.08.2009).

Kaynaklara metin içinde numara verilmemeli ve aşağıdaki örneklerde olduğu gibi belirtilmelidir.

Örnekler:
... x maddesi atmosferde kirliliğe neden olmaktadır (Landen 2002). Landen (2002) x maddesinin atmosferde kirliliğe neden olduğunu belirtmiştir. İki yazarlı bir çalışma kaynak olarak verilecekse, (Landen & Bruce 2002) veya Landen & Bruce (2002)'ye göre. ... şeklinde olmuştur; diye verilmelidir. Üç veya daha fazla yazar söz konusu ise, (Landen *et al.* 2002) veya Landen *et al.* (2002)'ye göre .... olduğu gösterilmiştir; diye yazılmalıdır.

Şekil ve Tablolar: Tablo dışında kalan fotoğraf, resim, çizim ve grafik gibi göstermeler "Şekil" olarak verilmelidir. Resim, şekil ve grafikler, net ve ofset baskı tekniğine uygun olmalıdır. Her tablo ve şeklin metin içindeki yerlerine konmalıdır. Tüm tablo ve şekiller yazı boyunca sırayla numaralandırılmalı (Tablo 1., Şekil. 1), başlık ve açıklamalar içermelidir. Şekillerin sıra numaraları ve başlıkları, alta, tabloların ki ise üstlerine yazılır.

Şekiller (tablo dışında kalan fotoğraf, resim, çizim ve grafik gibi) tek tek dosyalar halinde en az **300 dpi** çözünürlükte ve **tif** dosyası olarak şekil numaraları dosya isminde belirtilmiş şekilde ayrıca sisteme ek dosya olarak yüklenmelidir.

Sunulan yazılar, öncelikle Dergi Yayın Kurulu tarafından ön incelemeye tabii tutulur. **Dergi Yayın Kurulu, yayınlanabilecek nitelikte bulmadığı veya yazım kurallarına uygun hazırlanmayan yazıları hakemlere göndermeden red kararı verme hakkına sahiptir.** Değerlendirmeye alınabilecek olan yazılar, incelenmek üzere iki ayrı hakeme gönderilir. Dergi Yayın Kurulu, hakem raporlarını dikkate alarak yazıların yayınlanmak üzere kabul edilip edilmemesine karar verir.

SUİSTİMAL İNCELEMELERİ VE ŞİKAYETLER

Dergide yayınlanmış veya yayınlanma sürecine girmiş her türlü yazı hakkındaki suistimal şüphesi ve suistimal şüphesiyle yapılan şikayetler dergi Yayın Kurulu tarafından değerlendirilir. Yayın kurulu suistimal şüphesini veya şikayeti değerlendirirken COPE (Committee on Publication Ethics)'un yönergelerine bağlı kalır. Şüphe veya şikayet sürecinde şikayet taraflarıyla hiçbir bağlantısı olmayan bir ombudsman belirlenerek karar verilir. Şikayetler baş editöre tujns@trakya.edu.tr adresi kullanılarak yapılabilir.

YAYIN SONRASI DEĞİŞİKLİK VE GERİÇEKME İSTEĞİ

Dergide yazının yayınlanması sonrası yazar sırasında değişiklik, yazar ismi çıkarma, ekleme ya da yazının geriçekilmesi tujns@trakya.edu.tr adresine yapılacak bir başvuru ile gerçekleştirilebilir. Gönderilecek e-postada mutlaka gerekçe ve kanıtlar sunulmalıdır. Sunulan gerekçe ve kanıtlar Yayın Kurulu tarafından görüşülüp karara bağlanır. Yukarıda belirtilen değişiklik ve geri çekme istekleri oluştuğunda tüm yazarların dergiye gönderecekleri yazılar işlem süresi içerisinde otomatik olarak reddedilir.

ÜYELİK/AYRI BASKI/ERİŞİM

Dergi üyelik gerektirmeyip Açık Erişime sahiptir. Dergide yazısı basılan tüm sorumlu yazarlara 15 ayrı baskı ve yazının çıktığı 1 dergi ücretsiz gönderilmektedir. Dergide yayınlanan tüm yazılara erişim ücretsiz olup full-text pdf dosyaları CC-BY 4.0 uluslararası lisansı kapsamında kullanılabilir.

REKLAM VERME

Dergiye reklam vermek üzere tujns@trakya.edu.tr adresine yapılacak başvurular dergi sahibi tarafından değerlendirilecektir.

Baş Editör **:** Doç. Dr. Kadri KIRAN

Trakya Üniversitesi
Fen Bilimleri Enstitüsü
Balkan Yerleşkesi
22030 - EDİRNE

Tel : 0284 235 82 30
Fax : 0284 235 82 37
e-mail : tujns@trakya.edu.tr

Author Guidelines

Trakya University Journal of Natural Sciences
(Trakya Univ J Nat Sci)

Trakya University Journal of Natural Sciences, is published twice a year in April and in October and includes theoretical and experimental articles in the fields of **Biology, Biotechnology, Environmental Sciences, Biochemistry, Biophysics, Fisheries Sciences, Agriculture, Veterinary and Animal Sciences, Forestry, Genetics, Food Sciences** and **Basic Medicine Sciences**. Original studies, research notes, reviews, technical notes, letters to the Editor and book reviews can be published in the journal. The publishing language for all articles in the journal is **English**. On the other hand, authors are required to provide a Turkish abstract also. The Turkish version of the abstract will be supply by the journal for foreign authors. Abstracts should include introduction, material and methods, results and discussion sections in summary. The authors should pay attention to research and publication ethics Committee on Publication Ethics (COPE) in preparation of their manuscripts before submission by considering national and international valid ethics. An approval of Ethics and Animal Welfare Committee is mandatory for submissions based on experimental animals and this approval should be provided during submission of the manuscripts. Articles which have not been published elsewhere previously and whose copyright has not been given to anywhere else should be submitted. All responsibilities related to published articles in Trakya University Journal of Natural Sciences belong to the authors.

Submitting articles

Articles should be submitted on the web through http://dergipark.gov.tr/trkjnat and all submissions should be performed online.

Authors, who are already a member of the DergiPark system, can enter in the login section using their "user name" and "password" to submit their articles.

Authors entering the DergiPark system for the first time to submit an article will enter in the "**REGISTER**" section to submit their articles.

Article preparation rules

Articles should be submitted to the Journal using **MS Word** preparing **12 points Times New Roman** font and 1.5 raw spacing. Author names and contact info must be in first page,article must continue in second page without author names and contact info. Whole article should have numbered with **line number** restarting each page. The author's name must not be specified any academic titles. If studies supported by a foundation, this support should have been written in the acknowledgement section.

Articles should be arranged as below:

Authors: The name(s) of the author(s) should not be abbreviated and must be written under the title one by one, with surnames in capital letters. Address(es) should be written in full. Corresponding authors in multiple authored submissions should be indicated, and the address and e-mail of the corresponding author should be written just under the author(s) list. **No other information about the manuscript should be included in this page. The main manuscript text should start with the following new page and should not include any author-contact information.**

Title: Should be short and explanatory and written in capital letters and centered.

Abstract and keywords: Turkish and English abstracts should not exceed 250 words. "Keywords" should be written under the abstract in small letters and all keywords should be written using a comma after all. Keywords should not be replica of the title words, if it is not obligatory. Abstract should begin "Abstract" word from the left side of the page. The main and sub headers (if present) should not be numbered.

Introduction: The aim of the submitted and history of the previous studies should be indicated in this section. SI (Systeme International) system and abbreviation should be used in the article. Other abbreviations- should be explained once in their first appearance in the text. No "." sign should be used after abbreviations except those used at the end of a sentence (…the determined distance is 45 m. Therefore, …).

Material and Method: If the submitted study is experimental, methods of the experiments should be given in detail. The method(s) used in the article should be descriptive for others to repeat. If a widely known experimental method is used, the method does not need to be explained in detail. In this situation, indicating only the name of the experimental method or citing the study who used the method for the first time will be enough.

Results: Obtained results should be given in this section without any comment. Results can be explained with tables, figures or graphics, if necessary.

Discussion: Results must be discussed, but unnecessary duplications should be avoided. In this section, rather than giving literature data, authors should focus on their results considering similarities and differences with and between previously conducted researches, and should discuss possible reasons of similarities and differences. The contribution to science and importance of the obtained results should also be mentioned as much as possible in this section.

Acknowledgements: Should be as short as possible. Thanks are usually made to institutions or individuals who support the study or to experts who reviewed the article before submitting to the journal. Acknowledgement section should be given before the references section in a separate header.

References: Unpublished information should not be given as a reference (examples of unpublished references: articles in preparation or submitted somewhere, unpublished data or observations, data obtained based on interviews with individuals, reports, lecture notes, seminars, etc.). However, thesis completed and signed by a jury and articles with DOI numbers given can be used as reference. References should be given at the end of the text, sorted alphabetically by author's surname and should be given with numbering.

Articles: Surname of author, first letter of author's first name, publication year, article title, the *name of the journal,* volume, issue, page numbers. Journal name is written in italics.

Example:

Articles with single author

Surname, N. Year. Article title (First letter of all words small). *Whole name of journal*, Volume (Issue)**:** page range.

Aybeke, M. 2016. The detection of appropriate organic fertilizer and mycorrhizal method enhancing salt stress tolerance in rice (*Oryza sativa* L.) under field conditions. *Trakya University Journal of Natural Sciences,* 17(1): 17-27.

Articles with two or more authors

Surname1, N1. & Surname2**,** N2. Year. Article title (First letter of all words small). *Whole name of journal*, Volume (Issue)**:** page range.

Dursun, A. & Fent, M. 2016. Contributions to The Cicadomorpha and Fulgoromorpha (Hemiptera) fauna of Turkish Thrace region. *Trakya University Journal of Natural Sciences,* 17(2): 123-128.

Surname1, N1., Surname2**,** N2. & Surname3, N. Year. Article title (First letter of words small). *Whole name of journal*, Volume (Issue)**:** page range.

Becenen, N., Uluçam, G. & Altun, Ö. 2017. Synthesis and antimicrobial activity of iron cyclohexanedicarboxylic acid and examination of pH effect on extraction in water and organic phases.*Trakya University Journal of Natural Sciences,* 18(1): 1-7.

Book: Surname of author, first letter of author's first name, Year. *Book title* (name of translator or book editor if present), volume, edition number, press, city, page number.

Example:

Surname, N. Year. *Book Title* (First letter of words small and italic), volume, edition number, press, city, page number.

Czechowski, W., Radchenko, A., Czechowska, W. & Vepsäläinen, K. 2012. *The ants of Poland with reference to the myrmecofauna of Europe*. Museum and Institute of Zoology PAS, Warsaw, 496 pp.

Book Section: Surname of author, first letter of the author's first name, Year. Section name, page range. In: (Editor of Book, *Book title,* press, city, page number).

Example:

Surname, N. Year. Section name, page range. In: (Editor of Book, *Book title* (First letter of words small and italic), press, city, page number)

Jansson, A. 1995. Family Corixidae Leach, 1815—The water boatmen. Pp. 26–56. In: Aukema, B. & Rieger, Ch. (eds) Catalogue of the Heteroptera of the Palaearctic Region. Vol. 1. Enicocephalomorpha, Dipsocoromorpha, Nepomorpha, Gerromorphaand Leptopodomorpha. The Netherlands Entomological Society, Amsterdam, xxvi + 222 pp.

Congress, Symposium: Surname, N. Year. Presentation title (first letters of all words small), page range. Name of Congress/Symposium, Date (day range and month), place.

Example:

Bracko, G., Kiran, K., & Karaman, C. 2015. The ant fauna of Greek Thrace, 33-34. Paper presented at the 6th Central European Workshop of Myrmecology, 24-27 July, Debrecen-Hungary.

Internet: If any information is taken from an internet source (articles published in journals and taken from internet excluded), internet address should be written in full in references section and access date should be indicated.

Surname**,** N. Year. Name of study (First letter of words small) (Web page: http://www.....) (Date accessed: 12.08.2009).

Hatch, S. 2001. Student sperception of online education. Multimedia CBT Systems. (Web page: http://www.scu.edu.au/schools/sawd/moconf/papers2001/hatch.pdf) (Date accessed: 12.08.2009).

References within the text should not be numbered and indicated as in the following examples.

Examples:

... atmospheric pollution is causing by x matter (Landen 2002). If an article has two authors, it should be indicated in the text as (Landen & Bruce 2002) or ... according to Landen & Bruce (2002) .... If there are three or more authors, references should be indicated as (Landen *et al.* 2002) or according to Landen *et al.* 2002 ...

Graphics and tables: All photos, pictures, drawings and graphics except tables should be indicated as Figures. Pictures, figures and graphics should be clear and ready to print with offset technique. The places of all tables and figures should be indicated in the text. All tables and figures should be numbered within the text respectively (Table 1, Fig. 1). Figure numbers and legends are written below the figures, table numbers and legends are written above the tables.

All figures (all pictures, drawings and graphics except table) should also be uploaded to the system separately with 300dpi resolution at least as .tif file using the figure numbers in the files name.

Submitted articles are subjected to prior review by the Editorial Board. Editorial Board has the right to reject the articles which are considered of low quality for publish or those which are insufficiently prepared according to the author guidelines. The articles accepted for consideration for evaluation will be sent to two different referees. Editorial Board decides to accept or reject the submissions for publication by taking into account the reports of referees.

EXPLOITATION ENQUIRY AND COMPLAINTS

All kinds of exploitation doubts and complaints about manuscripts, either published or in publication process, are evaluated by the Editorial Board. The Editorial Board strictly follows the directives of COPE (Committee on Publication Ethics) during the evaluations. An ombudsman who has no connection with the parts in any stage of the complaint is appointed and a decision is made. Complaints can be sent to the editor in chief by sending an e-mail to tujns@trakya.edu.tr.

POST-PUBLICATION CHANGE AND WITHDRAWAL OF A MANUSCRIPT

Changes in author ordering, removal or addition of a new author in and withdrawal of a published manuscript can be realized by sending an application to tujns@trakya.edu.tr. The application e-mail should include the reason of the requested change with the evidences. The reasons and the evidences are discussed and finalized by the Editorial Board. Further submissions of authors of a formerly accepted manuscript undergoing a change process are automatically sent back to the authors until the final decision of the manuscript in process.

ADVERTISING

Advertising applications sent to tujns@trakya.edu.tr will be evaluated by the journal owner.

Editor-in-Chief **:** Dr. Kadri KIRAN

Trakya Üniversitesi
Fen Bilimleri Enstitüsü
Balkan Yerleşkesi
22030 - EDİRNE-TURKEY

Phone : +90 284 235 82 30
Fax : +90 284 235 82 37
e-mail : tujns@trakya.edu.tr